MINISTRY OF NATIONAL EDUCATION

THE ANNALS OF "DUNAREA DE JOS" UNIVERSITY OF GALATI

Fascicle IX
METALLURGY AND MATERIALS SCIENCE

YEAR XXXI (XXXVI),
March 2013, no.1

ISSN 1453-083X

2013
GALATI UNIVERSITY PRESS

THE ANNALS OF "DUNAREA DE JOS" UNIVERSITY OF GALATI.
FASCICLE IX. METALLURGY AND MATERIALS SCIENCE
N^0. 1 – 2013, ISSN 1453 – 083X

Table of Content

THE ANNALS OF "DUNAREA DE JOS" UNIVERSITY OF GALATI.
FASCICLE IX. METALLURGY AND MATERIALS SCIENCE
N^0. 1 – 2013, ISSN 1453 – 083X

STRUCTURE-PROPERTY CORRELATION OF COMPOSITE MATERIALS BASED ON Cu-Mo OBTAINED BY PVD METHOD

Lucica ORAC[1], Vera GRECHANYUC[2]
Olga MITOSERIU[1], Stela CONSTANTINESCU[1]
[1]University "Dunarea de Jos" of Galati, Romania
[2]University of Building and Architecture, Kiev, Ukrain
email: lucia_orac@yahoo.com

ABSTRACT

The paper describes reviews referring to determination of working parameters of the development processes of composites in copper matrix, by vapour-phase deposition method. The molybdenum was used as complementary phase. Structural characterization of coatings developed by optical microscopy and electronic scanning and effects of surface structure on their characteristics were presented. The specificity of the technology for obtaining Cu-Mo composites is a condition to formation a special laminated structure. The mechanical characteristics of the condensate depending on the amount of molibden. An important role in forming the structure and characteristics is played by the defects which were formed in the condensate during the transfer in the liquid phase as drops. Electrochemical tests have shown that the corrosion resistance of the composites obtained by PVD method is higher than pure copper.

KEYWORDS: PVD, coatings, defects, electrochemical corrosion

1. Introduction

One of the main causes of the limitation to the use of materials for electrical contacts free of Ag or other nobel matals, is the fast corrosive damage when operating in wet environment.

Cu-Mo (12% max. Mo) composite materials are produced by simultaneous evaporation from separate Cu and Mo crucibles with subsequent condensation of the vapor flow on OL-37 steel layer of 15 to 20mm thickness and 800 mm diameter. The surface of the disk-support on which condensation of the vapor flow takes place was machined until a roughness of R_a=0.63 was obtained.

The analysis of chemical composition and structure of composites based on copper and molybdenum content allowed to determine the variation of these elements from layer to layer (of up to 20-25% to 4-5 mas.) and the distribution gredient of these elements in the layers.

The mechanical properties of the Cu-Mo composite materials, depend on molibden content.

The condensate obtained as plates of 0.7-1.2mm thickness has been used for the study of corrosion resistance [1].

2. Results and experimental research

To obtain composite materials based on copper and molybdenum, copper, molybdenum and calcium fluoride powder have been used; their characteristics are presented in Table 1. For evaporation, use is made of copper ingots of 100mm diameter and 70mm diameter molybdenum. The ingots were blanked to 98.5, respectively 68.5mm size to avoid their jam in the evaporation process.

Table1. *Material marks that were used to obtain composite materials based on copper and molybdenum*

Materials	Marck	Standard
Cu	M0b, M00, M0, M1, M2	GOST 859-78
Mo	MCVP	TU 48-19-247-87
CaF_2	c	GOST 7167-77

Calcium fluoride powder was pressed with a press-type P-457 at a pressure of 240 to 300MPa, in a number of pills of 30 mm diameter and 15 to 20mm thickness. The CaF_2 pills were used to form a separate layer of the disc-holder, where vapor flow condensation takes place. Due to the separation layer the condense separates easily from the holder/support.

The chemical composition of the condensates was determined by chemico-analytical methods [2]. The chemical composition was determined at the Electrotechnical Research Institute in Bucharest, according to STAS STAS 1706/1-85 and 1706/17-71 using spectrometric methods.

The results, which re the arithmetic average of tens of tests on samples with different thicknesses, are presented in Table 2.

Table 2. *Chemical composition of the composites*

Sample code	Chemical composition, %	
	Cu	Mo
1	98.8	1.2
2	96.09	3.91
3	94.9	5.1
4	93.2	6.8
5	91.6	8.4
6	87.7	12.3

By electronic microscopy in cross –section and from the spot analyses EDX it could be noticed the stratified distribution of both molybden and copper (Figure 1).

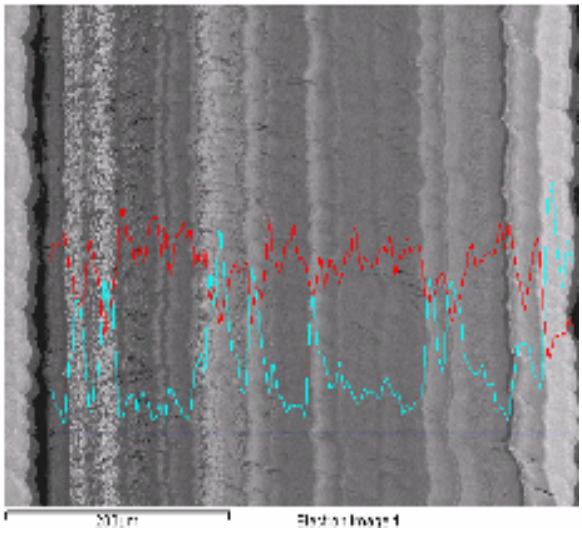

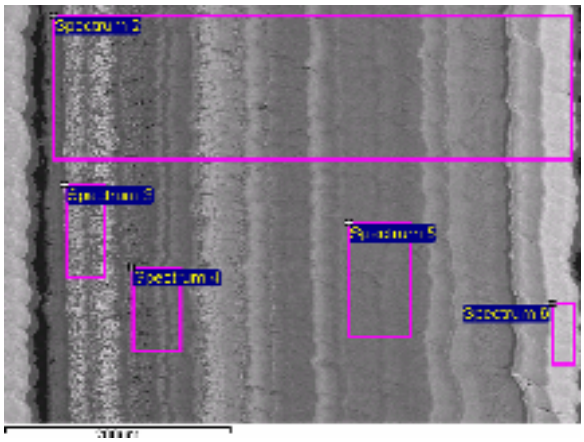

Fig. 1. *Analyses EDX in cross section and spots for the stratified composite, Cu - Mo (8.4% Mo)*

Processing option: All elements analysed (Normalised)

All results in weight %

Spectrum	Cu	Mo	Total
Spectrum 2	91.85	8.15	100
Spectrum 3	91.80	8.20	100
Spectrum 4	92.02	7.98	100
Spectrum 5	92.14	7.86	100
Spectrum 6	91.6	8.4	100

The structure of Cu-Mo composites is in the form of blocks. For each block it is characteristic an arbitrary periodic striped structure. The period of stripes repetition is 150 ±3μm.

Composites were obtained in Cu-Mo micro layers with a structure sufficiently balanced by condensation at temperatures above the melting temperature to 0.3 than the melting temperature of the lowest fusible component (°C).

The mechanical characteristics were determined from the tensile test results of flat samples in vacuum with 15 mm length on a 1248-R plant as per Standard of Ukraine 9651-84.

Samples were cut from the composite with thickness of 0.9 - 1.4mm in the initial state and after annealing in vacuum to 1170K for 3h.

The experiments were done at room temperature in open air and vacuum, of max. 0.1Pa at a temperature of 370-1070K from 100 to 100degrees. At each temperature three to six samples were studied. The deformation rate of the sample during the experiment was 2 mm/min, which corresponds to the relative speed of deformation ~ $2.2 \cdot 10^{-3}$ s^{-1} [3].

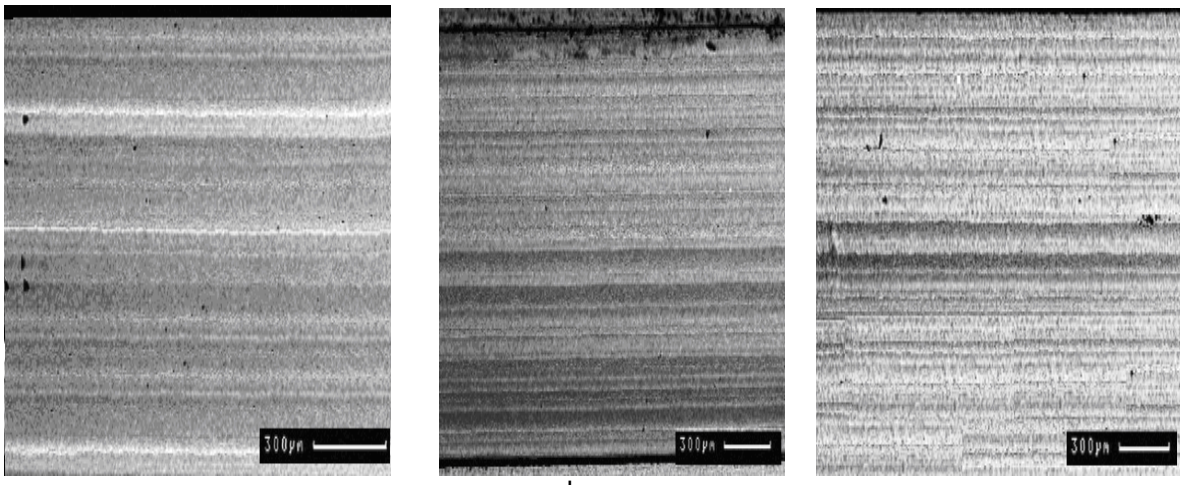

a b c

Fig. 2. *Microstructures a) Cu -5.1% Mo, b) Cu -8.4% Mo, c) Cu -12.3% Mo magnification x 200*

Table 3. *The mechanical characteristics of the condensate depending on the amount of molibden*

Composition	Mechanical characteristics					
	Before annealing			After annealing		
	R_{p02}	R_m	δ	R_{p02}	R_m	δ
	[MPa]		[%]	[MPa]		[%]
Cu-2.5-5.0Mo	210-370	300-430	10.3-7.3	200-360	295-420	17.6 – 9.5
Cu-5.1-8.0Mo	380-530	440-630	7.25-3.4	365-510	425-600	9.45-4.9
Cu-8.1-12Mo	550-750	635-785	3.25-1.8	520-695	605-730	4.85-3.9

From the charts made, the conventional yielding limit $R_{p0,2}$, resistance limit R_m, relative elongation δ were calculated.

The mechanical characteristics of Cu-Mo composites as to the content of molybdenum are shown in Table 3.

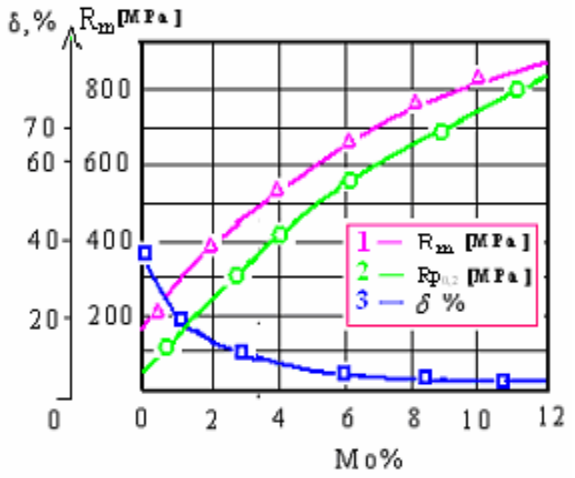

Fig. 3. *Variation of the mechanical strength R_m, yielding point and relative elongation depending on the concentration of Mo*

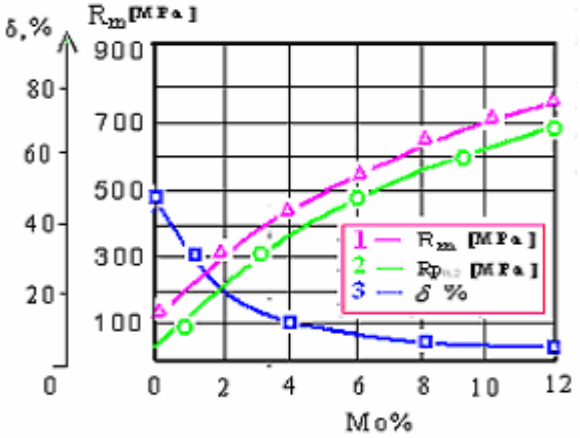

Fig. 4. *Variation of the mechanical strength R_m, yielding point and relative elongation depending on the concentration of Mo. (after vacuum annealing at 1170K)*

The results of tensile vacuum elongation checks showed that with increasing molybdenum content values R_m, $R_{p\,0,2}$ increased and δ decreased almost to „zero" values at Mo concentration ~ 14%.

The variation of the mechanical strength, yielding point and relative elongation depending on the concentration of Mo is given in Figure 3.

Similar values of the mechanical characteristics of these materials were obtained after vacuum annealing of the samples at a temperature of 1170K for three hours (Figure 4).

It is noted some decrease in strength characteristics by 8 - 10% and increased plasticity by 10 - 25% with increasing mean square deviation (3.3-5%) of the values of these parameters compared to the initial condition of the materials [4]. An important role in forming the structure and characteristics is played by the defects which were formed in the condensate during the transfer in the liquid phase as drops. For the most part these droplets grow, forming irregular spheres. These spheres, being in the previous layer, cause in the vapor flow disruption of crystallization of the next layers. The dislevel which is formed by such particles, is passed to each micro and macro-layer until the final surface of the composite (Figure 5), subject to the influence of throwing and melting condensation.

Fig. 5. *The structure of the sample surface without cutting*

Metallographic analysis of structural defects, subject to the transfer of the liquid phase allows us to conclude that there is a possibility of disturbance of the crystallization and the occurrence of such defects in the composite structure.

Electrochemical tests have shown that the corrosion resistance of the composites obtained by PVD method is higher than pure copper.

Figure 6 presents the Taefel curves for Cu-Mo composites produced by PVD method.

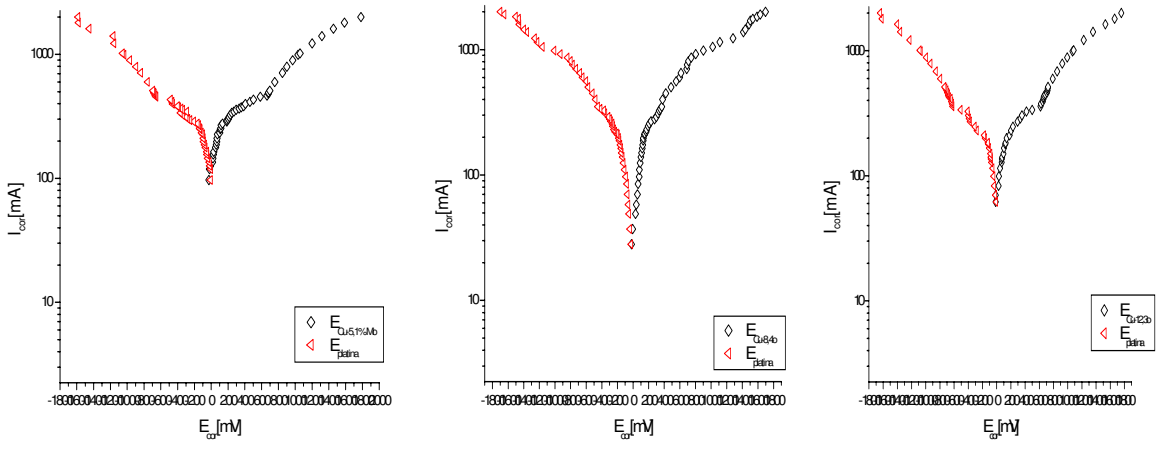

a) b) c)

Fig. 6*. Taefel curves for Cu-Mo composites produced by PVD method: a) Cu-5.1% Mo, b) Cu-8.4% Mo, c) Cu-12.3% Mo*

In Figure 6 it is observed that the current density of corrosion of the blank sample is higher than the composite samples, leading to the conclusion of increased resistance to corrosion of the composite samples, the visual appearance of the sample surfaces being clean without oxide stains [5].

Table 4. *Behaviour of Cu-Mo composites produced by PVD method, when tesed for corrosion by galvanostatic method*

Cu	**Mo**	**Current density** j_{cor}	**Corrosion rate** v_{cor}	**Penetration index p**	**Resistance group**
[%]		$[A/m^2]$	$[g/m^2 \cdot h]$	[mm/an]	
94.9	5.1	17.7	0.0056	0.0054	highly resistant
91.6	8.4	15.6	0.0049	0.0048	highly resistant
81.5	12.3	14.2	0.0042	0.0041	highly resistant

The values of current density, corrosion rate and penetration indices when tested for corrosion by the galvanostatic method are given in table 4.

Corrosion resistance of composites obtained by the two methods - PVD, electrochemical - is better than that of pure copper.

3. Conclusions

-The composites obtained by physical vapor deposition increase, forming chains and conglomerates actually very important because they increase the resistance to high temperatures.

-The structure of Cu-Mo composites is in the form of blocks. For each block it is characteristic an arbitrary striped structure. The period of stripes repetition is 150 ± 3mm.

-The results of the vacum elongation tests shown that with higher amounts of molibden the values of $R_m, R_{p\,0,2}$, increase, while δ decreases down to „zero" at a concentration of Mo ~ 12%.

-An important role in forming the structure and characteristics is played by the defects which were formed in the condensate during the transfer in the liquid phase as drops.

-Electrochemical tests have showed that the corrosion resistance of the composites obtained by PVD method is higher than pure copper.

References

[1] V.G. Grechanyuk - *Comparative assessment of anticorrosion resistence of copper base composite materials in various conditions*, Electrical contacts and electrods, Institute of Materials Science, Kiev I.N. Frantevicia NAN Ukraina, (2004), p. 38-41.

[2]. S. Constantinescu, O. Mitoşeriu - *Microstructural and layers superficial properties by the CVD method*, The Annals of "Dunarea de Jos" University of Galati, Fascicle IX. Metallurgy and Materials Science, nr.2/2004, ISSN 1453-083X, p. 51 –55.

[3]. S. Constantinescu, T. Radu - *The effect of heat treatment parameters on the structure and properties of the thick plates made from steel X60,* The Journal International Metallurgy, nr. 4/2004, p.28-32.

[4]. S. Constantinescu, L. Orac - *Material properties and methods of control,* Ed. Europlus, Galati, Romania, ISBN: 973 – 30 – 1709 – 4, (2007).

[5]. V.G. Grechanyuk, V.A. Denisenco, L. Orac - *Structurre and corrosive firmness of composition materials on basis of copper and molybdenum electron beam technology metod*, The Annals of 'Dunărea de Jos' University of Galaţi, Fascicle IX Metallurgy and Material Science,Vol. 1, (2007).

THE ANNALS OF "DUNAREA DE JOS" UNIVERSITY OF GALATI.
FASCICLE IX. METALLURGY AND MATERIALS SCIENCE
N^0. 1 – 2013, ISSN 1453 – 083X

ANODIZATION TREATMENT OF Ti6Al4V IN ELECTROLYTES CONTAINING HF

Emanuela-Daniela STOICA[1,2], Fedor S. FEDOROV[2], Maria NICOLAE[1], Margitta UHLEMANN[2], Annett GEBERT[2]
[1]Materials Science and Engineering Faculty, Politehnica University of Bucharest, Romania,
[2]IFW Dresden, Institute of Complex Materials
email: stoicaemanueladaniela@yahoo.com

ABSTRACT

The Ti6Al4V alloy is already well-known likely material for implant applications. As well as pure titanium, Ti6Al4V alloy possess the ability to form spontaneously a thin passive oxide layer on the surface. This oxide layer provides an enhanced biocompatibility and may be optimum for the osseointegration if it is applied a tailoring of the surface topology and chemistry. The present paper addresses a study of Ti6Al4V surface modification by anodization as function of HF concentration in electrolyte and time, with the purpose to achieve an ordered porous titanium oxide layer. Prior to the anodization treatment the as-prepared surfaces were microstructurally characterized by SEM, EDX and XRD. The oxidized surfaces were subjected to SEM measurement in order to observe the achieved morphology.

KEYWORDS: anodization, nanotube, nanopore, oxide, HF concentration

1. Introduction

Titanium and its alloys are the most used metallic materials for biomedical applications, due to their mechanical, biological and chemical properties. The α+β titanium alloys, such as Ti6Al4V and Ti6Al7Nb, are well-known metallic materials used for implant applications. Ti6Al4V possesses a good corrosion resistance and good physical properties even if there are some limitations regarding the mechanical properties (high Young's modulus value) [1].

Its biocompatibility is related to spontaneous formation of TiO_2 thin adherent layer. This layer is specific to titanium and its alloys and beside TiO_2 contains also the alloying element oxides (Al and V are valve metals [2]) such as Al_2O_3 and V_2O_5.

In recent years the surface modification techniques on "classical metallic biomaterials" showed a great interest for many researchers [3-4]. The anodization treatment is a new electrochemical method for surface modification [5]. Most of the anodization studies on Ti6Al4V were performed in electrolytes containing different amounts of NH_4F [6-8], NaF [7] or HF [8].

The present study is focused firstly on obtaining nanotubular oxide layers on Ti6Al4V substrate using the anodization technique in HF mixtures with H_3PO_4 and secondly, tno characterizing the achieved layers as function of electrolyte composition and anodization time.

2. Experimental results

2.1. Alloys characterization

The cast alloy Ti6Al4V disks (2 mm thickness and 11mm diameter) were microstructurally investigated before the anodization process. The samples were metallographically prepared and the polished surfaces were etched in a solution of 2% HF for a couple of seconds and subsequently analyzed using scanning electron microscopy (SEM) and energy dispersive X-ray analysis (EDX). Furthermore the samples were subjected to the x-ray diffraction analysis (XRD).

The chemical composition of cast alloy samples was determined using inductively coupled plasma optical emission spectrometry analysis (ICP-OES). A very good agreement with the nominal composition was revealed.

2.2. Anodization treatment

Prior to the anodization treatment, the Ti6Al4V disks were ground with emery papers up to 2500,

polished with 6µm diamond paste and cleaned by sonication in ethanol and distillated water. The electrochemical cell consisted of a two-electrode configuration with platinum foil as a counter electrode and Ti6Al4V sample as working electrode with a 0.28cm^2 surface area exposed to the electrolyte. The anodization experiments were carried out using a high-voltage potentiostat 2400 Source Meter Keithley connected to a digital multimeter (Keithley 2700 Multimeter /Data Acquisition System) interfaced to a computer. The electrolyte used for anodization treatment was a solution of 1 M H_3PO_4 with addition of 0.1 wt. % HF (E1) and 0.2 wt.%HF (E2) at room temperature. The anodization treatment comprised a potential ramp from open circuit potential (OCP) to 20V with a sweep rate of 20mV/s [6]. The potential of 20V was held constant for 2400s, 3600s and 7200s in each electrolyte. After the anodization treatment all samples were rinsed in distilled water and dried.

The structural and morphological characterization of the oxide layers was carried out with the Leo 1530 Scanning Electron Microscope (SEM). Moreover, the SEM analysis performed on nanotubular/nanoporous oxide layers allows us to measure the D_{inner} (inner diameter), D_{tube} (intertube distance), t_{wall} (wall thickness). The measurement error limit was around ± 5nm for D_{inner}, D_{tube} and around ±2 nm for t_{wall}.

3. Results and discussions

3.1. Alloys characterization prior anodization

The microstructure characteristics are important aspects for further electrochemical response of an alloy.

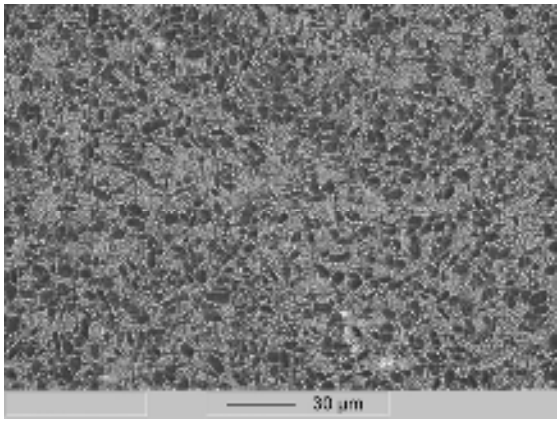

***Fig. 1**. SEM images (BSE mode) of a Ti6Al4V sample cross section*

Hence, a detailed analysis of the Ti6Al4V substrates was conducted by means of SEM and XRD.

Fig. 1 shows a SEM image in the composition of an HF etched cross-sectional area of a Ti6Al4V disk sample. The Ti6Al4V microstructure is clearly revealed with both phases α and β.

The EDX measurement (Fig. 2) shows that α-phase corresponds to the dark contrast areas and the β-phase to the bright areas. The α-phase contains the Al element while the β-phase comprises the V element. The phase distribution is important for subsequent studies since, in electrolytes containing HF, the electrochemical behaviors of the α and β-phases may be different [6], [9].

The chemical composition of the investigated Ti6Al4V samples (as determined by ICP-OES) was 89.19% Ti, 6.27% Al and 4.07% V. Thus, it is in very good agreement with the nominal composition.

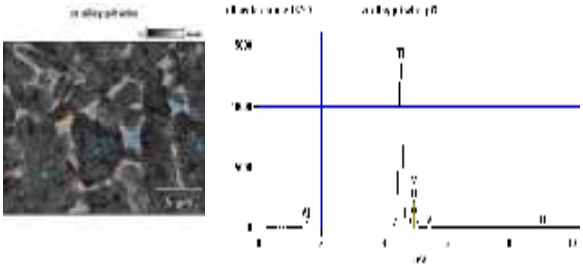

***Fig. 2**. EDX images of a Ti6Al4V sample*

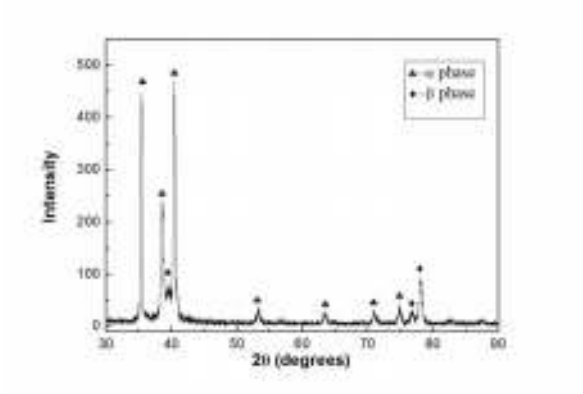

***Fig. 3**. XRD pattern of Ti6Al4V sample*

The alloys XRD patterns (Fig.3) have shown that the main intensity diffraction peaks correspond to the α-phase, since this phase is the major one. The main β-phase reflections were recorded around 2θ=76.8°and 2θ=77.8°.

3.2. Characterization of the anodized alloys surface

Scanning electron microscopy was employed for the structural and morphological characterization of the Ti6Al4V sample surfaces after the anodization process.

The anodization treatment in both electrolytes for 2400s and 7200s has shown only etched surfaces.

Thus, it can be assumed that the HF concentration of electrolytes is less important since for more and less than 3600 s the result was the same. This phenomenon is attributed to the last stages in the mechanism of TiO_2 growth [12-14]. The HR-SEM image of the alloy surface anodized in E1, for 3600s (Fig.4) shows that the alloy phases are differently affected by the treatment in fluoride-containing solution. Under these conditions on α-phase region a nanotubular oxide structure (Fig. 5) had formed, while on the β-phase region only a porous oxide structure was observed. In literature, it was found similar behavior of the α and β regions on Ti6Al4V anodized surface even the electrolytes were NH_4F [6], or HF [8] solutions.

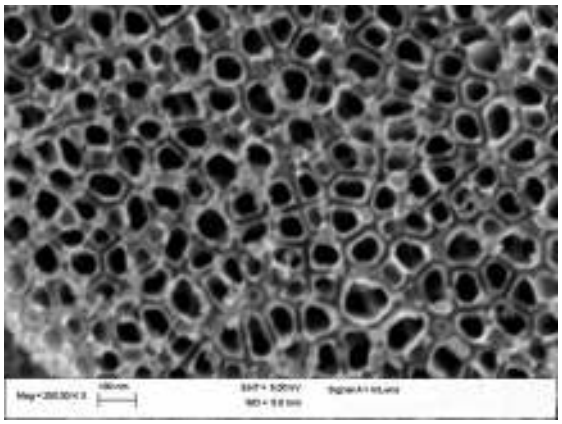

***Fig. 4**. Ti6Al4V HR-SEM image of α surface anodized in E1, for 3600s*

The D_{inner} of the tubes growth on α-region was around 70nm while the D_{tube} and t_{wall} were around 90nm and 20nm, respectively. Moreover, the nanopores D_{inner} growth on β-region could be measured and the value was around 60nm.

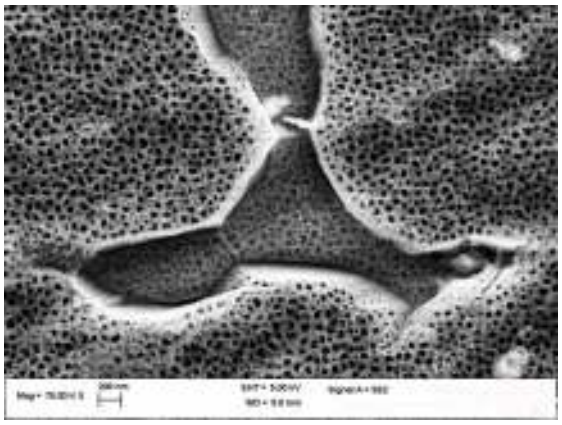

***Fig. 5**. Ti6Al4V HR-SEM image of α+β surface anodized in E1, for 3600s*

The nanopores D_{inner} is smaller than the nanotubes one, this aspect may be typical for Ti6Al4V anodized surface [6]. It should be mentioned that this method has certain limitations regarding measurement accuracy, and, for this reason an error limit of 5nm was taken.

For the second electrolyte E2, with higher HF concentration, for 3600s polarization a porous structure was achieved for both α and β regions (Fig. 6).

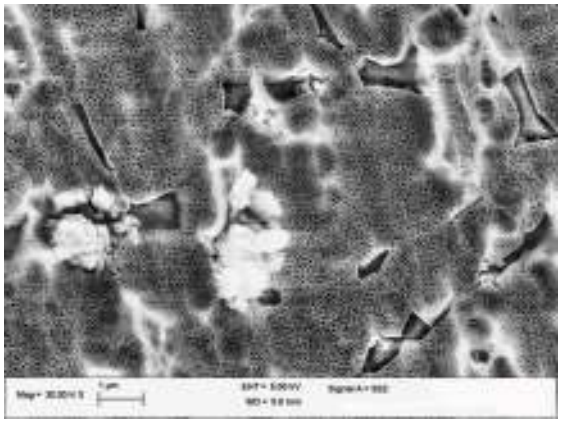

***Fig. 6.** Ti6Al4V SEM image of α+β surface anodized in E2, for 3600s*

The α-regions have shown a much ordered nanoporous structure (Fig.7). This aspect was also found in literature [6] for α-phase region. The nanopores D_{inner} was found around 60nm (±5nm).

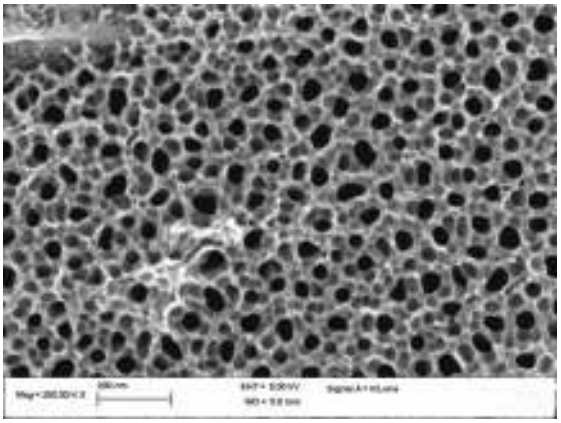

***Fig. 7.** Ti6Al4V HR-SEM image of α+β surface anodized in E2, for 3600s*

The behavior of the phases of the α+β titanium alloys is different depending of the β stabilizer element.

Thus, even if Ti6Al7Nb is also an α+β titanium alloys, in literature it was found that anodization in HF electrolyte contain led to upper ordered nanoporous layer growth on β-region [9].

4. Conclusions

The investigations regarding the anodization behavior of the α+β Ti6Al4V alloy were conducted in H_3PO_4/ 0.1 wt% HF (E1) and 0.2 wt% HF (E2) electrolytes applying a potential of 20V for up to 7200s potential and then sweeping the potential with 20mV/s. Nanotubular oxide structures were obtained and it was demonstrated that the optimum polarization time is 3600s for an 0.1wt% HF concentration (E1). The D_{inner} of the oxide nanotubes were about 70nm. while the β-phase regions showed only a random disordered nanoporous structure. Furthermore, at 2400s and 7200s anodization time no nanotubular or nanoporous layers were observed.

It can be concluded that employing the presented anodization parameters a nanotubular oxide structure was observed already after 3600s in electrolyte with less HF concentration.

Acknowledgment

The work has been funded by the Sectoral Operational Programme Human Resources Development 2007-2013 of the Romanian Ministry of Labour, Family and Social Protection through the Financial Agreement POSDRU/88/1.5/S/61178.

References

[1]. D. M. Brunette, P. Tengvall, M. Textor, P. Thomsen - *Titanium in Medicine: Material Science, Surface Science, Engineering, Biological Responses and Medical Applications*, 1st edition Springer; Berlin, (2001), pp.14-19.

[2]. **M.M. Lohrengel** - *Thin anodic oxide layers on aluminium and other valve metals: high field regime*, Materials Science and Engineering, Vol. R11, pp.243-294, (1993).

[3]. X. Liu, P. Chu, C. Ding - *Surface modification of titanium, titanium alloys, and related materials for biomedical applications,* Materials Science and Engineering: Reports: Vol. R47, pp.49-121, (2004).

[4]. K. Subramani - *Titanium Surface Modification Techniques for Implant Fabrication – From Microscale to the Nanoscale*, Journal of Biomimetics, Biomaterials, and Tissue Engineering. Vol. 5, pp.39-56, (2010).

[5]. V. Zwilling, E. Darquel Ceretti - *Structure and physicochemistry of anodic oxide films on titanium and TA6V alloy*, Surface and Interface Analysis, Vol.27, pp. 629-637, (1999).

[6]. J.M. Macak, H. Tsuchiya, L. Taveira, A. Ghicov, P. Schmuki - *Self-organized nanotubular oxide layers on Ti-6Al-7Nb and Ti-6Al-4V formed by anodization in NH_4F solutions*, Journal of Biomedical Materials Research. Part A, Vol. 75, pp. 928-33, (2005).

[7]. E. Matykina, a. Conde, J. de Damborenea, D.M.Y. Marero, M. a. Arenas - *Growth of TiO2-based nanotubes on Ti–6Al–4V alloy*, Electrochimica Acta, Vol.56, pp.9209-9218, 2011.

[8]. H. Lukáčová, B. Plešingerová, M. Vojtko, G. Bán - *Electrochemical treatment of Ti6Al4V (1. Part)* - Acta Metallurgica Slovaca, Vol.16, pp. 186-193, (2010).

[9]. H.-C. Choe - *Nanotubular surface and morphology of Ti-binary and Ti-ternary alloys for biocompatibility*, Thin Solid Films, Vol.519, pp.4652-4657, (2011).

[10]. E. Matykina, J.M. Hernandez-López, A. Conde, C. Domingo, J.J. de Damborenea, M. A. Arenas - *Morphologies of nanostructured TiO2 doped with F on Ti–6Al–4V alloy*, Electrochimica Acta, Vol.56, pp.2221-2229, (2011).

[11]. A. Kaczmarek, T. Klekiel, E. Krasicka-Cydzik - *Fluoride concentration effect on the anodic growth of self-aligned oxide nanotube array on Ti6Al7Nb alloy*, Surface and Interface Analysis, Vol.42, pp.510-514, (2010).

[12]. G. Crawford, N. Chawla - *Porous hierarchical TiO_2 nanostructures: Processing and microstructure relationships*, Acta Materialia, Vol.57, pp. 854-867, (2009).

[13]. S.E. Pust, D. Scharnweber, C. Nunes Kirchner, G. Wittstock - *Heterogeneous Distribution of Reactivity on Metallic Biomaterials: Scanning Probe Microscopy Studies of the Biphasic Ti Alloy Ti6Al4V*, Advanced Materials, Vol.19, pp.878-882, (2007).

[14]. P. Roy, S. Berger, P. Schmuki - *TiO_2 nanotubes: synthesis and applications*, Angewandte Chemie (International Ed. in English), Vol. 50, pp.2904-39, (2011).

THE ANNALS OF "DUNAREA DE JOS" UNIVERSITY OF GALATI.
FASCICLE IX. METALLURGY AND MATERIALS SCIENCE
N^0. 1 – 2013, ISSN 1453 – 083X

THE PRE-BIBLICAL METALLURGICAL ART ON THE BIBLICAL TERRITORY

Strul MOISA[1], Rodica WENKERT[2]
[1]Ben-Gurion University of the Negev, Beer-Sheva, Israel,
[2]Soroka University Medical Center, Beer-Sheva, Israel,
emails: smoisa@bgu.ac.il; rodicawe@clalit.org.il

ABSTRACT

The Old Testament describes in detail the metallurgical achievements, both in the period before the conquest and colonization of the promised land (mostly related to the manufacturing of the Tabernacle, in this sense, the gold chandelier with seven branches, also known as the menorah, is an exceptional example), and the period after the conquest and colonization of the promised land (the sea of bronze pillars Boaz and Jachin, the 10 golden candlesticks with seven arms, etc., famous artifacts of Solomon's Temple facilities, are good examples). Question: at that time, did the Jews have the technical and technological knowledge necessary to create things in order to reach the great achievements of the metallurgical processes described in the Old Testament? This article tries to answer this question.

KEYWORDS: Canaan, pre-biblical metallurgy, casting, lost wax casting, Nahal Mishmar`s Treasure

1. Introduction

Even before it was colonized by the Jews, The Promised Land – known as Canaan – was inhabited by other peoples (Canaanites, Amorites, Philistines, etc.). At that time, those peoples already had a certain degree of culture and civilization, including a high level of metallurgical creativity and development.

As a result of the contact with these peoples, the Israelites were able to absorb technology, in addition to technological knowledge that they already had from the previous period which also includes the Egyptian slavery period; exception is the iron manufacturing[1]. For requirements of the subject matter, the pre-biblical time is the chalcolithic period (or Copper Age, 4500-3300 BC). For the two reference coordinates – time (the pre-biblical period)/geographical area/(Canaan) - based on archaeological material, two things with connection to the metallurgical aspects will be presented: (1) casting as a widely used pre-biblical metallurgical process, and (2) the treasure from Nahal Mishmar.

2. Casting, a widely used pre-biblical metallurgical process

Before it was colonized by the Israelites, the land of Canaan was inhabited by other peoples.

These people had reached a high level of metallurgical development and creativity. For example, in Canaanite temples were discovered many statues cast in bronze, mostly of small size.

An example is the figurine in Figure 1, dated sec. 17 BC: in figure 1a[2], we can see the original casting mold, made of stone; Figure 1b is the statue of a worship idol, cast in modern conditions in the original stone mold. In pre-biblical times, casting was one of the most important technological processes, used for the fabrication of copper objects.

The general scheme of development of processes for manufacturing objects by casting is shown in Figure 2. The raw material used was copper ore which may contain impurities of arsenic[3].

[1] A good example is the conflict with the Philistines, described in Kings1.

[2] The mold was discovered following excavations near Naharya (northern Israel), in a place where a Canaanite temple existed.

[3] The Nahal Mishmar`s treasure – most copper-arsenic bronze artifacts constitutes an eloquent example.

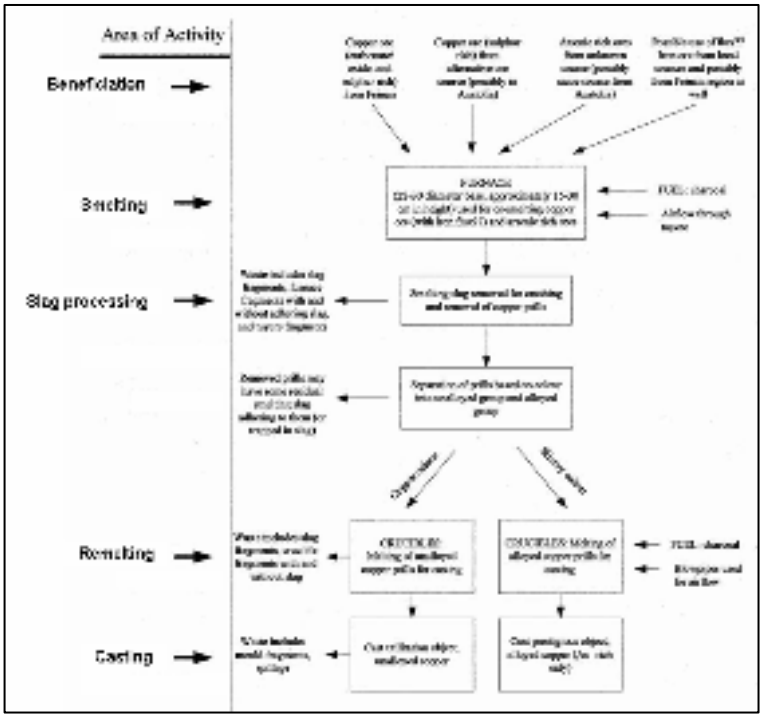

Fig. 1. *Canaanite religious idol* ***Fig. 2.*** *General scheme for manufactured artifacts by casting process*

As reference, the mineral exists in appreciable quantities as carbonate- malachite, $Cu_2CO_3(OH)_2$. The process used was pyro-metallurgical: thermal dissociation in a coal bed at temperatures of 700^0C.[4]

The first two activities in the scheme shown in Figure 1 are *de facto* extractive metallurgy.

The result, after melting, is a mass of clay which included copper grains[5]. The casting was done in disposable forms (sand, wax models, etc.) or forms with multiple uses (stone), etc., to a wide range of uses: cult and ornament objects, work tools (knives, chisels, axes, etc.), etc.

Lost Wax Casting process is one of the oldest techniques of casting metal - about 5000 years [2, 3, and 4]. Initially, the process was used for idols, ornaments, jewelry, etc.

But it seems that the Middle East has the first use of this process. In the Middle East, the Lost Wax Casting process has been used increasingly wider in Mesopotamia and Sumer (for statues made of copper and later bronze) since 3500 years BC; something later, the method is found in Anatolia.

The ancients quickly understood the advantages of the process: obtaining artifacts with complex configurations, versatility, repeatability, minimal finishing operations, the technique can be used for a large variety of metals and alloys (copper, gold, silver, bronze, etc.), etc.[6]

The majority of artifacts belonging to the Treasury from Nahal Mishmar were made by Lost Wax Casting process.

Made no later than 3700 years BC, this means that the first use of this process in the region was for the artifacts discovered in Nahal Mishmar.

3. The Treasure from Nahal Mishmar

We are in 1961. The team of archaeologists led by Pesach Bar Master was engaged in the search for possible additional scrolls in the Judean Desert, near the Dead Sea, where manuscripts from famous Oumran were discovered.

The geographical point at coordinates 31°38'0.93"N 35°36'4.34"E (located between Masada

[4] The melting process is carried out in two phases: (*)carbonate dissociation: $Cu_2CO_3(OH)_2 \rightarrow 2CuO + CO_2 \uparrow + H_2O \uparrow$ and (**)metal oxide dissociation: $2CuO \rightarrow 2Cu + O2 \uparrow$

[5] The slug will be eliminated later - totally or partially, and the copper granules obtained, following the melting procedure.

[6] In antiquity, the technique was known in India, China, Thailand, and was used by the Greeks, the Romans, the Aztecs and the Mayans, but also in Mexico and by the African population near the Benin bay. Many pieces found in Pharaoh Tutankhamen's tomb (1333-1324 BC) were also made through this process.

and Ein Gedi) is a cave accessible with difficulty, today called the Nahal Mishmar's Treasure.

In this cave were discovered 442 objects, wrapped in a mattress of straw, a real treasure (Fig.3).

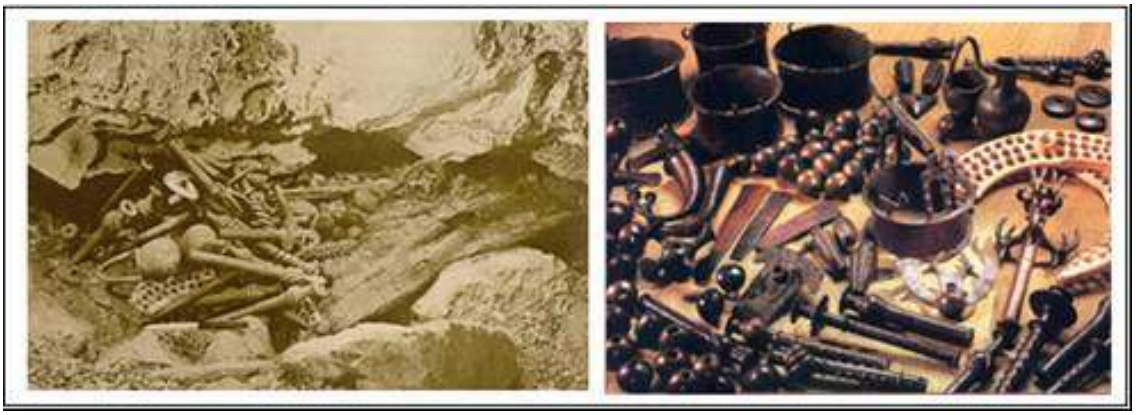

Fig. 3. *Treasure of Nahal Mishmar: left: at finding time; right: after preservation*

This treasure is the largest group of ancient copper objects, found so far in the Middle East. Among these objects, 429 were made of copper-arsenic alloy (4-12% arsenic). This arsenic-bronze is the first alloy in the history of civilization [6]. 10 crowns, 256 mace heads, 118 scepters, 16 work tools chisel shaped were inventoried. Also, the thesaurus contains a set of objects of other materials: six of hematite, five of hippopotamus ivory and one of elephant ivory. Their esthetics is exceptional and they are so sophisticated that in many cases modern artisans are surprised. The shape and decoration of each artifact is unusual. Many are so strange that they it defy accurate definition. An additional aspect: each artifact is in itself unique, given that there are no two identical objects.

Fig. 4. *Examples of artifacts from the Nahal Mishmar's treasure*

Some additional examples are shown in Figure 4: a crown (center), a two-headed (left), a scepter with three-deer heads (right)[7].

The fact that 338 of objects represent deities,

• copper was associated with other minerals rich in arsenic [koutekit (Cu_5As_2) domeikite (Cu_3As)] and sulfur [Covelit (CuS)].

• Carbon-14 dating of the reed mat in which

[7] An explanation accepted by most researchers is that the objects found were objects of worship and belonged to Ein Gedi temple discovered. This temple is known in literature as the Chalcolithic Temple and the distance between Nahal Mishmar and Ein Gedi is about 12 km. Researchers believe that at the time of reference, for reasons of insecurity, the objects were transferred temporarily from Ein Gedi temple in a temporary place of refuge, the cave from Nahalal Mishmar. The reason for insecurity is not well defined, but depositors should have to return the treasure back to the Ein Gedi. The fact is that they did not returned it and the treasury had to wait for the team of archaeologists led by Pesach.

deity heads, scepters, supports the hypothesis that the antique warehouse complex was used for ceremonial and religious needs. The metal particles were studied for geo-chemistry-mineralogy. For this purpose, a variety of methods of investigation were used: SEM equipped with EDS (morphology and chemistry), ICP-AFS (chemical analysis), XRD (mineralogical composition).

A few results:

• chemical analysis of most minerals: 40.5% Cu, 10% As, 4% CaO, 2% $P_2 0_5$, 6.7% $Al_2 0_3$, 25.3% $Si0_2$, 1.5% $Fe_2 0_3$, 1.8% $Na_2 0$, 1 2% $K_2 O$, 1.1% $Ti0_2$, 0.3% SO_3, 0.4% MgO, 2700 ppm Zn, 1600 ppm Mn, 400 ppm Ba, 360 ppm Pb, 100 ppm Ag, 55 ppm V, 25 ppm Sb.

• EDS analysis results of mineral elements: 71% Cu and 29% As.

the objects were wrapped suggests that it dates to at least 3700 BC.

Artefacts are particularly beautiful, with complex geometry, which explains the skill, professionalism and experience of the Canaan artisans[8]. Saas notes [7]: *The treasures from the Judean Desert represent the acme of the metallurgical skill of Chalcolithic artisans, working from 4500 to 3150 B.C.E., when copper and copper-arsenic alloys were first widely used in the Near East ...*

In parallel, it should be emphasized that the combination of primitive art, religion and metallurgy is striking in this case. Many of the artefacts were made by Lost Wax Casting process. Also, additional procedures were used: casting in open forms, casting in closed forms, etc. Several types of artefacts and their sections are shown in Figure 5.

Fig. 5. *Some examples of artifacts types from the Nahal Mishmar`s treasure*

As mentioned before, the material from which the Nahal Mishmar artefacts were made is arsenic bronze, the first alloy in the history of civilization, developed around 4000 BC.

Arsenic is a rare element in the earth's crust: its abundance is at about $5x10^{-4}$ % estimated. However, it often accompanies ores of gold, silver, lead and copper, thus becoming a by-product. Perhaps at first, this bronze was made by accident, likely caused by the similarity of colors both metalliferous ores and green-light the flame when heating in the furnace. One thing is sure: both "metallurgical" ancient and user - that could even be one and the same person - quickly realized that the pieces made of arsenic bronze have superior both technological properties (casting and forging capability) and use properties (toughness, hardness) compared to the similar parts made of copper.

Regarding the starting question: did the Jews of that time hold technical and technological knowledge necessary to create things of the great achievements of metallurgical order described in the Old Testament?

An affirmative answer can be given: the Jews came into contact with people who had a high level of metallurgical development and creativity, which allowed the technological knowledge assimilation.

[8] Today, the artifacts are exhibited at the Israel Museum in Jerusalem, Department of Antiquities.

4. Conclusions

• In pre-biblical times, casting was a widely used metallurgical process.

• Pre-biblical peoples held a high level of development and metallurgical creativity.

• In addition to technological knowledge already held in previous periods and by contact with these people, the Israelites could absorb metallurgical technology.

• Metallurgical achievements described in the Old Testament had the necessary technological knowledge support in order to be materialized.

References

[1]. S. Moisa - *Biblia si Metalurgia* (in Romanian), Editura Galaxia Gutenberg, (2011).

[2]. http://www.goldbulletin.org/assets/file/goldbulletin/downloads/Hunt_2_13.pdf L. B. Hunt, *The long history of lost wax casting*.

[3]. Moorey, P. R. S. - *Early Metallurgy in Mesopotamia*, in The Beginning of the Use of Metals and Alloys. Paper from the Second International Conference on the Beginning of the Use of Metals and Alloys, Zhengzhou, China, 21-26 October 1986., ed. R. Maddin Cambridge, Massachusetts & London, England: The MIT Press. (1988)

[4]. Muhly, J. D. - *The Beginnings of Metallurgy in the Old World*, in *The Beginning of the Use of Metals and Alloys*. Paper from the Second International Conference on the Beginning of the Use of Metals and Alloys, Zhengzhou, China, 21-26 October 1986., ed. R. Maddin Cambridge, Massachusetts & London, England: The MIT Press, (1988).

[5]. Moorey, P. R. S. - *The Chalcolithic Hoard from Nahal Mishmar, Israel*, in *World Archaeology* vol. 20 (1988), pg. 171–189.

[6]. S. llani, A. Rosenfeld - *Ore source of arsenic copper tools from Israel during Chalcolithic and Early Bronze ages,* in *Terra Nova,* vol. 6 (1994), pag. 177-179.

[7]. S. L. Saas - *The Substance of Civilization*, Arcade Publishing, New York, (1998), pag. 59.

THE ANNALS OF "DUNAREA DE JOS" UNIVERSITY OF GALATI.
FASCICLE IX. METALLURGY AND MATERIALS SCIENCE
N^0. 1 – 2013, ISSN 1453 – 083X

IMPROVEMENT OF PROPERTIES OF HEAVY PLATES BY SECONDARY STEELMAKING TECHNOLOGIES AND ROLLING CONDITIONS

Viorel MUNTEANU, Marius BODOR
"Dunarea de Jos" University of Galati
email: munteanu_viorel48@yahoo.com

ABSTRACT

In order to obtain the mechanical and technological characteristics required for controlled rolled plates it is necessary to realize a very low content of sulphur by desulphurized mixtures using CaO-Al_2O_3-CaF_2 and injection of powdered SiCa or core wire SiCa. This paper presents the influence of rolling conditions on mechanical properties, the influence of the rolling schedule and the temperature range of the end rolling of the microstructure.

KEYWORDS: heavy plates, secondary metallurgy, rolling schedule, impact strength, fractures strength

1. Introduction

As a result of the progress made in the industrial manufacture of micro-alloyed steels, their application area has been extended to fields where requirements include high strength and toughness characteristics at low temperatures, on the one hand, and an adequate weldability in harsh ground conditions, on the other **[3, 4, 5]**.

The fulfillment of the mechanical and technological characteristics required for controlled rolled plates designed for pipes with a large diameter of 1420 mm for transporting oil and natural gas from the arctic regions calls for a high technological level of the whole manufacture flow: steelmaking, treatment in the ladle, casting, heating and rolling.

2. Industrial experiments

The steel was produced in the 180t BOF furnace.

The chemical composition of the experimental heats is shown in Table 1.

Table 1. *Chemical composition of experimental heats*

No.	Elements, %								
	C	Mn	Si	P	S	Al	Nb	V	C_E
1.	0.08	1.65	0.27	0.010	0.008	0.025	0.040	0.06	0.3670
2.	0.08	1.74	0.27	0.010	0.012	0.025	0.042	0.07	0.3040
3.	0.08	1.43	0.25	0.018	0.008	0.038	0.033	0.07	0.3323
4.	0.07	1.65	0.32	0.020	0.010	0.050	0.043	0.05	0.3550
5.	0.08	1.63	0.51	0.022	0.0045	0.028	0.042	0.07	0.3657
6.	0.07	1.56	0.38	0.023	0.0035	0.010	0.031	0.05	0.3400
7.	0.06	1.57	0.43	0.018	0.0035	0.040	0.020	0.06	0.3337
8.	0.08	1.55	0.42	0.020	0.0035	0.090	0.040	0.06	0.3503
9.	0.07	1.60	0.50	0.020	0.0035	0.068	0.033	0.05	0.3467
10.	0.06	1.50	0.42	0.017	0.0035	0.045	0.024	0.04	0.3180
11.	0.06	1.58	0.38	0.018	0.0038	0.030	0.067	0.05	0.3333
12.	0.07	1.55	0.35	0.018	0.0038	0.025	0.074	0.05	0.3383
13.	0.07	1.48	0.37	0.013	0.0025	0.030	0.046	0.05	0.3267
14.	0.11	1.48	0.43	0.022	0.005	0.062	0.044	0.07	0.3707
15.	0.10	1.48	0.44	0.016	0.004	0.09	0.04	0.06	0.3587
16.	0.09	1.53	0.40	0.020	0.004	0.04	0.04	0.05	0.3550

In order to achieve the lowest sulphur content possible, the steelmaking practice was based on the principle of sulphur removal in each possible stage, as follows:

a) sulphur removal from pig-iron in the ladle with soda, reaching sulphur contents of 0.020% maximum;

b) a high degree of descaling of the pig-iron surface in the transfer ladle;

c) use of scrap of known origin with a low sulphur content;

d) use of lime with a minimum content of 90% CaO and a high reactivity;

e) the practice of elaborating a high alkalinity scale, the achievement of a maximum distribution scale/scale ratio and high degree of retention in the furnace;

f) sulphur removal in the ladle using de-sulphurized mixtures of $CaO-Al_2O_3-CaF_2$ by using lumps of SiCa in spouts and continuous argon bubbling through a porous plug (heats 5-16);

g) injection of powdered SiCa, about 1.5kg/t (heat 13), and use of the continuous pipe with SiCa, about 1.2kg/t (heat 12).

The steel was continuously cast with spout protection in refractory tubes from the ladle to the tundish, obtaining slabs of 250x1500x(2800-4200) mm. The refractory lining of the ladle and the tundish was basic, so as to get a high degree of exogene inclusions.

The slabs were heated before rolling in the gravity – discharge furnace; the trimming temperature being about 1150^{o}C, with temperatures of about 1220^{o}C being reached.

The slabs were rolled into plates, to establish:

- the rolling pattern, with two (pattern No. 1), and three (pattern No. 2) strain times;

- the condition of the temperatures at the end of rolling and of the associated degrees of reduction that would assure the tensile characteristics specified for X 70 grade steel plates.

The patterns and the temperatures at the end of rolling, experimentally used, are shown in Fig. 1. The final thickness ranged between 15.7 and 23.2mm and the plate width between 2400mm and 4600mm.

After rolling the plates, the samples were taken to test for the following:

-microstructural analysis;

-tension with the determination of R_m, $R_{po,2}$ A5%;

-Charpy V notch impact strength on transverse specimens tested at -20^{o}C (KCV_T -20^{o}C);

-impact strength on U-notched test specimens taken transversally and tested at -60^{o}C (KCU_{3T} -60^{o}C).

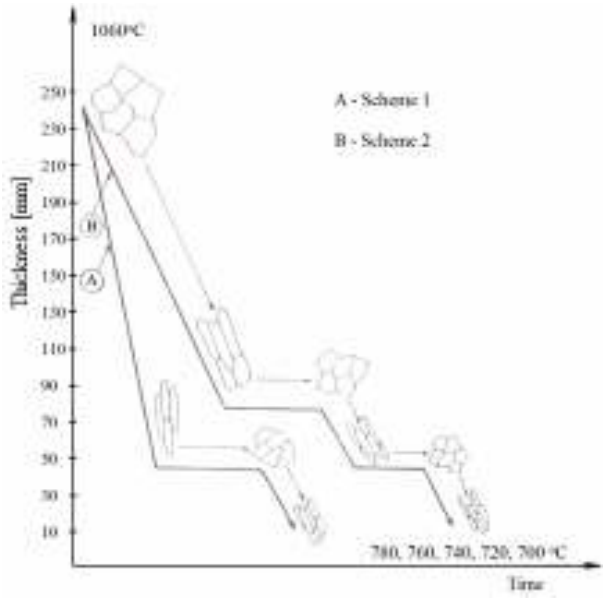

Fig. 1. *Rolling scheme applied within the industrial scale experiments*

The results obtained were processed and shown graphically indicating the influence of different technological factors on the degree of tensile characteristics.

3. Influence of sulphur content

Literature data **[1, 2, 4]** show the deleterious influence of sulphur on the mechanical properties of the steel, particularly on the toughness; for this reason the quantitative settling of this effect was kept under observation during working. The experimental values of the toughness obtained for the 1-16 heats in optimum rolled conditions, depending on the sulphur content, are mentioned in Fig. 2 (KCV_T -20^{o}C) and Fig. 3 (KCU_3 -60^{o}C).

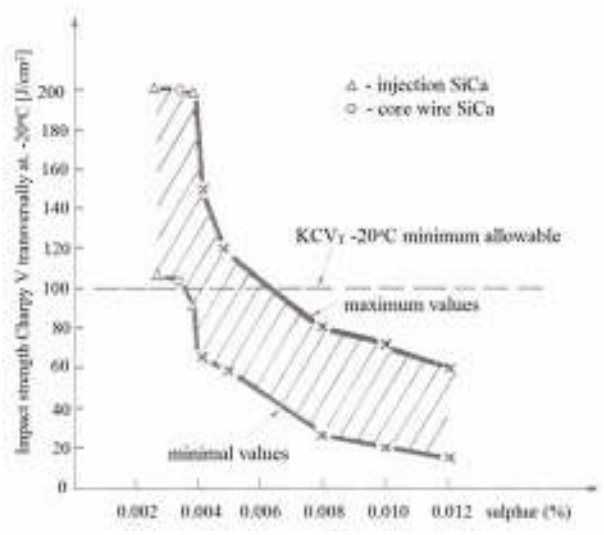

Fig. 2. *Influence of sulphur content on impact strength KCV_T -20°C*

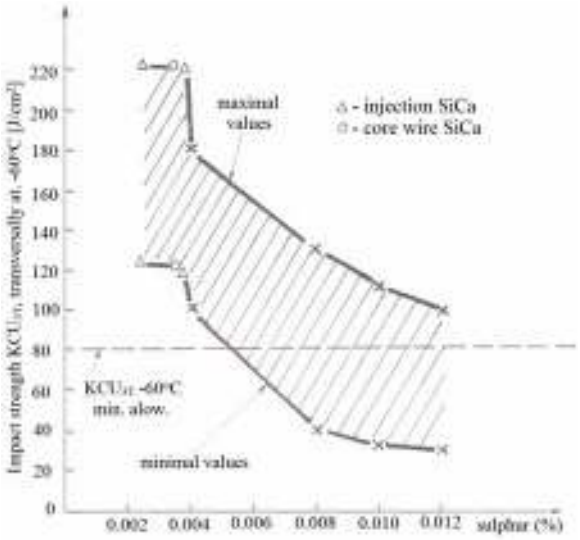

Fig. 3. *Influence of sulphur content on impact strength KCU_{3T} at. -60°C*

The data analyses presented in Figs. 5 and 6 confirm the following:

- stress decreasing of the toughness values KCV_T -20°C and KCU_{3T} -60°C due to increased sulphur content, particularly over 0.004%;
- stress sensitivity of the toughness values determined on the V notch test pieces, in ratio to the increase of sulphur;
- necessity of achieving a sulphur content under 0.004%.

Evidently, to meet these conditions some supplementary technological measurements must be taken for steel melting and casting.

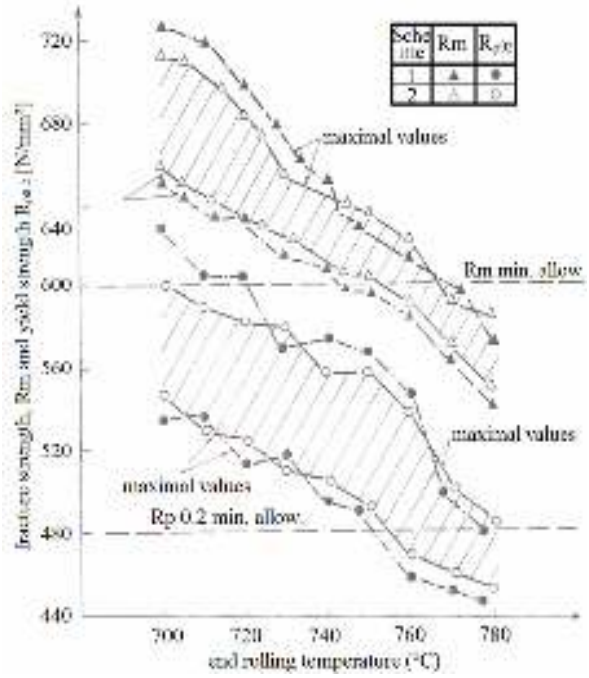

Fig. 4. *Influence of rolling scheme and end rolling temperature on fractures strength and yield strength*

4. Influence of rolling conditions on mechanical properties

Rolling methods and technological parameters used:

- heating temperature for plastic deformation;
- plastic deformation temperature;
- practicable reducing degree;
- temperature range of ultimate plastic deformation;
- deformation degree associated with the final temperature of the deformation determines the kinetic process of the:
  - ● dissolving and precipitation of the micro-alloying element combination, V and Nb with those of the interstice, C and N;
  - ● phase transformation γ-α at cooling after deformation resulting in the required microstructure and mechanical characteristics.

For these reasons, the aim of the experiments was to determine the influence of the rolling condition on the structural and mechanical properties and hence, the adoption of the optimum rolling technology.

4.1. Influence of the Rolling Schedule and Temperature Range of the End Rolling on the Microstructure

Metallographic test pieces were taken from the rolled plates in accordance with the scheme of Fig. 1 with a range of temperature between 700-780^{o}C for the rolling. The test pieces were prepared in accordance with classic methods and X 200 analyzed, in longitudinal section to the rolling direction.

The analyses of the microstructure show the more advanced degree of fineness for the same temperature during end rolling when schedule N 2 with three times of deformation was used.

Concerning rolling temperatures, it was noted that the grain becomes finer as the temperature is lowered during rolling to between 780 and 740^{o}C.

The decrease of temperature during and rolling to under 740^{o}C, particularly under 700^{o}C, leads to the partial refining of the grain **[6]**.

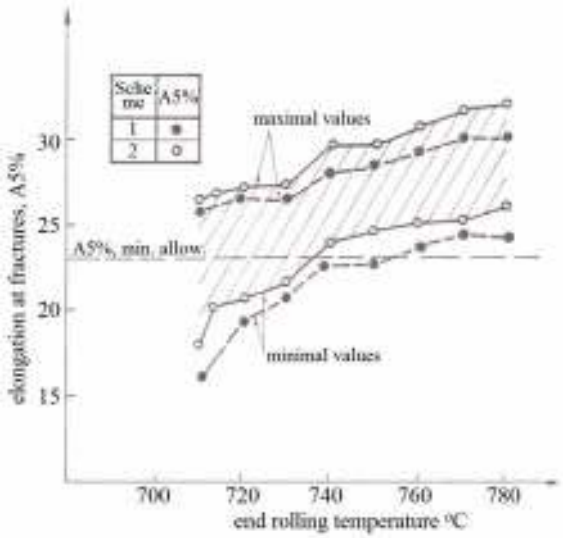

Fig. 5. *Influence of rolling scheme and end rolling temperature on elongation at fracture*

4.2. The Influence of Rolling Conditions on Such Mechanical Characteristics as Resistance, Plasticity and Toughness

From controlled rolled plates in different conditions some test specimens were taken for tension and toughness tests.

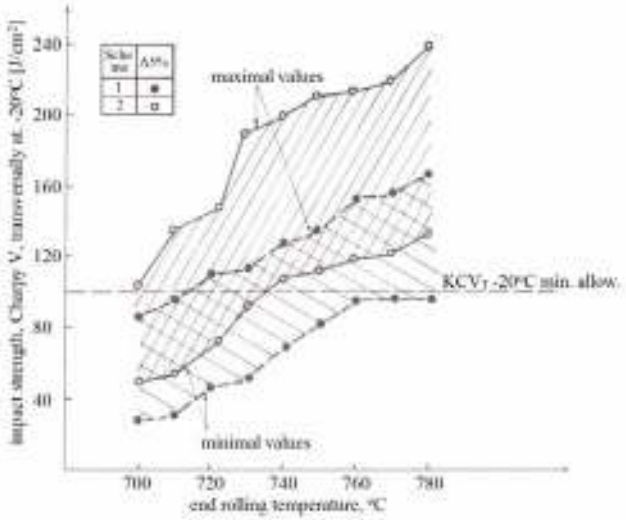

Fig. 6. *Influence of rolling scheme and end rolling temperature on impact strength KCV$_T$ -20^{o}C*

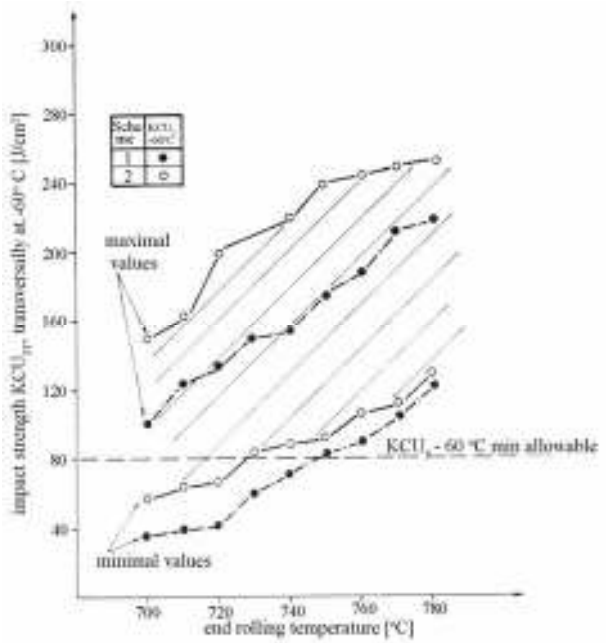

***Fig. 7**. Influence of rolling scheme and end rolling temperature on impact strength KCU_{3T} -60^{o}C*

Figs. 4, 5, 6 and 7, for heats 5-13 with sulphur content of max. 0.0045%, present the dependence on characteristics such as: resistance, plasticity and toughness in the rolling schedule with deformation time 1 and 2 and 2 and 3 for each schedule, temperature of rolling being in the range of 700-780^{o}C.

Irrespective of the rolling chart, the results obtained indicate a close relationship between values of mechanical characteristics and end rolling temperatures; the strength properties (R_m, $R_{po,2}$) increase, and those of plasticity (A 5%) and toughness (KCV_T -20^{o}C, KCU_{3T} -60^{o}C) decrease from 780 to 700^{o}C.

Regarding the rolling scheme used with 2 or 3 deformation times, one can note a certain influence on the plasticity characteristics (Fig. 5) and toughness (Figs. 6 and 7). Higher values of these characteristics can be obtained for all end rolling temperature in the case of application of scheme No. 2 with 3 rolling times, probably in accordance with a greater degree of fineness of the ferritic grain.

In reference to the minimal allowable values for mechanical characteristics, one can state that a whole assembly of completely satisfactory properties is achievable only in the case of scheme No. 2 of rolling, for rolling temperatures situated in the range of 740-780^{o}C.

Thus, the industrial manufacture of plates of grade X 70 is tied in with keeping within very close limits during the whole rolling process **[7, 8]**.

4.3. Influence of Slab Heating Temperature on the Level of Mechanical Characteristics

To examine the influence of this parameter slabs pertaining to heats No. 5-13 were heated with a view to rolling at temperatures of about 1150^{o}C and 1220^{o}C.

All slabs, irrespective of their heating temperature, were rolled according to the scheme No. 2 with 3 deformation times, the end rolling temperature being situated in all cases in the optimal range of 740 – 750^{o}C.

The results obtained, statistically processed, are presented in Table 2.

The analysis of data in Table 2 points to the influence of slab heating temperature on the level of mechanical properties, this probably being in relation with differences in the processes of the precipitation of both nitride and carbonitrides of Nb and V and the process of austenitic grain growing.

In the case of slab heating to a temperature of 1220^{o}C, there is an advanced dissociation of precipitates. Depending on these conditions, there is stronger growth of austenitic grain compared with the case of heating up to 1150^{o}C.

The initial structural characteristics before deformation affect final results after deformations; for the same conditions of rolling a coarser initial austenitic grain leads; to the formation of austenitic grains of larger size, causing a reduction in plasticity and toughness properties.

Table 2. *Influence of slab heating temperature on the level of mechanical characteristics*

Heating temperatures of slabs	Values of mechanical characteristics	Mechanical characteristics				
		R_m	$R_{po,2}$	A5	KCV_T -20°C	KCU_{3T} -60°C
[°C]		[N/mm^2]		[%]	[J/cm^2]	
1150°C	Maximum	640	540	30	210	260
	Minimum	605	490	25	115	165
	Mean	625	518	27.5	157	207
1220°C	Maximum	675	550	26	185	225
	Minimum	635	510	22	87	103
	Mean	653	538	23.5	110	148

The increase in impact strength characteristics at a heating temperature of 1220°C, as compared with 1150°C, is explainable through differences in the development of dissolution and precipitation processes. In the case of temperature up to 1220°C, the dissolution of nitrides and carbonitrides is complete, and the precipitation is accomplished during cooling after rolling, and after phase transformation γ-α, resulting in a hardening by precipitation of the ferritic grains.

In connection with minimal imposed values for mechanical characteristics, one can state that an adequate complex is obtainable only in the case of heating temperature of maximum 1150°C.

5. Conclusions

A. The experiments on an industrial scale in the manufacturing of plates of steel X 70 have proved the necessity of achieving steel with maximum sulphur content of 0.0045% and with a high grade of purity in exogenous and endogenous inclusions as a result of the adopting of certain technological measures adequate for both steel melting and pouring.

B. The achievement after rolling of the entire complex of structural and mechanical properties imposed on plates of grade X 70 requires the control within precise limits of all technological parameters, such as:

-heating temperatures of slabs;

-succession of deformation and recrystallizations operations (rolling chart);

-degrees and temperatures of deformation;

-end rolling temperatures;

-deformation degrees associated with end rolling temperatures.

Acknowledgements

Bodor Marius would like to acknowledge the support provided by the European Union, Romanian Government and "Dunărea de Jos" University of Galaţi, through the project POSDRU – 107/1.5/S/76822.

References

[1]. Orton P. J. - *An overview of line pipe micro alloying*, 1-3 October, Washington, USA, p. 334, (1975).

[2]. Rizescu C., et al. - *Aspecte privind realizarea la C. S. Galaţi a oţelurilor sudabile cu limita de curgereri dicată destinate construcţiilor metalice puternic solicitate,* Sesiunea ştiinţifică a Academiei R.S.R., (1983).

[3]. Ianc P., et al. - *Thermomechanical processing of micro alloying austenite*, The metallurgical society of AIME, Pitsburg, SUA, 1981, p. 361.

[4]. Ianc P. et al. - *Research works on niobium, molybdenum and vanadium steels for large size structural pipe lines*, American society for metals, Philadelphia, USA, (1983).

[5]. Tadakki T., Kazuaki M., Yasuo K., Kenji T., Isao K. - *Development of super tough acicular ferrite steel for line pipe optimization of carbon and niobium content in low carbon steel*, HSLA Conference, (1983).

[6]. S. A. Golovanenco, T. K. Sergeeva - *Microstructural aspects of failure caused by hydrogen embrittlement of gas pipeline steels,* Proceedings of an international seminar, Moscow, 20-22.03. (1984).

[7]. N. M. Fonstein, D. A. Litvinenko - *The influence of structure on fracture toughness of low-alloy pipe steels*, Proceedings of an international seminar, Moscow, 20-22.03. (1984).

[8]. B. M. Ovsiannikov, M. V. Pirusski - *Progress in the methods of fracture resistance evaluation in low-alloy steels*, Proceedings of an international seminar, Moscow, 20-22.03. (1984).

THE ANNALS OF "DUNAREA DE JOS" UNIVERSITY OF GALATI.
FASCICLE IX. METALLURGY AND MATERIALS SCIENCE
N^0. 1 – 2013, ISSN 1453 – 083X

FEM ANALYSIS OF THE SPUR GEARS PRESS–ROLLING PROCESS

Ionuţ MARIAN[1], Monica SAS-BOCA[1], Luciana RUS[1], Marius TINTELECAN[1], Ramona – Crina SUCIU[2], Dan Noveanu[1], Liviu NISTOR[1]

[1]Technical University of Cluj – Napoca, Cluj-Napoca
[2]National Institute for R&D of Isotopic and Molecular Technologies, Cluj-Napoca
email: Marian.Ionut@ipm.utcluj.ro

ABSTRACT

This paper presents the FEM (finite element method) analysis of the pressing-rolling process, a new method for obtaining spur gears. Using symmetries, the 3D geometrical model was created for tools and for the initial blank. The FEM analysis was carried out using Forge 2009, a specialized software for studying the plastic deformation processes. The objective of this study is to describe the evolution of the pressing and rolling forces in the press-rolling process.

KEYWORDS: FEM analysis, pressing, rolling, gear

1. Introduction

The main tooth forming techniques are casting, cutting, and forming processes (Fig. 1). Rolling techniques are divided into two categories as described in Fig. 2. According to this description press-rolling process is part of the forming techniques, more exactly, a longitudinal rolling process.

The rolling process is one of the forming processes used in industrial processing which has evolved over time from producing necessary prefabricated for other processes, finished products with simple shape, to obtaining products with complex shape and high dimensional precision complex form [2].

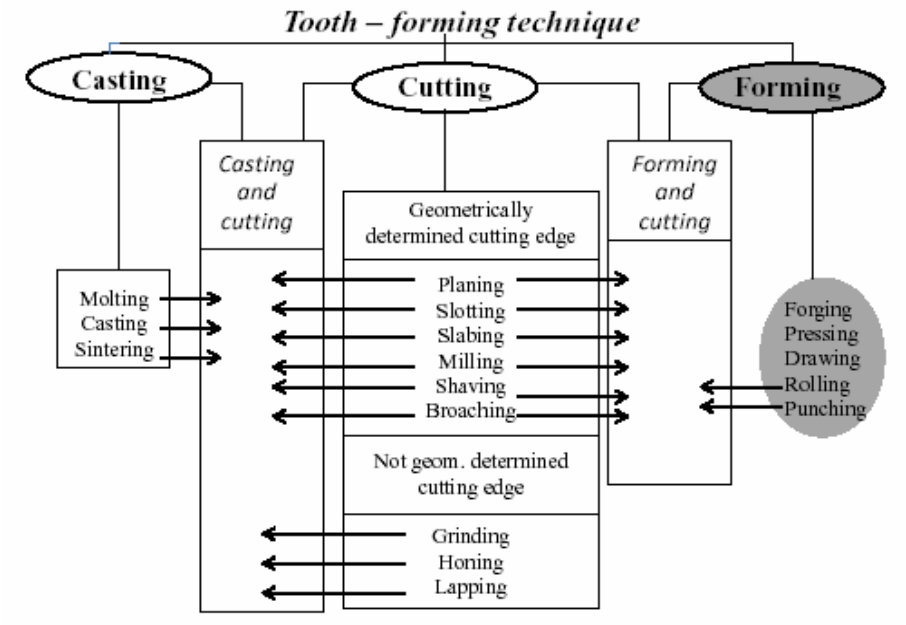

Fig. 1. *Tooth-forming techniques [1]*

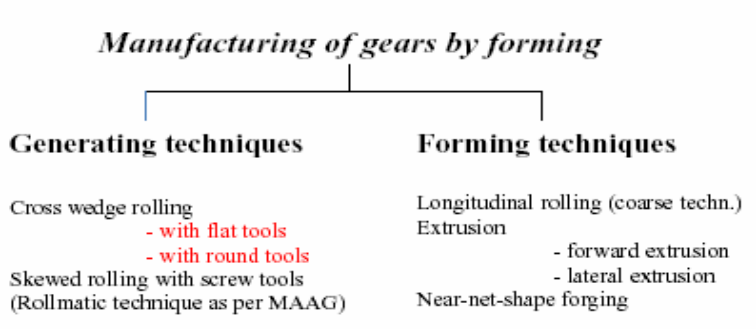

Fig. 2. *Various processes for gear manufacturing [1]*

By rolling we understand the deforming process supported by the metallic material passing through two or more rotating cylinders [3]. Longitudinal rolling with roll of grooved parts can be classified according to the manner of the deformation:

-superficial pressure (grooves are made successively (Fig. 3 a));

-deep pressure (grooves are made simultaneously (Fig. 3 b)). According to previous classifications, the press-rolling process (Fig. 4) to obtain spur gears is a longitudinal rolling process with deep pressing. Because in practice acting multiple cylinders (rolls) with rotation axis in the same plane is difficult, in the press – rolling process advance of work piece in the process and the friction between it and the roll, spinning the roll. So the study of this process is reduced to the study of longitudinal profiles rolling process with specification that this process takes place vertically direction, which means that the process is directly influenced by the weight of the work piece. To achieve simulation of the press-rolling process is necessary to describe the analytical model in order to calculate the rolling force and the pressing force.

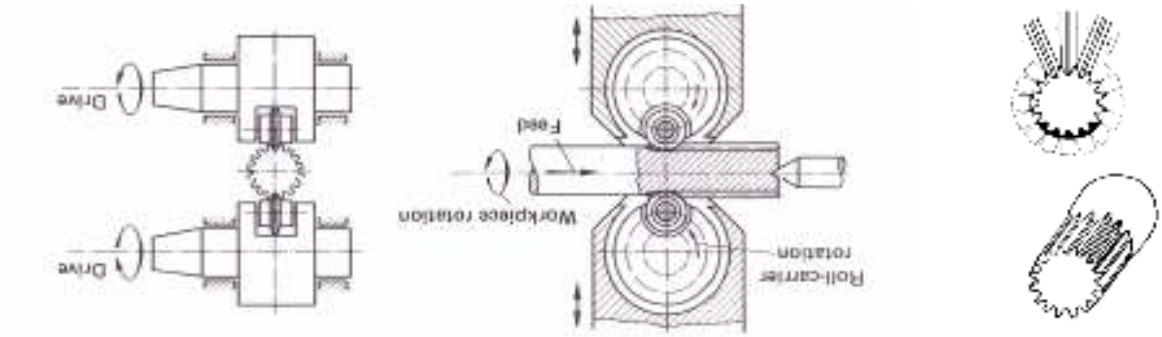

a) b)

Fig. 3. *Longitudinal rolling of grooved parts with: a) superficial pressing [4] b) deep pressing [5]*

The rolling force in flat rolling is determined by the relationship:

$$F = n \cdot b_m \cdot \sigma_m \cdot l_c \quad (1)$$

where: n number of rolls;
b_m average widening;
lc *contact arc length*
D_R roll diameter;

$$l_c \cdot b_m = S_c = \sqrt{\frac{D_R}{8}\left(D_s + D_i\right)} \quad (2)$$

$$\sigma_m = \sigma_d \left[2\left(D_s / D_i\right)^{\delta} = 1\right] \quad (3)$$

S_c – contact area;

σ_m work piece average resistance to deformation;

D_S initial diameter of work piece;

D_i - inner diameter of the gear.

$$\delta = 1 + \frac{\mu}{tg\frac{\alpha}{2}} \quad (4)$$

μ - friction coefficient and α the contact angle between roll and work piece.

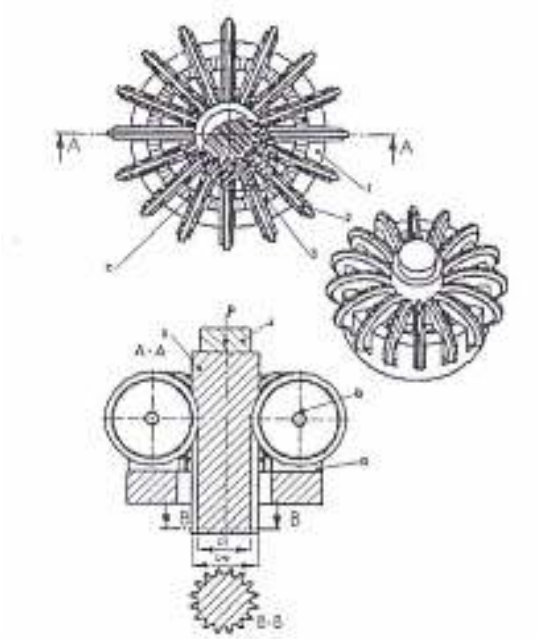

Significance notations 1 - support, 2 - rolls, 3 - roller hub barrel type, 4 - puncher, 5 - cylindrical work piece, a-roll slot, b-circular bearing, c-bearing support for the barrel roll.

Fig. 4. *Press- rolling process [2]*

Pressing force is calculated using the equation:

$$P = P_D + P_a - G \quad (5)$$

where:

-P_d [2] the force required for material deformation from diameter D_S to diameter D_i;

$$P = \sigma_m \cdot \frac{\pi}{4}\left(D_s^2 - D_i^2\right) \quad (6)$$

- P_a [2] force necessary to overcome reactions from support is given by the relation;

$$P_a = n \cdot p_s \cdot S_c \cdot 2 \cdot \frac{\mu_f}{\alpha} \cdot \frac{d_f}{D_R} \quad (7)$$

- p_s - specific pressure;
- μ_f - coefficient of friction in the bearings;
- d_f - spindle diameter roll;
- p -specific pressure exerted on the roller
- G - work piece weight.

According to the laboratory work "Experimental Determination of the coefficient of friction in longitudinal rolling" the simultaneous measurement method of rolling force and the force of contraction [7], the coefficient of friction is calculated using the relationship and the Fig. 5.

Fig. 5. *Graphical representation of forces in press-rolling process, longitudinal section*

where:

- F = N rolling force;

$$\mu = \frac{T}{2N\cos\frac{\alpha}{2}} + tg\,\frac{\alpha}{2} \quad (8)$$

- μ coefficient of friction, force of contraction;
- T for longitudinal rolling;
- α grab angle.

Considering the force of contraction T of the lamination process equal to the pressing force P from the press-rolling process and adding the necessary force to prevail the reactions from bearings and the force of gravity can be written:

$$P = nF\left(\mu - tg\,\frac{\alpha}{2}\right)\cos\frac{\alpha}{2} + P_a - G \quad (9)$$

From equations 5 and 9, matching the first terms of the relations, the relation to calculate the rolling force for one roll can be written:

$$F = \frac{\sigma_m \cdot \frac{\pi}{4}\left(D_s^2 - D_i^2\right)}{n \cdot \left(\mu - tg\,\frac{\alpha}{2}\right)\cos\frac{\alpha}{2}} \quad (10)$$

2. Simulation

2.1. Geometries and materials

The geometries of the billet, the active roll and the stem were generated in "Solid Works" and the meshes within their space domains in "Forge 2009". Fig. 6 shows the initial meshes of the billet and the tooling in cross section. For saving the computer RAM source and computation time [6] in the FEM analyses was carried out on 1/46 section from billet, stem and 1/2 section from one active roll.

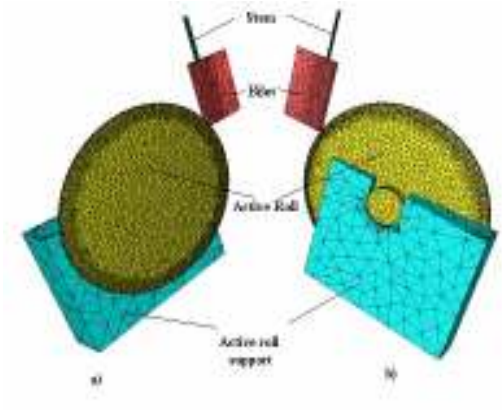

Fig. 6. *Sections trough the press rolling process: a) back view b) front view*

The puncher (stem) and the support were considered as perfectly rigid tools (for this tool is not necessary to define the material). The work piece material is Al99% and roll material is steel DIN 1.7350 X210Cr12.

2.2. Simulation parameters

Process parameters are presented in the following Table 1. The initial work piece, the tools and the environment temperature were considered 20°C. The stem speed during the process is 10mm/s. The coefficient of the friction at the interface active roll-work piece and stem-work piece is 0.7 and friction coefficient at interface active roll-support was chosen 0.1 (dry friction).

Table 1. *Simulation process parameters*

Billet length [mm]	30
Billet diameter [mm] Billet temperature [^{o}C]	38….41 20
Tooling temperature [^{o}C]	20
Friction factor at interface billet-active roll	0.7
Friction factor at interface active roll - holder	0.1

Also, the heat transfer coefficient between tool-work piece and air been incorporated in finite element analysis.

4. Results and discussions

The graphs shape rolling force (obtained by simulations) is similar to the pressing force (Fig. 7).

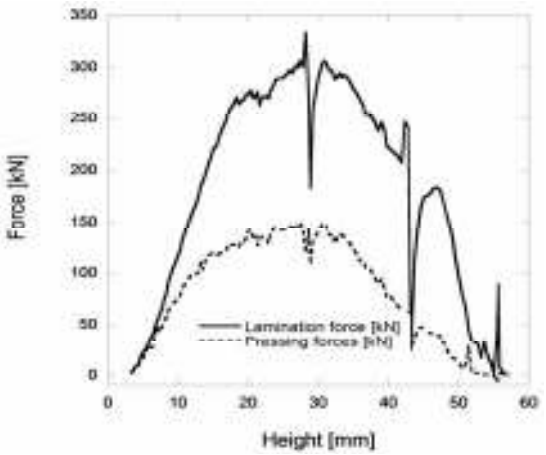

Fig. 7. *Graphics of forces obtained by simulation of rolling force and pressing force*

In the study of the press force evolution we can find three main phases (zones) specific to the evolution of the work piece during the rolling process:

1. entry zone:
   - adjustment roll zone (just for open bearing);
   - work piece clamping zone;
2. pseudo stationary flow zone,
3. exit zone:
   - step 1 - this zone begin when the ma material start to flow in reverse direction of rolling;
   - step 2
   - level a) - the force necessary to deform the material in rolling directions decreases and the force necessary for deform the material how flow in reverse direction is increased;
   - level b) - where the force decreases to zero, the negative value of the force jump (point P) corresponding to the action of part weight cumulating with the part velocity.

All these zones are described in Fig. 8.

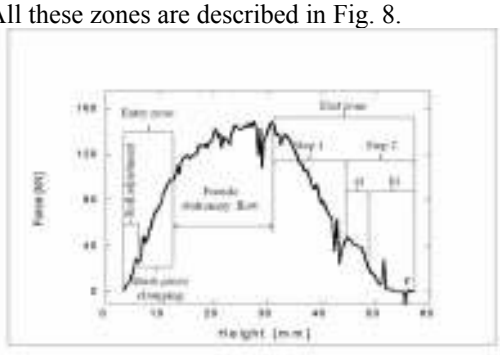

Fig. 8. *Phases of pressing force evolution in press-rolling process*

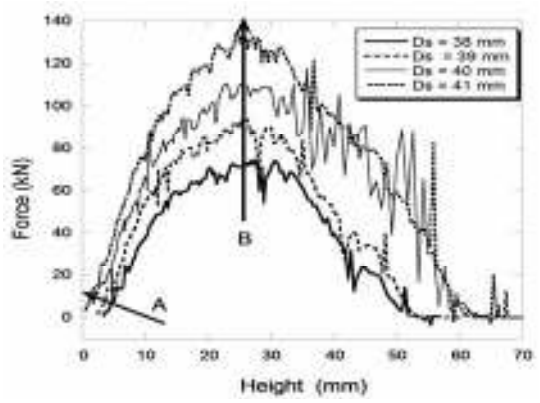

Fig. 9. *Pressing force evolution and punching stroke according to the initial work piece diameter*

The following comparative study of the evolution of the pressing force required for the pressing-rolling process and considering the process input variable initial work piece diameter (Ds).

Thus the initial work piece diameter directly influences the press-rolling process as shown in Fig. 9.

- arrow A in Fig. 9 indicates that the pressing force increases with the increase of the work piece diameter;

- arrow B in Fig. 9 indicates that the increasing diameter changes the parameters of the deformation area (increase grip angle, length of contact arc, while achieving a more complete filling of the outbreak strain exactly the gear tooth) while increasing the punching required course.

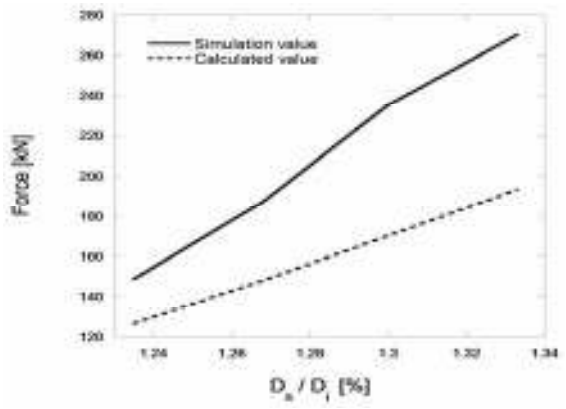

Fig. 10. *Pressing force evolution*

Comparing the pressing force obtained by numerical modeling of the process using FEM with results obtained using the analytical model we can draw the graph presented in Fig. 10.

Consequently, one can say that the graph of force calculated analytically calculated force closely follows the numerical chart. Calculation errors are largely due to the simplifying assumptions considered in theoretical relationships pressing force.

5. Conclusions

Process necessary force is greater than that calculated using mathematical relations, it is because the work piece sectional area changes its input in the process (between the punch and focus discharge work piece deformation occurs). Work piece diameter with increasing pressing force initially increases and travel needed punching process. The pressure is directly influenced by the weight of work piece.

Acknowledgment

This paper was supported by the project "Doctoral studies in engineering sciences for developing the knowledge based society – SIDOC", contract no. POSDRU/88/1.5/S/600788, project co-funded from the European Social Fund through the Sectorial Operational Program for Human Resources 2007-2013.

References

[1]. R. Neugebauer, M. Putz, U. Hellfritzsch - *Improved Process Design and Quality for Gear Manufacturing with Flat and Round Rolling***,** CIRP Annals - Manufacturing Technology Volume 56, Issue 1, Pages 307-312, (2007).

[2]. L. Nistor, D. Frunza - *Evaluarea forţei în obţinerea danturii roţilor dinţate cu dinţi drepţi prin presare - laminare* (The force evaluation for straight toot gears manufacturing by pressing – rolling), Metalurgia, vol. 58, pg. 14-18, no.5/2006.

[3]. L. Nistor - Laminarea metalelor (Metal rolling) Polytechnic Institute Cluj-Napoca, (1988).

[4]. K. Lange - *Handbook of metal forming*, Copyright, (1985).

[5]. I. Drăgan - *Tehnologia deformărilor plastice* (Plastic deformations technology), E.D.P Bucureşti, (1979).

[6]. H. You-feng, X. Shui-sheng, C. Lei, H. Guo-Jie, F. Yao - *FEM simulation of aluminum extrusion process in porthole die with pockets,* Trans. Nonferros Met. Soc. China, vol. 20, pg. 1067-1071, (2010).

[7]. Adriana Neag, Mariana Pop - *Deformări plastic*e - *Aplicaţii* (Plastic deformation-Aplication) - U.T. Press Cluj Napoca, (2009).

THE ANNALS OF "DUNAREA DE JOS" UNIVERSITY OF GALATI.
FASCICLE IX. METALLURGY AND MATERIALS SCIENCE
N^0. 1 – 2013, ISSN 1453 – 083X

METHODS OF PROTECTION OF NATIONAL ARCHITECTURE MONUMENTS

Gh. CROITORU[1], Ig. COLESNIC[2]
[1]Institute of Scientific Research in Construction „INCERCOM", Chisinau;
[2]Institute of Power Engineering of the Academy of Sciences of Moldova
email: gcroitoru@mail.ru

ABSTRACT

The paper discusses the problem of monuments conservation in terms of technical implementation and based on the importance of conservation of historical content, and it helps to skillfully handle the complicated untypical tasks on all surfaces, be it facade repair, building waterproof, or wood protection.

Also, we studied the causes of weathering and fracture of facade construction materials of old buildings. In the restoration process, we suggest using materials from sacrificial, sanitizing and compression plasters and the correct application of desalination compresses, which is a reliable, effective method of salts removal. In addition to special sand-blasting and chemical cleaning of dirt, interior walls may be cleaned using a removable latex film for eliminating contaminants.

KEYWORDS: restoration, monuments, desalination, conservation, stone-strengthener

1. Introduction

Restoration of buildings and constructions is an extremely difficult type of work that requires the joint work of various specialists, and especially restoration architects, engineers and construction technicians.

The purpose of measures of monuments protection is their long-term conservation. Cultural heritage is extremely important to society, especially for the possibility to know our own history on the example of real historical evidence. This statement is true for small regions in particular, and for Europe as a whole. Heritage Preservation is a component of the quality of life. We consider the complex problem of monument preservation not only in terms of technical implementation, but also from the point of view of historical content conservation, helping to skillfully handle complex atypical tasks on all surfaces be it facade repair, building waterproofing, or wood protection.

The slightest mistake can lead to loss of irreplaceable cultural heritage. With the constant improvement of technology and searching opportunities for conservation of our cultural heritage, we have carefully and conscientiously select concepts and draw up recommendations for the use of products. This includes understanding and recognition of coexisting, and sometimes almost opposite concepts in the restoration of monuments: restoration using a new material, or preservation and strengthening of the initial state.

2. Case study

The restoration of an important architectural monument cannot in any way be compared with the construction of new buildings from ground. When constructing new facilities there are opportunities for an extensive reorientation and technical improvements, while during reconstruction activities, and even more so for conservation, we must start from the existing state of the structure. From here follow a number of special factors that must be considered to ensure that restoration activities are successful. A careful examination and analysis of the situation, the examination carried out on site, as well as laboratory tests of material samples, are an integral part of activities planned for reconstruction (Fig. 1).

Studies conducted by us as on a construction site and in our laboratories allow us to find cost-effective materials and methods of their application, ideally meeting the goals set for restoration or construction.

Based on these studies, specific recommendations are given with the name of the material, its processing method and timing of works.

These carefully crafted recommendations provide guidance to the contractor industry. Not only the technical features, but also historical, architectural and restoration details are taken into account, as it is necessary to preserve facade appearance with minimal intervention. For this purpose, in most cases a thorough examination of the structure is a must; further monitoring of work performance is advised.

Fig. 1. *Exterior of historic buildings 17th-19th centuries in Chisinau*

3. Methodology and results of a complex study

3.1. Causes of weathering and destruction of building materials

Every professional in construction knows the white beards, as if growing from the damp masonry in older buildings. They can lead to plaster peeling or even to stone breakaway. Non-professionals often refer to these salt layers as wall nitrate - a concept that barely meets the actual state of things.

The salts are not only a necessary component of life on earth, but also a component of many building materials based on minerals. Salt solubility plays an important role in the process destroying the clutch, and there is a close connection between salt and humidity. Ingress of water and dissolved salts in the pores of building materials is in most cases the root cause of weathering.

The penetration of water often causes a range of complex physical and chemical processes which in turn can lead to erosion.

Without the presence of excess moisture in the material, damage caused by frost, as well as chemical and biological corrosion, would not have such frightening proportions. Salts dissolved in water affect the construction masonry of porous materials and in the case of mechanical and chemical stress, can lead to destruction.

The penetration paths of moisture in the construction masonry are varied. Water can rise through capillaries, penetrate into the masonry under pressure as leaking moisture or with the rain through open pores, cracks and construction joints.

The water in the gaseous state can penetrate into the masonry as the result of hygroscopic water absorption and capillary condensation.

It is not possible to draw a clear boundary between physical and chemical corrosion. A typical chemical process is, for example, the loss of a binder component of the building material because of its transformation into a soluble salt (solvent corrosion). The process of crystallization of salts formed at the same time is often associated with an increase in their volume, and this process is characterized as a physical one.

Typical types of physical weathering are:

- the crystallization of salts;
- the hydration salts;
- freezing and thawing;
- hygroscopic expansion/shrinkage.

Biological corrosion, i.e. the damage of masonry by organisms such as algae, lichen, moss and bacteria, can cause chemical damage due to corrosive metabolic products (e.g. chemicals), and the green cover formed on the clutch works as a moisture collector and prevents the normal drying of building materials.

In fact, the list of destructive processes associated with salt and humidity is much larger than the excerpt presented on these pages.

3.2. The process of desalination and purification

Compress for desalting. For a durable and successful protection of the buildings affected by salts, a complex of measures should be performed not only to block the incoming water, but also to remove the existing salts.

In addition to mechanical and chemical methods of fighting salts, which due to their destructive effect are not allowed in restoration, there is a proven physical method of extraction of salts with a desalting compress. Desalination refers to a clear reduction of destructive salts contained in porous building materials. Used in the restoration of sacrificial, sanitizing and compression plasters, the correct application of demineralization compresses is a reliable method of removing salts, proved to be effective.

Due to compress application on the masonry, the area capable to evaporate the water located in the clutch, shifts. Salts dissolved in water, have the ability to move from a building material in the pack so that the crystallization of salts occurred in the new evaporation zone outside the architectural element. At the same time compresses are not a decorative element and are not used to further protection of the masonry. Compresses are used temporarily, without causing damage to masonry, and can be reversible in nature.

Careful cleaning of the foundation. It is widely believed that the crust of dirt, which is formed on the surface of building material, can be used as a protective layer. As a rule, this statement is incorrect.

In contrast, the crust of dirt has a large internal surface, and is an excellent absorbent material for moisture and airborne gaseous and particulate (dust) emissions. These substances react inside the crust of mud and accelerate the process of destruction, even if their effect is not noticeable at first.

For dirt removal, there are several technical and aesthetic justifications:

- removal of risk factors related to the accumulation of salts and deceleration of drying;
- preparation of the foundation for further preservation activities because of recovery of capillary water absorption;
- removal of unsightly external contamination.

In addition to a special sand-blasting and chemical cleaning of dirt, the cleaning of the interior building walls may be performed using the method of removable latex film.

None of the currently used methods for dirt removal is optimal for internal cleaning. Regular cleaning requires too much water or too much dust is produced. A suitable method could be the laser treatment, but its application on large surfaces is not justified in economic terms.

Products based on special latex dispersion fill this gap. They contain a small amount of water, which quickly evaporates when applied to the wall.

Material polymerizes into a sticky elastic film with active components on the surface intended for cleaning. After hardening of the film, it is removed together with the dirt.

3.3. Preservation of natural stone

Blocking natural stone expansion. Very many natural rocks contain clay minerals which can expand. In most cases, these are layered silicates, which in structure resemble a book.

Due to the electrochemical "magnetic" property in the presence of sufficient moisture, they can retain and set free the moisture between the "pages of the book," i.e. in the intermediate layers.

The layers of minerals saturated with moisture come loose like an accordion (Fig. 2).

If the amount of moisture decreases, the fibers come together again, creating tension in the masonry structure. These destructive processes are called hygroscopic expansion or shrinkage. The action of a unique product against expansion is based on the "turning off" of clay minerals. After treatment with protective material, the positively charged metal cations, found in the intermediate layers and responsible for the expansion, are replaced with the active ingredient of the protective material. As a result, there is a significant reduction in the hygroscopic expansion while maintaining the other characteristics of the material. Subsequent treatment of the surface water repellents enhances the action of the anti-expansion product.

Fig. 2. *Microstructure of clay material predisposed to expansion*

Stone hardening on the basis of "classical" stone-hardeners.

Stone-hardeners on the basis of silicic acid ester ($Si(OR)_4$) by reaction with water, form reinforcing silicagel (SiO_2 aq):

$$Si(OR)_4 + H_2O \rightarrow SiO_2 \text{ aq} + 4\ ROH$$

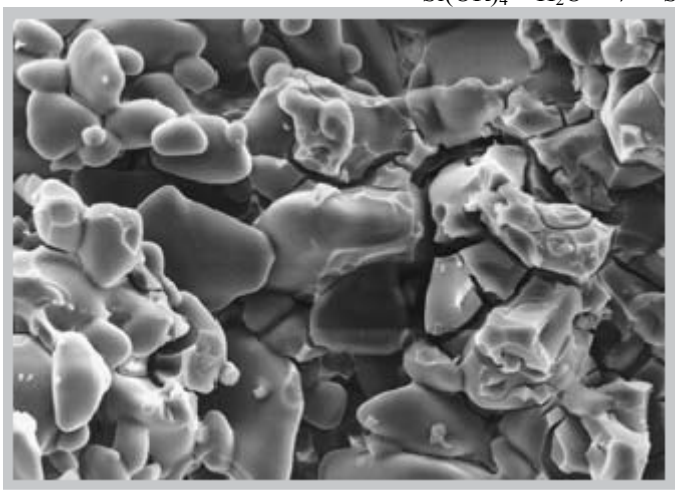

***Fig. 3**. Silica in rock pores at 300-fold increase with the electron microscope*

The active substance - silicic acid ester (Fig. 3) being a liquid, solvent addition during processing is not necessary. The ability to prepare various proportions of the mixed molecules of the active ingredient allows the variation of strengthener properties, especially in the amount of formed gel. That is, the amount of the gel, resulting in the reaction of the active substance within the pore space. Further variations in the depth of impregnation and reaction rates are achieved by varying the type and amount of added catalyst and solvents.

Through targeted experiments combining these options, a wide range of these stone hardeners was obtained. Thus, it is possible to select an individual product that is suitable for hardening any foundation (Fig. 4).

***Fig. 4.** Process of restoration of facades and column capitols*

All the classic hardeners based on silicic acid ester have one characteristic feature: silica gel is obtained from the fluid and does not form a dense structure, i.e. it creates a secondary porosity within the treated capillaries. This porosity ensures the porosity of the capillary conductivity and conductivity of water vapor in the reinforced material.

Stone strengthening using elastic hardeners.

A very small amount of gel particles of "classical" stone strengtheners reduces the area of its application on foundations with normal pores diameters. Usual hardeners are only in part suitable to strengthen the building materials with an initially large pores or with pores that increased as a result of weathering, the, and only in certain conditions.

These problematic materials include tuff, a variety of plasters, capable of expansion natural stone, cane-fiber sandstone. The reasons may be the original distribution of pore radii of natural stone, or microcracks formed due to weathering, for example,

in the case of expansion able natural stone such as cane-fiber sandstone.

Plasticized stone hardeners.

Hence the need to strengthen the previously mentioned foundations with advanced stone hardeners. In the 90's were designed silicic acid esters, meeting these requirements were designed.

With the introduction of plasticizing particles, the resulting silica becomes more elastic. The internal stresses arising from the reactions are reduced and silica gel bridges are formed (Fig. 5). Due to the release of this product group, it became possible to strengthen the very porous by nature or heavily damaged structures.

A positive side effect of these materials in comparison with classical hardeners is the improvement of characteristics of the treated material regarding expansion and shrinkage.

Through processing, the elastic modulus increases faster than the rate of strength.

a) *b)* *c)*

Fig. 5. *Stone strengthening on the basis of plasticized stone hardener: a) separation of the gel plates in about 10 μm; b) the picture registers the type and regularity of the separation of gel plates of about 10 μm; c) visible explicit linking of the gel structure in the pore space. 900-fold magnification, soft fritted saturated glass*

The purpose for the restoration of stone material is in most cases not only to strengthen the stone structure, but to improve of many other indicators, depending on the type and intensity of weathering.

Based on the similarity of silicic acid ester with most types of natural stone, as well as due to the fact that masonry is often composed of layers of different materials, the desire to solve all problems with one product is quite understandable. Stone hardeners on the basis of silicic acid ester used in silica foundations, set in motion two interrelated mechanisms. First, the ester of silicic acid is attached in a chemical reaction to the quartz substrate, and, secondly, it forms in the pore space of the foundation a three-dimensional silicate structure, which, without direct connection leads to the stabilization of the material. On calcite foundations only the second mechanism takes place. To achieve the chemical addition of silicic acid ester to the calcite foundation specially developed for this purpose, adhesion promoters are used. These substances interact with covalent compounds of quartz and polar compounds of limestone, and involve the two above-mentioned mechanisms.

3.4. Innovative processes for in-depth strengthening

Strengthening during the process of vacuum circulation (VKF)

The VKF method is based on the use of back pressure technology during which the monuments, statues and facade parts are packed in a tight film, resistant to solvents (Fig. 6). If only a portion of the facade is subjected to the process, the places of contact of the film with the rock are isolated with sealing material and batten bars made of solid wood. Then, a powerful vacuum pump removes the air trapped in the film bag and pore space, while the figure itself turns into a vacuum pot. Upon reaching the desired index of relative vacuum (200-900 mbar), a specially designed reinforcing material is added, which is evenly and deeply absorbed into the stone.

Areas with open pores and the most damaged areas in the stone are filled in the first place, more dense structures - a little slower. The excess of restorative material is returned to the installation where it is again included in the cycle.

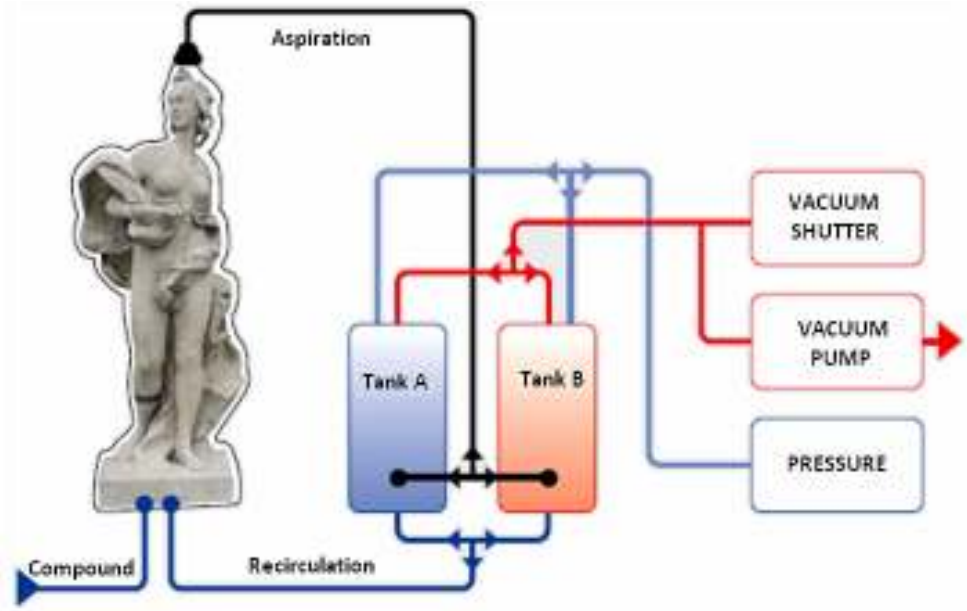

Fig. 6. *Surface hardening during the process of vacuum circulation (VKF)*

Advantages of the method:

- the pore space is completely filled with protecting material;
- the damaged material is homogenized with the intact material;
- a complete impregnation can be carried out on the site;
- the process can be repeated as many times as it's needed;
- the porous stone structure is saved, compatible with the raw material of stone;
- the intervals between subsequent restorations significantly increases.

3.5. The current process to enhance the load bearing capacity of vaults

Vaults impregnation

At the turn of the 19th and 20th centuries, vaults of many churches in the Republic of Moldova were constructed using mostly "porous limestone." After one century, many of these constructions have very severe damage and loss of hardness. In addition, the vaults often show significant changes in surface appearance, in the form of salt efflorescence, dirt, shedding up to the formation of mud cake.

This damage reduces the strength of the material and causes the loss of the original relief pattern. In some cases the size of the arch cross-section is greatly reduced, which may lead to loss of bearing capacity of the foundation, up to the danger of building collapse.

Often, historic vaults of buildings are demolished for these reasons and then reconstructed. Now it is not necessary to do that.

On the basis of experimental research a method for strengthening vaults was developed, based on the impregnation of masonry arches with a special compound (Figure 7).

This method is used in conjunction with a system of special supporting plasters and thermal insulation, laid above the masonry arch.

Masonry joints take on certain functions in the structure and therefore must meet all necessary requirements and have certain properties. This applies not only to external, but also physical, mechanical and, above all, moisture characteristics. Thus, we have a wide range of mortars to fill the joints with different types of binding elements. The mortars are separated by areas of application, as well as within each group by color, grain size and strength.

As before, the application of plaster is an important part in the modern decoration of facades. As the surface layer, besides aesthetic purposes, they originally had the function of protecting the structure from environment effects. In the restoration of historic buildings, in most cases, this is not the only technical problem. Often, much more important is the problem of internal damage by salts or moisture coming from the foundation. Only in a few "lucky" cases a simple plaster can be used, often a special recipe has to be used for selected historic plasters. It is often necessary to respond to a specific situation, using special, modern products. Depending on the situation, it may be necessary:

- to ensure dry and free of efflorescence surfaces;
- to protect the adjacent historical surface, such as wall paintings.

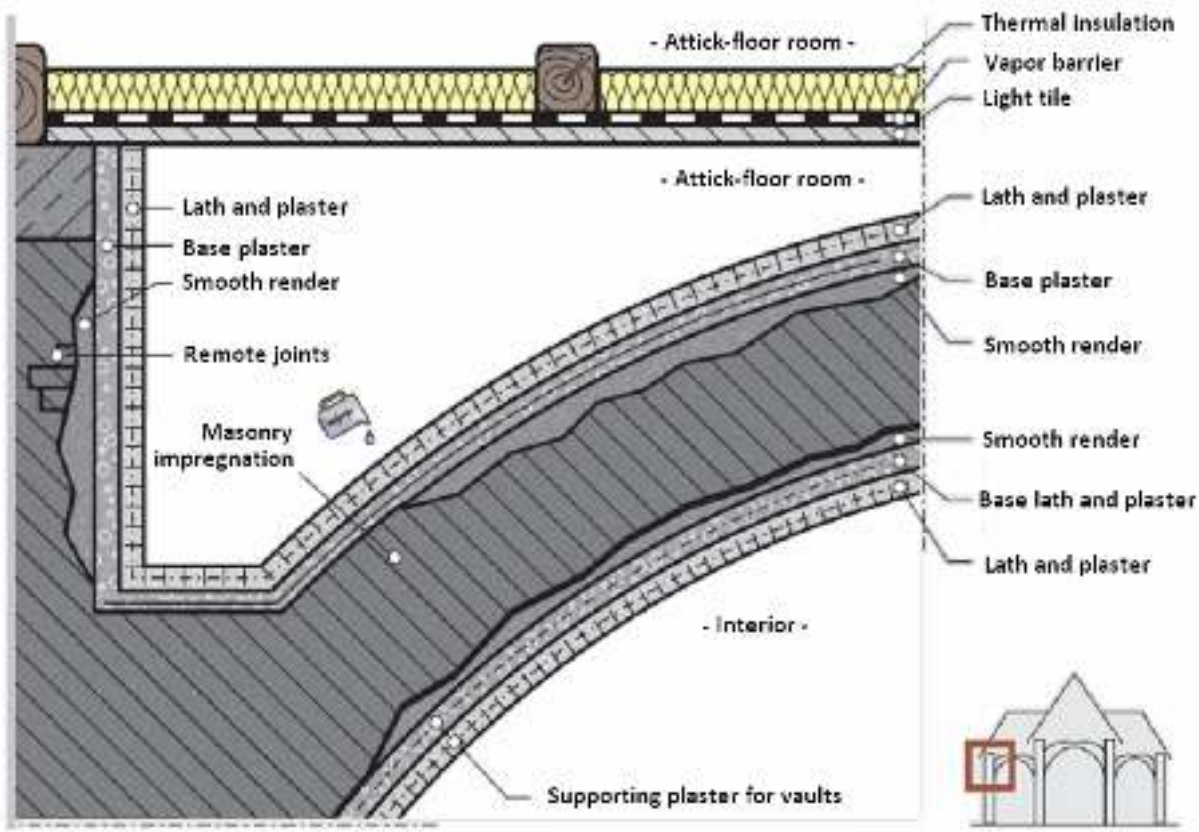

Fig. 7. *Enhancement of load bearing capacity of vaults*

Aim of restoration	Foundation	Features of mortars
Material suitable to the historical foundation	Mostly dry and salt-free	Capillary active with medium pore size
Dry and free of efflorescence freshly plastered surface for the most part without a direct connection to the original historic surface	Affected by moisture and harmful salts	Water repellent with a high pore volume in conjunction with a capillary-active plaster base
Freshly plastered surface in most cases with a direct link to the original historic surface	Affected by moisture and harmful salts	Capillary active with high pore size

Signifying plasters have in most cases, two important functions:

1. moving the evaporation boundaries of the moisture contained in the masonry into the plaster layer,

2. the accumulation of salts in the masonry without destroying the structure during crystallization.

The first problem is solved by the water-repellent, and at the same time open to water vapor diffusion properties of the plaster. The moisture that occurred in the masonry is forced into the initial layer of 1.5 to 3cm thickness to move to gaseous state, and further move to the surface as water vapors. Thus, in accordance with the second task, crystallized salt are stored in the pore space of the plaster and in the plaster under it.

4. Conclusion

Designing the protection of architectural monuments structures from moisture, weathering and destruction requires an individual approach. In all cases, one should apply a gentle but reliable solution taking into account alterations to the building structure during operation. Design requires justified use of historical and contemporary efficient materials, including concrete, if necessary.

In addition to a special sand-blasting and chemical cleaning of dirt, cleaning the interior walls

and facades of buildings may be performed using a removable latex film to eliminate contaminants.

On the basis of experimental research a method for strengthening the vaults was developed, based on the impregnation of masonry arches with a special compound. This method is used in conjunction with special support plasters and thermal insulation, laid above the masonry arch.

An integrated approach to the protection of architectural monuments structures from the negative impact of water and other negative factors, properly used, will allow reassuring them for years.

References

[1]. Курдюмов В. И. - *Краткий курс оснований и фундаментов.* СПб. (1902).
[2]. Кирнтейн Г. - *Строительное искусство. Руководство к возведению фабричных, гражданских и сельских строений*. Рига, (1915).
[3]. Раппопорт П. А. *Строительное производство Древней Руси* (X–XIII вв.) СПб.: Наука, (1994).
[4]. Покрышкин П. П. - *Краткие советы по вопросам ремонта памятников старины и искусства.* СПб. (1904).
[5]. Shanks, M. & Tilley C. - *Re-Constructing archaeology. Theory and practice,* Second Edition, London-New York: Routledge, (1992).
[6]. Corvo, F., Minotas, J., Delgado, J., Arroyave, C. -*Changes in atmospheric corrosion rate caused by chloride ions depending on rain regime,* Corrosion Science, 47, (2005), p. 883 -892.
[7]. Morselli, L., Bernardi, E., et al. - *Chemical compozition of vet and dry atmospheric depozitions in an urban environment: local, regional and long range influences,* Atm. Chem. (2008), 2 9, 3, p. 146 – 150.

THE ANNALS OF "DUNAREA DE JOS" UNIVERSITY OF GALATI.
FASCICLE IX. METALLURGY AND MATERIALS SCIENCE
N^0. 1 – 2013, ISSN 1453 – 083X

METALLIC MATRIX COMPOSITES WITH CERAMIC PARTICLES. WETTING CONDITIONS

G. NEAGU, Fl. ŞTEFĂNESCU, A. MIHAI, I. STAN, I. ODAGIU
Politehnica University of Bucharest
email: gigelneagu@yahoo.com

ABSTRACT

The paper presents the main aspects regarding the mixtures obtained made up from aluminium melts and different kinds of ceramic particles (silicon carbide and boron carbide). Synthetically discussed are the wetting conditions and the wetting coefficient and the possibilities to improve it insisting on the alloying metal bath, its overheating and the heat treatment of the particles with the aim to remove gases from the superficial layer. The critical acceleration necessary for the incorporation of particles into the melt for different temperatures was determined.

KEYWORDS: aluminium, silicon carbide particles, boron carbide particles, wettability, minimum acceleration

1. Introduction

In recent years the production of metallic composites has expanded the use of additional material in the form of particles due to some important advantages: much cheaper compared to fibres; isotropic materials or materials with controlled heterogeneity can be obtained; simple technologies can be used to incorporate the complementary material.

Compared to the organic matrix, metallic materials are used for the need to obtain composites that can be used at relatively high temperatures. For castings destined to be used at smaller temperatures than 400°C, aluminium and its alloys are used as matrix due to a sum of advantages (low cost, small density, acceptable mechanical properties, electrical and thermal conductivity, corrosion resistance, workability). Titanium used as alloying element improves the behaviour of aluminium at high temperatures [1].

Mechanical, thermal and electric properties of metallic composites depend, inter alia, on the type, quantity, size, shape, and complementary material distribution.

Generally, particles of graphite, ceramic metallic materials or glass are used to produce metallic composites with low density, high specific properties, dimensional stability, and, especially wear resistance.

Silicon carbide particles (cubic or hexagonal elementary cells) are frequently used to produce composites due to the low cost, small density, high specific mechanical properties, low thermal expansion coefficient, resistance to thermal shock, hardness etc.

Although less used, boron carbide is also an attractive material for the production of metallic composites. In aluminium-based composites boron carbide particles provide low density, thermal stability, hardness, wear resistance [2].

Due to the close values of densities ($\rho B4C=2.52g/cm^3$), the intensity of the settling process is diminished in aluminium melts ($\rho_{Al}=2.369g/cm^3$ at the melting point) [3].

Gravitational casting is still the simplest and least expensive method of producing metallic composites. Therefore, to produce aluminium particles mixtures remain a matter of general interest.

2. Wetting conditions

The wettability parameter, $\sigma_{lg}\cos\theta$ where σ_{lg} is the surface tension at the aluminium melt-gas interface and θ is the contact angle, allows analysing the wetting conditions in aluminium – silicon or boron carbide [4]. Positive values of this parameter indicate wetting conditions in the system. Evidently, non-wetting occurs when $\sigma_{lg}\cos\theta < 0$.

The values of the wettability parameter in different aluminium-based systems are presented in Table 1 and Figure 1. The calculations were made based on the values of the surface tension and the wetting angle, as presented by Rohatgi [5]. The wettability parameter values determined confirm non-wetting conditions in the two systems reported, in different conditions [2-3, 6-10].

It should be noted that the layer of alumina formed due to the high affinity of aluminium for oxygen prevent a correctly estimation of the contact angle.

Table 1. *Wettability parameter values*

System	T, [°C]	Wettability parameter, $\cdot 10^3$, [N·grd/m]	
		SiC	B_4C
Al	700	-238.85	- 425.5
	800	-178.95	- 362.95
	900	-161.21	- 275.69
Al-2Cu	700	-242.24	- 378.78
	800	-197.05	-342.38
	900	-145.56	-282.49
Al-4.5 Cu	800	-186.93	- 323.36
Al-2Mg	700	-193.34	- 325.36
	800	-147.04	- 117.12
	900	-120.72	- 66.40
Al-4.5Mg	800	-136.67	- 32.99

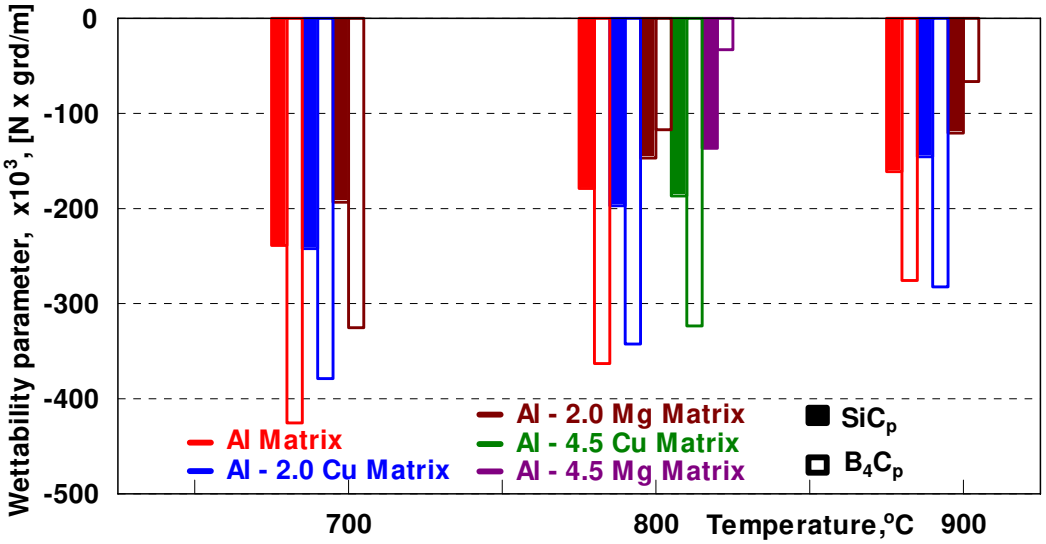

Fig. 1. *Wettability parameter*

The transfer of a silicon or boron carbide particle from the gaseous phase into the aluminium melt is complete when the gas - particle interface is replaced by a particle - liquid interface [11].

In the particular case of a cubic particle (l_p) moving with gravitational acceleration g, the total force that acts during its penetration into the metallic bath is:

$$F_t = G_p + F_\sigma + F_a , \quad (1)$$

where: G_p is the gravitational force; F_σ - the force determined by the superficial energy; F_a - Archimedes force.

If *Y* axis of an xOy coordinate system associated to the particle has the positive direction towards the melt surface, the particle will be incorporated when $F_t > 0$ [12].

The gravitational force can be determined by the equation:

$$G_p = m_p g , \quad (2)$$

where m_p is the mass of the particle.

In order to determine the force caused by the superficial energy ΔE_σ, it is necessary to take into account the following relationship:

$$F_\sigma = 6 l_p \sigma_{lg} \cos\theta , \quad (3)$$

Archimedes force is given by the following equation:

$$F_a = -\rho_l V_p g = -m_p g \frac{\rho_l}{\rho_p}, \quad (4)$$

where: ρ_l is the density of the liquid aluminium, V_p - the volume of the particle; ρ_p - the particle density.

Therefore, the necessary force for a particle to penetrate the metal bath is:

$$F_t = m_p g\left(1 - \frac{\rho_l}{\rho_p}\right) + 6 l_p \sigma_{lg} \cos\theta . \quad (5)$$

In non-wetting conditions, when $\rho_p < \rho_l$, for the two analysed systems it results that:

$$m_p g\left(1 - \frac{\rho_l}{\rho_p}\right) + 6 l_p \sigma_{lg} \cos\theta < 0 , \quad (6)$$

and the particle will float.

Therefore, to penetrate the melt, the particle needs a minimum acceleration:

$$a_p = -6 \frac{\sigma_{lg}}{l_p^2(\rho_p - \rho_l)} \cos\theta . \quad (7)$$

Different values of this parameter for aluminium melts are presented in Table 2. The calculations were performed by using Rohatgi's data and the following relations [13]:

$$\rho_{Al} = 2.369 - 3.11 \cdot 10^{-4}(T - T_{top}), \quad (8)$$

$$\rho_{Al-Mg} = 2.376 - 0.009\%Mg . \quad (9)$$

Table 2. *The values of minimum acceleration*

System	*T*, [°C]	$a_p \cdot 10^4$, [m/s^2]			
		SiC		B_4C	
		$l_p=10^{-4}$, [m]	$l_p=2\cdot10^{-4}$, [m]	$l_p=10^{-4}$, [m]	$l_p=2\cdot10^{-4}$, [m]
Al	700	16.79	4.2	156.2	39.05
	800	12.14	3.03	111.94	27.99
	900	10.56	2.64	73.31	18.33
Al-2Mg	700	13.62	3.4	120.5	30.13

3. Improvement of wetting

The high values calculated for the minimum acceleration impose the necessity to apply some methods to improve the wetting conditions. The simplest methods are:

- overheating of the melt. The presence of an oxide film at the aluminium melt surface drastically reduces the wetting angle. For pure aluminium the oxide layer formed at the surface of the melt, due to the small solubility of oxygen, is γ-Al2O3 [14].

The wetting becomes possible at higher temperatures when the oxide layer can be removed by a chemical reaction [15]:

4 Al (l) + 3 Al2O3 (s) = 3 Al2O (g) (10)

For aluminium and its alloys the effect of temperature on the superficial tension is to decrease it. In this way, the wetting angle between the melt and the complementary material reduces.

Some empirical relationships, such as those proposed by Keene or Shen, can be used to study the effect of temperature on the surface tension [16, 17]:

$$\sigma_{lg} = 985 - 0.19(T - 933)\ [mJ/m^2] \quad (11)$$

$$\sigma_{lg} = 890 - 0.182(T - 933)\ [mJ/m^2] \quad (12)$$

Generally, a longer time of contact at high temperatures improves the wetting conditions.

In an Al-SiCp system, at usual temperatures of the melts, the following reaction:

4Al + 3SiC ⇔ Al4C3 + 3Si (13)

causes the appearance of an undesirable compound [7].

Silicon, used as alloying element, may prevent the formation of this compound.

Boron carbide reacts with both solid and liquid aluminium. In solid state or for an overheating degree of the melt up to 110°C, it forms Al3BC or AlB2 compounds. Over this temperature Al3BC and Al3B48C2 are produced [18]. The appearance of these compounds is also undesirable because it leads to decomposition of complementary material

On the other hand, increasing temperature a reduction of apparent dynamic viscosity of the mixture occurs.

- heat treatment of dispersed material. A gas film exists on the surface of particles and blocks direct contact between the two components. Also this fine film favours ascension movement of the particles although $\rho_{Al} < \rho_p$ [19, 20].

- alloying or flux treatment of the melt. Some elements introduced in aluminium-based melts assure wetting conditions by:

- reducing of melt surface tension;

- lowering the interfacial energy between the melt and the particle;

- chemical reactions (reactive wetting).

Elements with high affinity to oxygen (lithium or magnesium for example) avoid the appearance of the oxide layer on the surface of the complementary material and diminish interfacial tension.

Introduced in the melt, magnesium creates also advantageous wetting conditions by the diminution of the melt surface tension. Such as, in accordance with Lang's equation, 1 wt% Mg reduces the aluminium surface melt by 5% approximately. Magnesium does not react with silicon carbide. Compared with magnesium tin has a much smaller effect [7, 19].

Titanium improves the wettability of silicon carbide due to the strong affinity for the complementary material constituting TiC, TiSi2 and Ti3SiC2 compounds [7].

Titanium presence in K2TiF6 favours improvement of wetting in Al-B4C system by the appearance of TiB_2 and TiC compounds at the surface of particles [A.R. Kennedy, 2001, Kertli, 2008).

4. Conclusions

Aluminium-silicon or boron carbide composites have low density, high specific properties, hardness and good wear resistance.

Gravitational casting is a simple and inexpensive method to be used for obtaining metallic composites parts.

Non-wetting conditions exist in the two-systems.

The high values calculated for minimum acceleration impose the necessity to apply some simple methods to improve the wetting conditions: overheating of the metallic bath, alloying or flux treatment of the melt.

Titanium leads to the improvement of wetting conditions as a result of the chemical reactions in the melt.

References

[1]. I.A. Ibrahim, A. Mohamed, E.J. Lavernia - *Particulate reinforced metal matrix composites – a review*, Journal of Materials Science 26 (1991), 1137-1156.

[2]. Q. Lin, P. Shen, F. Qiu, D. Zhang, Q. Jiang - *Wetting of polycrystalline* B_4C *by molten* Al *at 1173-1473K*, Scripta Materialia (2009), doi:10.1016/j.scriptamat.2009.02.024.

[3]. B. Previtali, D. Pocci, C. Taccardo - *Application of traditational casting process to aluminium matrix composites*, Composites: PartA (2008), 1606-1617.

[4]. D. Kokaefe, G. Ergin, V. Villeneuve, Y. Kokaefe - *Determination of wetting at elevated temperatures using image analysis*, Archives of Computational Materials Science and Surface Engineering, 1 (2009) 213-224.

[5]. P.K. Rohatgi - *Cast Metal Matrix/Composites*, Metals Handbook, Ninth Edition, Vol. 15, Casting, ASM International (1988) 840-854.

[6]. V. Laurent, D. Chatain, N. Eustathopoulos - *Wettability of* SiC *by aluminium and* Al-Si *alloys*, Journal of Materials Science 22 (1987) 244-250.

[7]. N. Sobczak, M. Ksiazek, W. Radziwill, J. Morgiel, W. Baliga, L. Stobierski - *Effect of titanium on wettability and interfaces in the* Al/SiC *system*, Proceedings of International Conference "High Temperature capillarity", Cracow, Poland (1997) 138-145.

[8]. J. Hashim, L. Looney, M.S.J. Hashmi - *The wettability of* SiC *particles by molten aluminium alloy*, Journal of Materials Processing Technology 119 (2001) 324-328.

[9]. E. Candan - *Effect of alloying elements to aluminium on the wettability of Al/SiC system*, Turkish Journal of Engineering & Environmental Sciences 26 (2002) 1-5.

[10]. I. Kerti, F. Toptan - *Microstructural variations in cast* B_4C*-reinforced aluminium matrix composites (AMCs)*, Materials Letters 62 (2008) 1215-1218.

[11]. P.K. Rohatgi, R. Asthana - *Transfer of Particles and Fibres from Gas to Liquid during Solidification Processing of Composites*, International Symposium of Advances in Cast Reinforced Metal Composites, Chicago, Illinois, U.S.A. (1988) 61-66

[12]. A.S. Kakar, F. Rana, D.M. Ştefănescu -*Kinetics of gas-to-liquid transfer of particles in metal matrix composites*, Materials Science and Engineering, Al 35 (1991) 95-100.

[13]. C. Garcia-Cordovilla, E. Louis, A. Pamies - *The surface tension of liquid pure aluminium and aluminium-magnesium alloy*, Journal of Materials Science 21 (1986) 2787-2792.

[14]. **M. Syversten** - *Oxide Skin Strength on Molten Aluminium*, Metallurgical and Materials Transactions B 37B (2006) 495-504.

[15]. N. Shinozaki, T. Fujita, K. Mukai - *Wettability of* Al_2O_3-MgO *substrates by molten aluminium*, Metallurgical and Materials Transactions B 33 (June 2002) 506-509.

[16]. B.J. Keene - *Review of data of surface tension of pure metals*, International Materials Review 38/4 (1993) 157-192.

[17]. P. Shen, H. Fujii, T. Matsumoto, K. Nogi - *Influence of substrate crystallographic orientation on the wettability and adhesion of* α-Al_2O_3 *single crystals by liquid* Al *and* Cu, Journal of Materials Science 40 (2005) 2329-2333.

[**18]. J.C. Viala, J. Bouix, G. Gonzales, C. Esnouf** - *Chemical reactivity of aluminium with boron carbide*, Journal of Materials Science 32 (1997) 4559-4573.

[19] B.C. Pai, G. Ramani, R.M. Pillai, K.G. Satyanarayana - *Review. Role of magnesium in cast aluminium alloy matrix composites*, Journal of Materials Science 30 (1995) 1903-1911.

[20]. W. Zhou, M.Z. Xu - *Casting of SiC Reinforced Metal Matrix Composites*, Journal of Materials Processing Technology 63 (1997) 358-363,

[21]. A.R. Kennedy, B. Brampton - *The reactive wetting and incorporation of* B_4C *particles into molten aluminium*, Scripta Materialia 44(2001) 1077-1082.

THE ANNALS OF "DUNAREA DE JOS" UNIVERSITY OF GALATI.
FASCICLE IX. METALLURGY AND MATERIALS SCIENCE
N^0. 1 – 2013, ISSN 1453 – 083X

AUTOMOTIVE POWERTRAIN MANAGEMENT

Florin POPA, Edward RAKOSI,
Gheorghe MANOLACHE, Victor RAKOSI
"Gheorghe Asachi" Technical University of Iasi, Romania
email: edwardrakosi@yahoo.com

ABSTRACT

Given the diversity of phenomena that occur during operation of automotive powertrain and their strong impact on the environment, this paper presents a unified approach to these problems. This is a complex pattern study, composed of a mathematical model, a simulation done by inserting subroutines in the software package MATLAB 6.5 and a CATIA V5R16 environment modeling. By customizing the model obtained can define it completely stabilized operating modes of propulsion systems and their dynamic, economic and pollution parameters. This provides, even the design phase, definition of additional constructive and functional criteria against the current, to ensure stable and economic operation, in an area as extensive.

KEYWORDS: automotive powertrain, stable and economic operation

1. Introduction

In the proposed modeling is adopted as a key assumption that the entire car's propulsion system is a mechanical system consisting of solid bodies, connecting inner and outer, with a rigid motion, as outlines in **Fig. 1**. In this figure, I is the reduced moment of inertia of the rotating elements of the propulsion engine, I' is the drive wheels reduced moment of inertia, and I'' is the reduced moment of inertia of the gearbox and main gear elements.

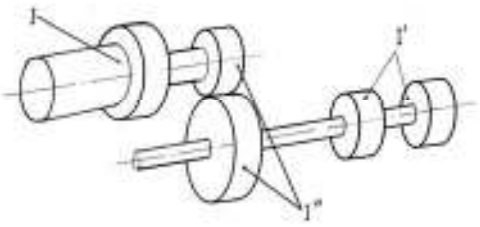

Fig. 1. *Mechanical equivalent of the entire system of the vehicle propulsion*

To study the movement of rigid, in the initial phase is necessary to generate equivalent mechanical model of the propulsion system, which involves calculating in different points the reduced masses of the real system and the corresponding reduced loads. Thus, the mechanical equivalent of automotive powertrain assembly is replaced by an equivalent mass, resulting in the model in **Fig. 2**, whose degree of freedom is given by the angle of rotation.

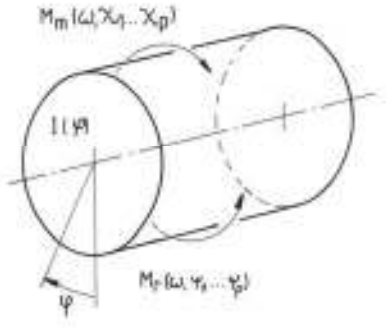

Fig. 2. *The mechanical equivalent of automotive powertrain assembly*

Considering the reduction point at the motor shaft level, mass moment of inertia, I, of the reduced mass is calculated, according to the equivalent kinetic energy criterion, by means of the relationship:

$$I = \sum_{j=1`}^{n_r} I_j \left(\frac{\omega_j}{\omega}\right)^2 + \sum_{i=1}^{n_j} m_i \left(\frac{v_i}{\omega}\right)^2 \qquad (1)$$

where:

I_j - is mass moment of inertia of the rotating j mass;

ω_j - angular velocity of the j mass;

m_i - mass of the i element moving translational;
v_i - speed of the m_i mass;
n_r - number of rotating masses;
ω - angular velocity of low mass I (usually equal to the angular velocity of the shaft to which they reduce).

The mathematical model of evolution of the mechanical equivalent of automotive powertrain assembly is provided as a starting point total energy conservation of I mass condition, so that:

$$d\frac{I(\varphi)\omega^2(\varphi)}{2}=\begin{bmatrix}M_m(\omega,\chi_1,\chi_2,..\chi_p)-\\-M_r(\omega,\psi_1,\psi_2,...,\psi_q)\end{bmatrix}d\varphi \quad (2)$$

and equivalent simplified form is:

$$\frac{\omega^2}{2}\frac{dI}{d\varphi}+I\frac{d\omega}{dt}=M_m-M_r \quad (3)$$

which is actually a mathematical model of mass movement I reduced its axis. Since the mass moment of inertia I variation depending on the angle of rotation φ is small, can introduce approximation,

$$\frac{dI}{d\varphi}=0 \quad (4)$$

equation (3) becomes:

$$I\frac{d\omega}{dt}=M_m-M_r \quad (5)$$

Analyzing this equation shows that the propulsion system operation may occur several situations, depending on the relationship in which the two moments, M_m and M_r. Thus, if the $M_m = M_r$ resulting from (5) that the angular acceleration $d\omega/dt = 0$, so the motor shaft angular velocity is constant. In this situation, powertrain operation is performed in a steady or stable. Equality of torque and moment resistant is done only at the intersection point ***a***, between the output characteristics of the engine and transmission input characteristics, as shown in **Fig. 3**.

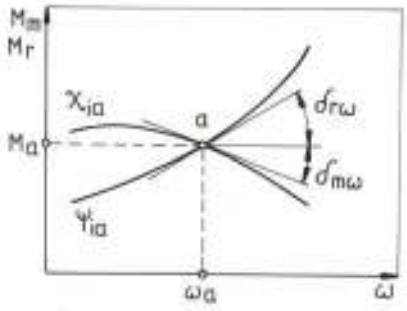

Fig. 3. *Coordinates defining the operating point of the propulsion system*

Coordinates of this point, called point of operation, is the parameters of the engine required power, represented by the torque M_a and the angular velocity ω_a during the stationary regime:

$$P_a = M_a\omega_a \quad (6)$$

Operating point stability analysis by analytical mechanical model involves studying evolution during transient processes. This development is defined by the solution of differential equation (5). Normally, to solve this equation requires knowledge of the functions that describe the output characteristics of the engine and the transmission input characteristics. But using the Taylor series development needs can be assessed in the general case, the performance of these functions in the vicinity of the operation, obtaining:

$$M_m(\omega,...,\chi_i,...)=M_m(\omega_a,...,\chi_{ia},...)+$$
$$+\frac{\partial M_m(\omega_a,...\chi_{ia},...)}{\partial\omega}\frac{\omega-\omega_a}{1!}+...$$
$$+\frac{\partial M_m(\omega_a,...\chi_{ia},...)}{\partial\chi_i}\frac{\chi_i-\chi_{ia}}{1!}+...$$

respectively, (7)

$$M_r(\omega,...,\Psi_i,...)=M_r(\omega_a,...,\Psi_{ia},...)+$$
$$+\frac{\partial M_r(\omega_a,...\Psi_{ia},...)}{\partial\omega}\frac{\omega-\omega_a}{1!}+... \quad (8)$$
$$+\frac{\partial M_r(\omega_a,...\Psi_{ia},...)}{\partial\Psi_i}\frac{\Psi_i-\Psi_{ia}}{1!}+...$$

the notations have the significance of **Fig. 3**.

Accepting a linear variation of characteristics M_m and M_r in the vicinity of the operation ***a***, which involves taking only the terms containing derivatives of order zero and first order of Taylor development and, second, entering the following variable transformations:

$$\omega=\omega_a+\Omega$$
$$\chi_i=\chi_{ia}+\mathrm{X} \quad (9)$$
$$\psi_i=\psi_{ia}+\Psi$$

and notation:

$$\Delta_{kl}=tg\delta_{kl} \quad (10)$$

Narrowing the difference $\Delta_{r\omega}-\Delta_{m\omega}=\Delta$, equation (5) becomes successively simplified forms:

$$I\frac{d\Omega}{dt}+\Delta\Omega=...+\Delta_{m\chi_i}\mathrm{X}_i-\Delta_{r\psi_i}\Psi_j+... \quad (11)$$

or still:

$$I\frac{d\Omega}{dt}+\Delta\Omega=C \quad (12)$$

where C is denoted by the algebraic sum of terms on the right, that is:

$$C=...+\Delta_{m\chi_i}\mathrm{X}_i-\Delta_{r\psi_i}\Psi_i+... \quad (13)$$

which means, in fact, the system disturbance occurs.

Solving differential equation (12) is based on the constant values I, Δ, C. But since, obviously, equivalent mechanical model is non-zero mass, we have $I\neq 0$. In this situation, to solve the equation will consider the following cases further developed.

1. If $\Delta \neq 0$ and $C \neq 0$, above equation becomes:

$$\frac{d\Omega}{C-\Delta\Omega}=\frac{dt}{I} \quad (14)$$

with solution:

$$\Omega=\frac{C}{\Delta}\left(1-e^{-\frac{\Delta}{I}t}\right) \quad (15)$$

2. When $\Delta = 0$ and $C \neq 0$ equation to customize the form:

$$I\frac{d\Omega}{dt}=C \quad (16)$$

with solution:

$$\Omega=\frac{C}{I}t \quad (17)$$

when we consider the initial condition $\Omega(0)=0$.

3. If the parameters defined $\Delta \neq 0$ and $C=0$, equation (12) becomes:

$$I\frac{d\Omega}{dt}+\Delta\Omega=0 \quad (18)$$

Solving the characteristic equation is obtained solution:

$$\Omega=\Omega_0 e^{-\frac{\Delta}{I}t} \quad (19)$$

where Ω_0 is the angular velocity value Ω at baseline, considered to $t = 0$.

If, however, the initial velocity is zero, that is:

$\Omega_0 = 0$

in (19) becomes apparent:

$\Omega = 0$

and

$\omega = \omega_a$

which is understandable because the disturbance is absent, that is $C = 0$.

Where:

$\Omega_0 \neq 0$

solution of the (18) equation remains to form (19):

4. A final case under consideration is given to values $\Delta = 0$, $C = 0$

In this case, equation (12) is also a simplified form, that is:

$$I\frac{d\Omega}{dt}=0 \quad (20)$$

with solution:

$$\Omega=\Omega_0 \quad (21)$$

same question with respect to Ω_0, as for **3**.

With the developed model, based on the solutions (15), (17), (18) and (21) can be extremely useful ***analysis*** of the ***stability of the vehicle propulsion system operation***. The first case analyzed is the situation defined by:

$\Delta < 0$

that is:

$tg\delta_{r\omega} < tg\delta_{m\omega}$

In this case, the angular velocity decreases or increases indefinitely to a change in operating point position ***a***; that, in this case the operating point is ***unstable***.

In the second case, considering the situation:

$\Delta = 0$ şi $C \neq 0$,

which translates into the condition:

$tg\delta_{r\omega} = tg\delta_{m\omega}$

In this case we also get an ***unstable*** operating point.

An interesting case, revealed by this analysis, occurs when $\Delta < 0$, or $\Delta = 0$, but in both cases $C=0$. This case leads to a ***metastable*** operating point. Clearly, this situation should be avoided because any accidental change of the angular speed leading to the change of operating point.

Finally we discuss the case when:

$\Delta > 0$

or

$tg\delta_{r\omega} > tg\delta_{m\omega}$

and

$C \neq 0$

In this case, the angular velocity varies in time, uniquely determined, between the old and new position of operating point. It follows that in this case operating point is ***stable***, a situation particularly advantageous in the operation of vehicle propulsion. If, in addition provided $\Delta > 0$ or $tg\delta_{r\omega} > tg\delta_{m\omega}$ is satisfied the condition $C = 0$, results that the operating point returns to the old position, remaining stable.

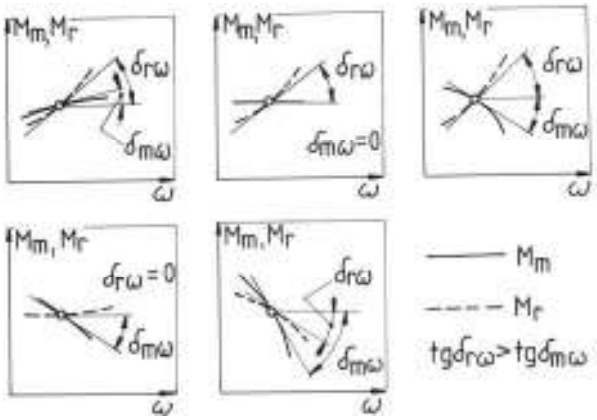

Fig. 4. *The relative positions of the characteristics that determine stable operation*

Modeling done in this phase of work and analysis on it, leading to a *general conclusion* that shows that *to achieve stable operation of automotive propulsion systems is necessary and sufficient for any*

operating point as the slope of the input characteristic is greater than the slope of the output characteristic.

In this sense, the **Fig.4** shows different mutual positioning of the input and output characteristics, leads in all cases to a stable operating point.

2. Simulations

Starting from the mathematical model developed has made a complex simulation of the propulsion system behavior in various constructive-functional situations, called ***MATCEL-PROP***.

The simulation was performed by inserting subroutines in the software package ***MATLAB 6.5*** and ***Excel*** program. Adding a tutorial conducted to facilitate the development program. They could thus reveal a series of theoretical results, described briefly below.

Determination of basic parameters required simulation was made for a typical car, ***VW Golf IV***; significant values are highlighted in **Fig. 5**.

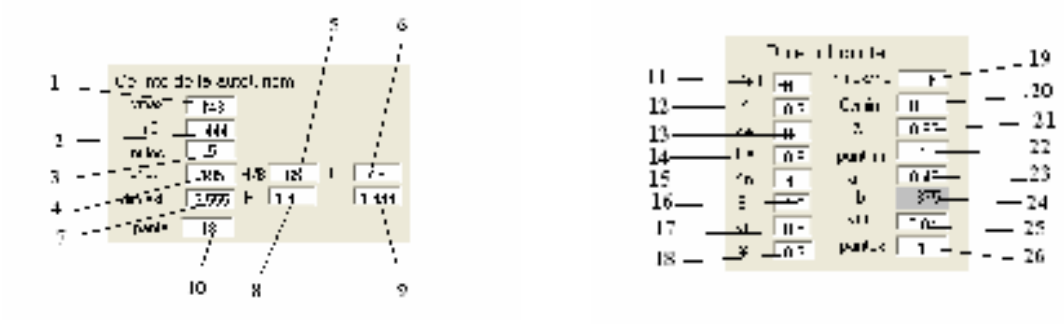

Fig. 5. *Basic parameters related coefficients picture*

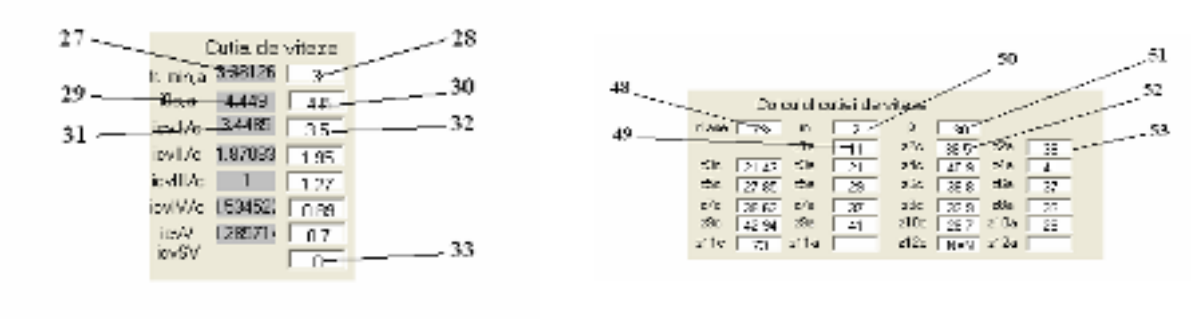

Fig. 6. *Verification of the simulation parameters*

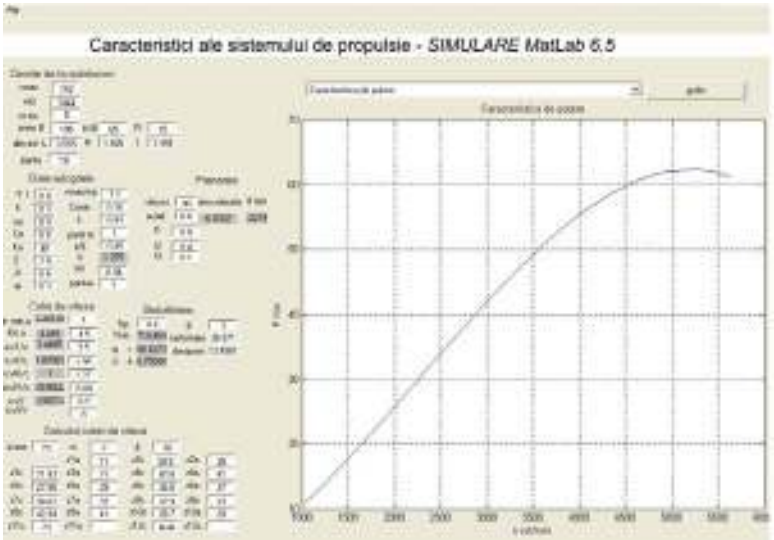

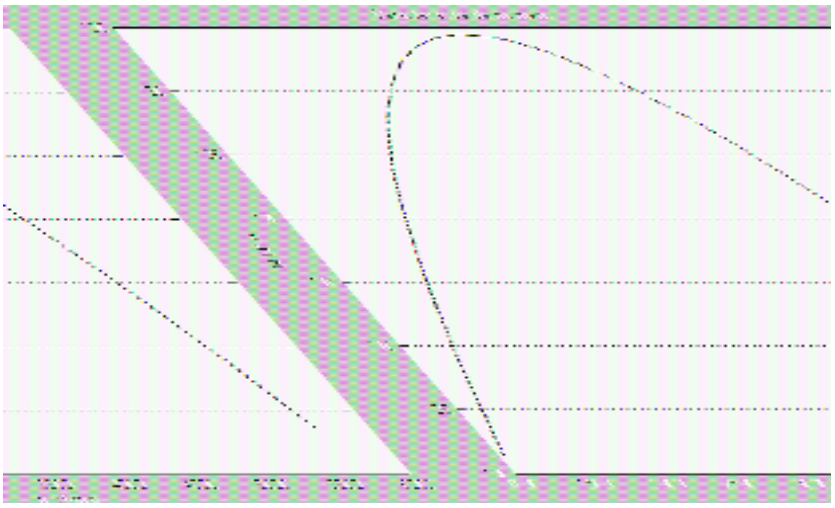

Fig. 7. *Characteristic of the propulsion system*

Fig. 7 highlights *characteristic* of the propulsion system model is chosen, it is the actual power and timing variations in the actual engine propulsion system obtained by simulation, in the form of an executable.

From these raw elements, further presented the most significant results of simulation ***MATCEL-PROP***, looks especially the problem of propulsion system stability. Were considered, in particular, common situation of equipment for the real propulsion system model of car chosen, designed to lead to some conclusions with applicative features, useful in terms of its mechanical and functional optimization. Results are summarized using the variation diagrams of engine torque, M_m, resistant torque reduced to motor shaft, M_{rr} and specific fuel consumption, c_e, depending on the angular velocity ω of motor shaft, presented in figures below.

For each case, algorithm simulation allows determining the position of the system operating point corresponding to maximum speed of the car. On the other hand, in order to emphasize the stability of propulsion, these diagrams contain the tangent lines to variation curves of torques in the operating point, $Fct.tan.M_m$, respectively, $Fct.tan.M_{rr}$. In this respect, a ***first case*** simulated and analyzed (***ES1***) with ***MATCEL-PROP*** considers basic equipment of the propulsion system, which includes an engine having the effective power value 64[kW], assimilated in the model with an engine power (P_e=P_m), and a 15" wheel diameter.

By assigning the value 4 for main gear ratio, i_0, variations in **Fig. 8** shows a ***stable operating point*** at maximum speed of 149 [km/h], and further characterized by an acceptable specific effective fuel consumption, respectively 173[g/kWh].

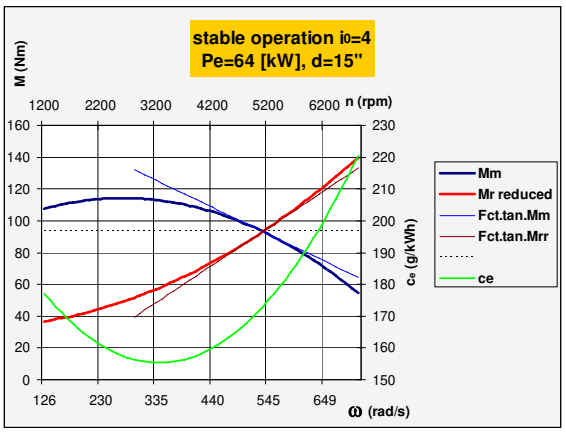

Fig. 8. *Conditions for stable operation of the propulsion system - highlighted by the simulation phase* ***ES1***

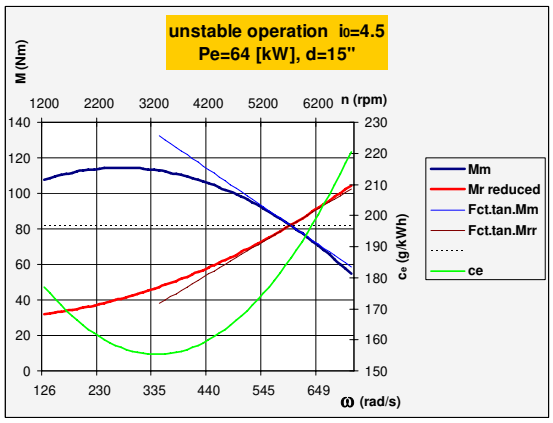

Fig. 9. *Conditions for unstable operation of the propulsion system - highlighted by the simulation phase* ***ES1***

Still increasing main gear ratio by only *0.5*, thus leading to the value i_0 = *4.5,* the propulsion system behavior becomes ***unstable,*** speed decreases slightly the value of 148 [km/h], there the premises so that it can not be kept constant, while the value of specific effective fuel consumption rises to 173 [g/kWh] to 186.4 [g/kWh], situation highlighted by the diagrams in **Fig. 9**. On the other hand, from baseline, summarized in **Fig. 8**, reducing by 0.5 the ratio main gear i_0, it reaches i_0=*3.5,* achieve a ***very stable*** operating point, leading to maximum speed 146.9 [km/h], very stable value, made with a specific effective fuel consumption of 162 [g/kWh], which confirms the downward trend of this important parameter, with increasing stability of the system drive. This condition simulated propulsion system is presented through results obtained in **Fig. 10**.

Continuing the iteration of the ***MATCEL-PROP***, the main gear ratio value i_0=*3* is reached ***extremely stable*** operation of the propulsion system, characterized by a maximum speed value of 136.3 [km/h], in turn extremely constant value, in fact the smallest of speed values highlighted in this stage of the simulation and effective specific fuel consumption decreased to 155.6 [g/kWh], situation presented in **Fig. 11**.

Simulate a situation leading to opposite results as shown in **Fig. 12**, the i_0=*5* value ratio of the main gear reach a ***very unstable*** operation, the operating point is characterized in this case by the speed increased to 144.9 [km/h], but can not be maintained, obtained at engine speed of 6200 [rpm] and effective specific fuel consumption increased to a value of 200.4 [g/kWh].

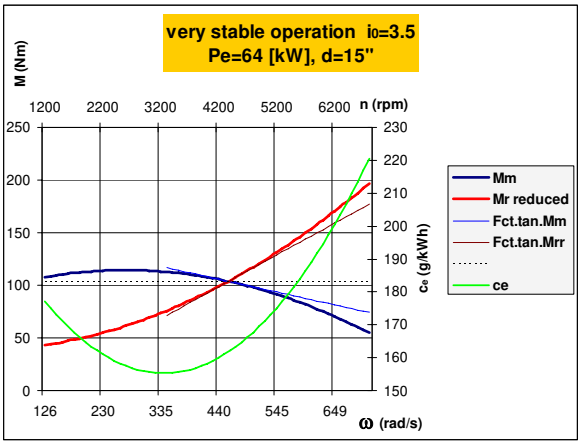

Fig. 10. *Conditions for very stable operation of the propulsion system - highlighted by the simulation phase* ***ES1***

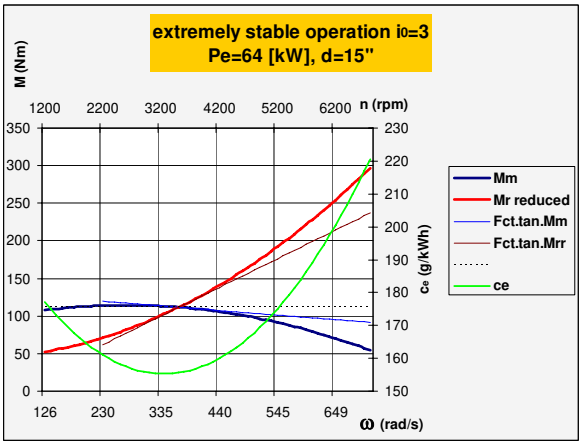

Fig. 11. *Conditions for extremely stable operation of the propulsion system - highlighted by the simulation phase* ***ES1***

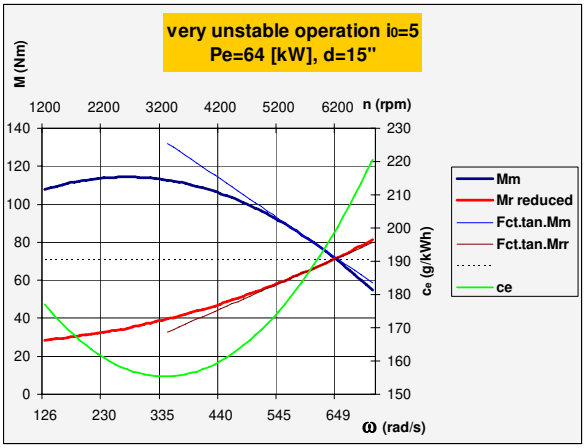

Fig. 12. *Conditions for very unstable operation of the propulsion system – highlighted by the simulation phase* ***ES1***

Simulation performed with ***MATCEL-PROP*** include a ***second phase*** of study (***ES2***), which takes into account the above stable conditions, characterized by the motorization of 64 [kW] and the

main gear ratio value $i_0=4$, but with two-stage change diameter wheels. Thus, a diameter of 15"was increased to 16". The ***third phase*** of study (***ES3***) addressed through simulation ***MATCEL-PROP*** envisages an engine characterized by increased power to 74 [kW], keeping the basic diameter of the wheel motors, thus is 15", but with the i_0 main gear ratio change, with steps of 0.5in the range of normal values. ***Stable*** operation is achieved with the main gear ratio $i_0=3.7$.

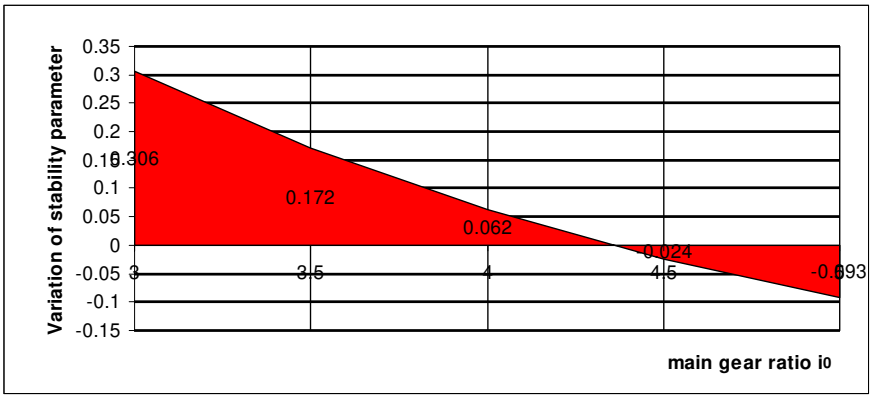

Fig. 13. *Variation of stability parameter with main gear ratio change obtained by simulating* ***MATCEL-PROP*** *for propulsion engine power of 64 [kW]*

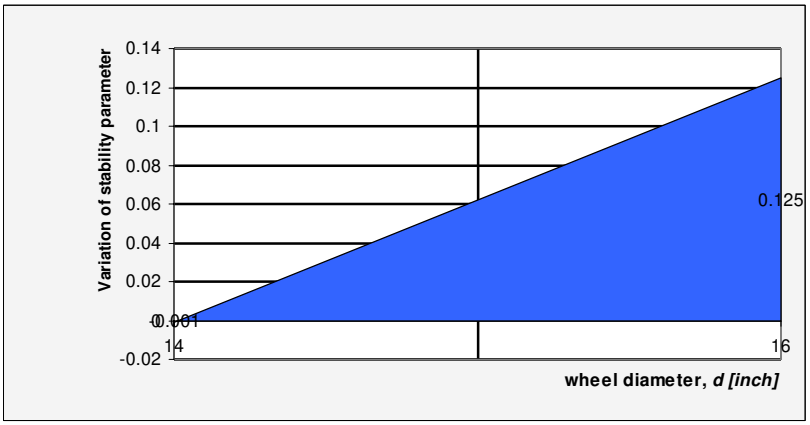

Fig. 14. *Variation of stability parameter obtained by simulating* ***MATCEL-PROP*** *for changing wheel diameter*

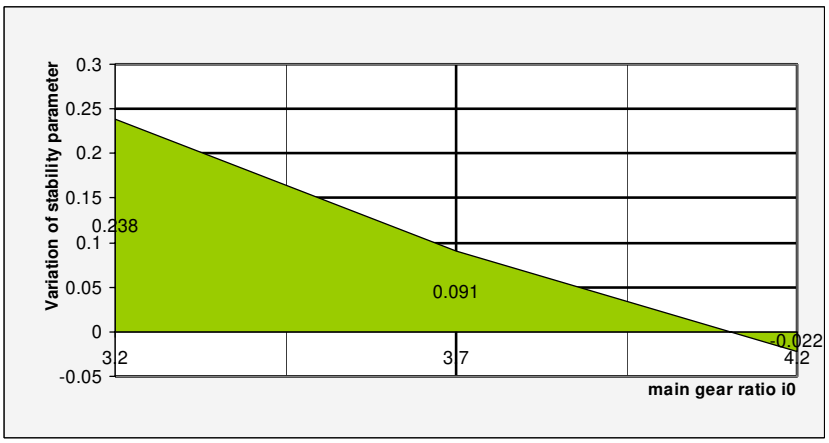

Fig. 15. *Variation of stability parameter with main gear ratio change obtained by simulating* ***MATCEL-PROP*** *for propulsion engine power of 74 [kW]*

The simulation is ***MATCEL-PROP*** addresses equally the ***fourth stage*** of the study (***ES4***), leaving, primarily from reduced engine power, thus is 54 [kW] and secondly, as described above, driving wheel diameter 15". Also, in this case is considered the i_0 main gear ratio change with steps of 0.5.

Initializing the study from i_0=*4.2* is reached to a ***stable*** operating state. The results obtained in the ***four stages of the study*** are summarized in **Fig. 13**, **Fig. 14**, **Fig. 15** and **Fig. 16**, actually describing simulated behavior of the propulsion system, assessed by the **stability parameter variation** Δ.

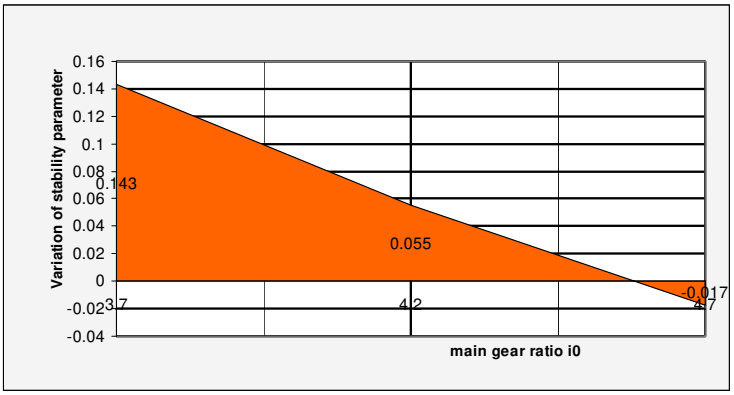

Fig. 16. *Variation of stability parameter with main gear ratio change obtained by simulating* ***MATCEL-PROP*** *for propulsion engine power of 54[kW]*

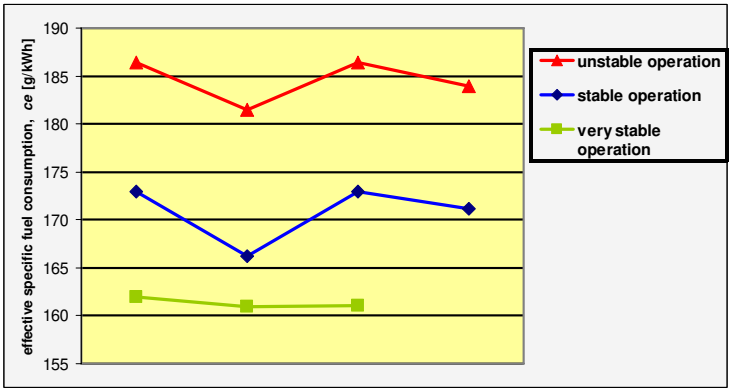

Fig. 17. *Evolution of effective specific fuel consumption values for different states of the propulsion system*

On the other hand, the evolution of specific fuel consumption values for different states of the propulsion system is highlighted in **Fig. 17**. It can thus be noted that increased stability during operation of the propulsion system, values of these inputs are reduced, which is very advantageous. Using the **Fig. 18 a, b, c** shown the variation of these inputs for the three states of the system, and that each state consumption values are very close together, being practically constant regardless of equipment and characteristics of propulsion system that obtains the condition of its.

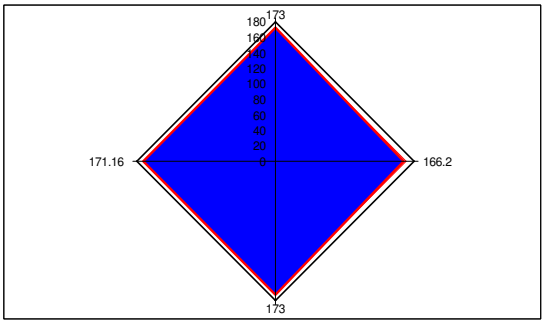

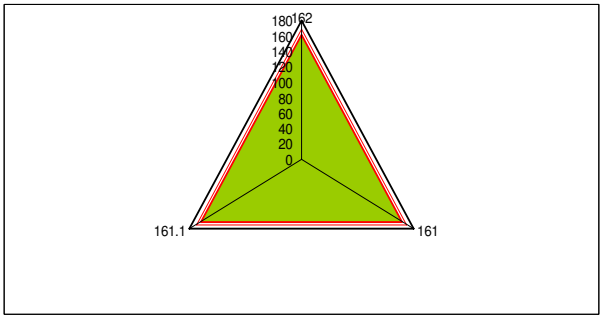

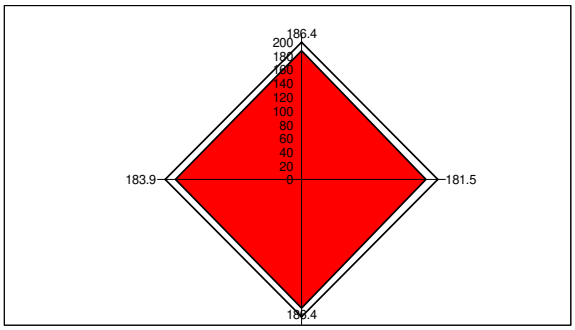

Fig. 18. a, b, c. *The range of values of effective specific fuel consumption corresponding of the three states of propulsion system*

Based on ***MATCEL-PROP*** **simulation**, design using ***CATIA V5R16*** environment has created a ***virtual model of transmission***, as a complex part of the propulsion system for the most stable operating situation highlighted. It was also considered the modeling of dynamic phenomena mainly in order to validate ***the equivalent mechanical model of the propulsion system.***

Since the equivalent model substitute the presence of trees, gears and other rotating masses, specific to propulsion system, also was considered useful an evaluation of a discrete model of the propulsion system, encompassing such elements assimilated in mechanical model.

3. Conclusions

In this work a model study was performed, which allows to define more completely stabilized operating modes of propulsion systems and their dynamic, economic and pollution parameters. This provides early-phase design, construction and functional definition of criteria additional to those present, to ensure stable operation and economic, in an area as extensive, contributing to an integrated management of automotive propulsion systems and the environment.

References

[1]. Heisler, Heinz - *Advanced Engine Technology*, SAE International, (1995).
[2]. Heisler, Heinz - *Advanced Vehicle Technology*, Elsevier Science, Reed Educational and Professional Publishing, 2nd edition, (2002).
[3]. Heywood, J.B - *Internal Combustion Engine Fundamentals*, McGraw-Hill Series in Mechanical Engineering, Library of Congress Cataloging-in-Publication Data, (1988).
[4]. Rakosi, E., Roşca, R., Manolache, Gh. - *Sisteme de propulsie pentru automobile,* Editura "Politehnium" Iaşi, (2006).

THE ANNALS OF "DUNAREA DE JOS" UNIVERSITY OF GALATI.
FASCICLE IX. METALLURGY AND MATERIALS SCIENCE
N^0. 1 – 2013, ISSN 1453 – 083X

QUALITY SURFACE ANALYSIS FOR POLARIZED GRID PLASMA NITRIDING

Mihai AXINTE, Manuela-Cristina PERJU, Carmen NEJNERU, Ion HOPULELE, Iulian CIMPOEŞU
"Gheorghe Asachi" Technical University from Iaşi
email: mihai.axinte@gmail.com

ABSTRACT

For the study regarding the effect of the polarized grid a prototype plasma nitriding facility was used. A polarized grid was placed inside the working chamber, into the space between the anode and cathode, a negative polarised grid.

The sample used for the tests has a special configuration, provided with three different diameter holes, to highlight the hollow cathode effect on the holes near by sample areas.

The chemical analysis for the deposited surface layer was made.

KEYWORDS: plasma nitriding, cathodic active screen grid, hollow cathode effect, scanning electron microscopy

1. Introduction

Plasma nitriding process and, in the last years, plasma nitriding assisted by glow discharge plasma are used for improving surface hardness, fatigue strength, and corrosion or wear resistance of industrial components for a wide range of different applications.

Recently, conventional plasma nitriding has been extensively used for the surface modification of different alloy steels. But, because of different problems in this technique, such as overheating of some parts due to the ''hollow cathode effect'' and non-uniform properties of work pieces by the ''edging effect'' [1], a new method of plasma nitriding, known as active screen plasma nitriding, has been developed [6–8]. Since plasma is generated also on the part and screen surface, the arcing damage and the ''edge effect'' can be avoided by this technique [5]. In this method, the components are surrounded by a metal screen or cage and a negative high voltage is applied to the part and to the screen, so the term ''active screen'' is employed [7]. Thus, the plasma generates on the screen rather than on the component surface, and heats it up. The screen has the major role of modifying the electric field.

Active screen has a role to change the electric field between the anode and cathode in this case the influence of cathode sputtering intensity and the way is this done, "protecting" partially corner and edge areas and areas with holes, where edge effects and hollow cathode may occur [4].

2. Experimental conditions

2.1. Sample preparation

Were used steel samples type 38CrMoAl09. The chemical composition for the used sample is presented in table 1, and it was determined using the Foundry Master spectrometer from the Department of Technologies and Equipments for Materials Processing in the Faculty Materials Science and Engineering from Iaşi.

Table 1. *Chemical composition for 38CrMoAl09 steel*

Element	Fe	C	S	Cr	Mo	Ni	Al	Cu	W	Ti
%	95.4	0.503	0.296	1.49	0.127	0.122	1.17	0.122	0.065	0.016

For the experiment we used a prototype plasma nitriding installation, built into the same department, previously mentioned. The installation is provided with a vacuum chamber, where the termochemical treatment takes place. The part is connected to the cathode and the chamber to the anode. In addition to the classical plasma nitriding facilities this one is provided with an active screen which enclosures the

part. This screen is made by stainless steel grid, by wire with d=0.5mm, holes of 0.5mm (Figure 4). This screen is connected to a DC electric, with variable voltage, electrically insulated by the part. The screen is cylindrical with d=65mm, opened at the bottom and top.

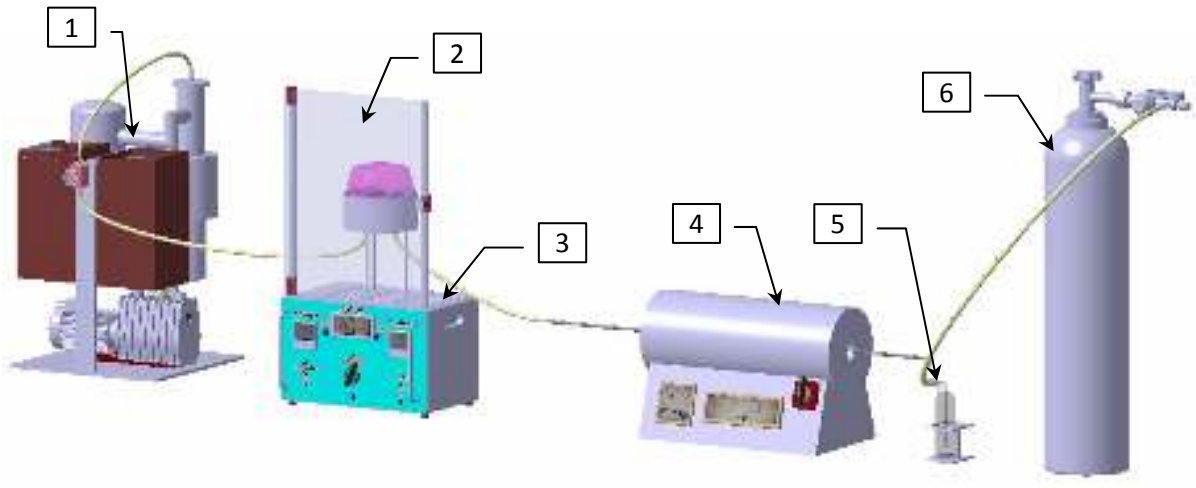

Fig. 1. *The 3D model for the built facility: 1) flow control valve for ammonia 2) vacuum device; 3) electric block and nitriding chamber; 4) ammonia dissociation device; 5) bubble meter; 6) tank of ammonia*

To simulate the real conditions in an industrial facility, and to highlight the hollow cathode effect and the edge effect, a cylindrical shape sample with specific geometry was used.

Perpendicular to the cylinder axis, 3 holes were made into the sample part: d_1=3mm, d_2=4mm, d_3=5mm. The distance between the holes of the axis is 8.75mm (Figure 5).

The installation contains the following main parts:

1. The discharge chamber with the vacuum system and the gas flowing system.

2. Electric installation for power and adjustments**.**

The discharge chamber contains the cathode which is the nitriding element, provided with a thermocouple to measure and to adjust the temperature, the voltage and the intensity discharge, [2]. Also the chamber is connencted to a vacuum chamber which ensures a pressure between up to 10^{-3}Torrs. For washing the working chamber with nitriding agent, the ammonia gas tank is connected to the working chamber through a gas supply pipe, with the flow control capabilities (Figure 1).

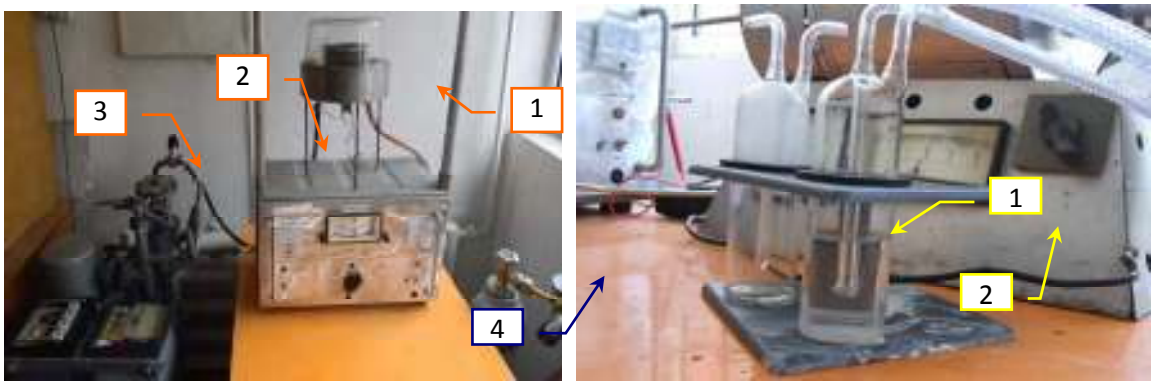

a) b)

Fig. 2. *a) Plasma nitriding installation, partial view: 1) plasma nitriding chamber; 2) electric block; 3) vacuum device; 4) tank of ammonia; b) Plasma nitriding installation detail: 1) bubble metter for gas dosage; 2) ammonia dissociation furnace*

Discharge regime parameters have been stabilized to the following values: temperature T=500˚C, pressure during treatment: P=2torr; cathode voltage: U_k=468V; cathode intensity I_k=0.18A; active screen voltage U_g= 250V, active screen intensity: I_g=0.007A; treatment time: t=7hours.

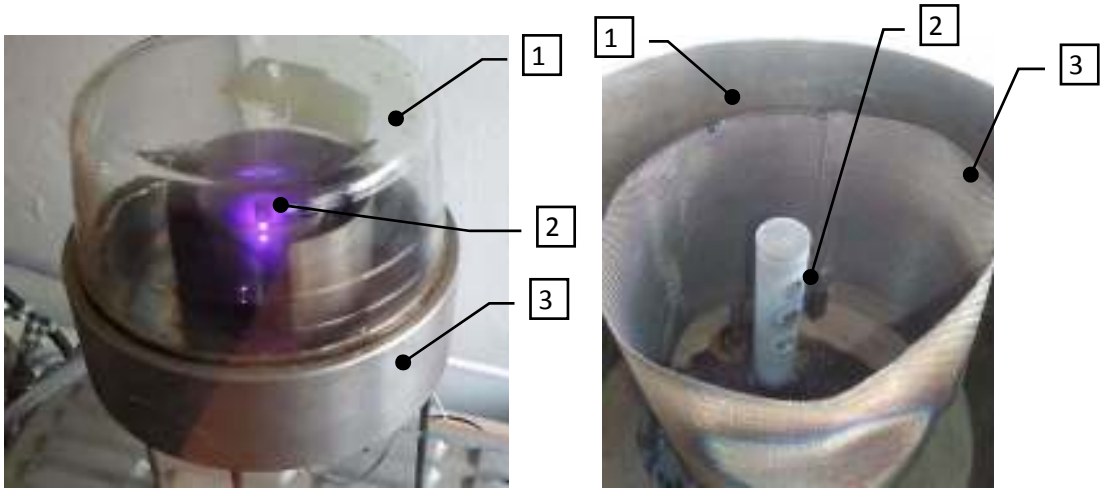

Fig. 3. *a) Discharge halo appearance during active screen plasma nitriding: 1) sealing glass cap; 2) the halo discharge during plasma nitriding; 3) chamber floor; b) appearance of the sample after nitriding: 1) anode; 2) sample; 3) grid active screen*

In this nitriding regime, the hollow cathode effect was completely removed in the small 3 mm hole, for 4 mm diameter hole the hollow cathode is fluctuating, in a transient state, being used as a condition of signaling to maintain the discharge parameters steady, not to reach the condition of occurrence of hollow cathode effect in the 3 mm hole. For the 5mm hole, the hollow cathode effect persisted permanently, as it is presented in Figure 3, where is presented a picture feature for thermo-chemical treatment regime.

After nitriding, the chamber was open, the aspect for the nitrided piece with active screen is shown in Figure 2.

2.2. Surface deposition

Taking into consideration the fact that the specimen studied has three holes with a different diameter and hollow cathode effect acted differently in each of the three holes, a set of micrographs were taken near each of these holes in order to observe the morphology of the deposition for each case. We observed that during ionic nitriding the hollow cathode effect is likely to occur mainly on the hole with 5 mm diameter size.

In this paper the hollow cathode effect and edge effect were studied on the proximity of 5mm diameter hole taking into account the characteristics of deposition with SEM and EDX type analyses. In figure 4 is shown the area next to the 5mm hole edge. Using the electronic scanning microscope, coupled with an EDX type QUANTAX – Bruker detector, the chemical analysis for the deposited surface layer was made.

3. Results and discussion

At high power magnification, 5000x, it is observed that due to the active screen, there was no problems regarding deposition. Because of this, the sputtered cathode surface is less rough than the classical treatment, resulting a uniform deposition.

A set of chemical analyses in three areas situated near the edge of the 5 mm hole was performed. The areas to perform the analysis are illustrated in Figure 5. The tables present the results obtained from the chemical analyses. Thus, in tables 2, 3 and 4 are presented the chemical composition of surface layers in area 1, 2 and 3 respectively, according to Figure 4.

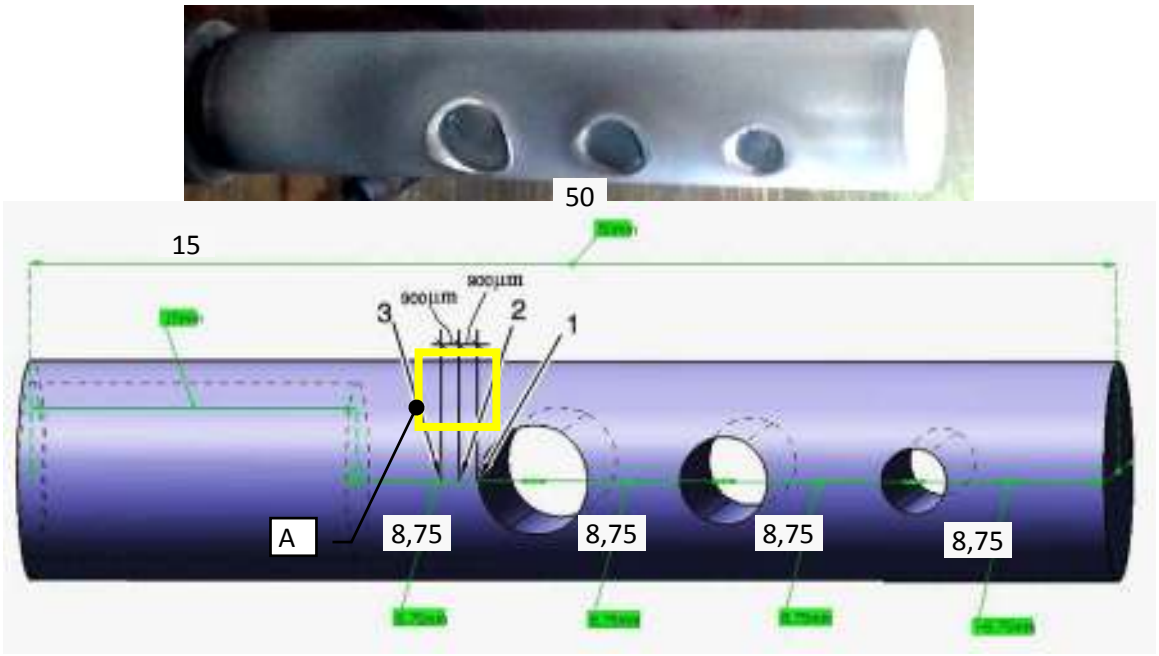

Fig. 4. *Schematic illustration for chemical analyses areas were close to the 5mm diameter hole: 1) edge area; 2) 0.9mm away from the edge; 3) 1.8mm away from the edge; A - area of sampling images close to the 5mm hole*

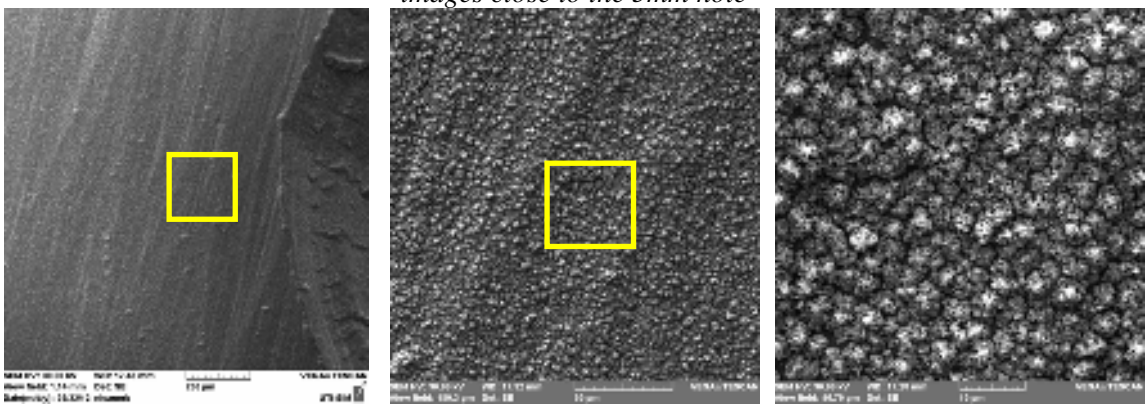

a) b) c)

Fig. 5. *Surface microstructures next to the 5mm hole obtained after plasma nitriding thermochemical treatment with active screen. S.E.M photographs on different scales: a) 200x; b) 1500x; c) 5000x*

Table 2. *Chemical composition of the layer in area 1, near the 5mm diameter hole*

Element	Iron	Nitrogen	Oxygen	Chromium	Carbon	Aluminum	Silicon
%	Balance	7.747	7.111	1.946	0.452	1.117	0.608

Table 3. *Chemical composition of the layer in area 2, 0.9mm near the 5mm diameter hole*

Element	Iron	Nitrogen	Oxygen	Chromium	Carbon	Aluminum	Silicon
%	Balance	9.611	8.289	1.678	1.501	0.921	0.521

Table 4. *Chemical composition of the layer in area 3, 1.8 mm near the 5mm diameter hole*

Element	Iron	Nitrogen	Oxygen	Chromium	Carbon	Aluminum	Silicon
%	Balance	9.092	5.740	1.539	1.531	0.929	0.421

From THE EDX analysis, at can be seen that in zone 1, near the hole there is a lower percentage of N physico-chemical absorbed on the surface – 7.74%, compared to the points located at a specific distance from the hole wall, 9.611% N at 0.9mm in area 2, and 9.092% on the surface at 1.8mm in area 3. The following pictures are graphic representations of distributions of chemical elements in the deposited layer near the 5 mm diameter hole.

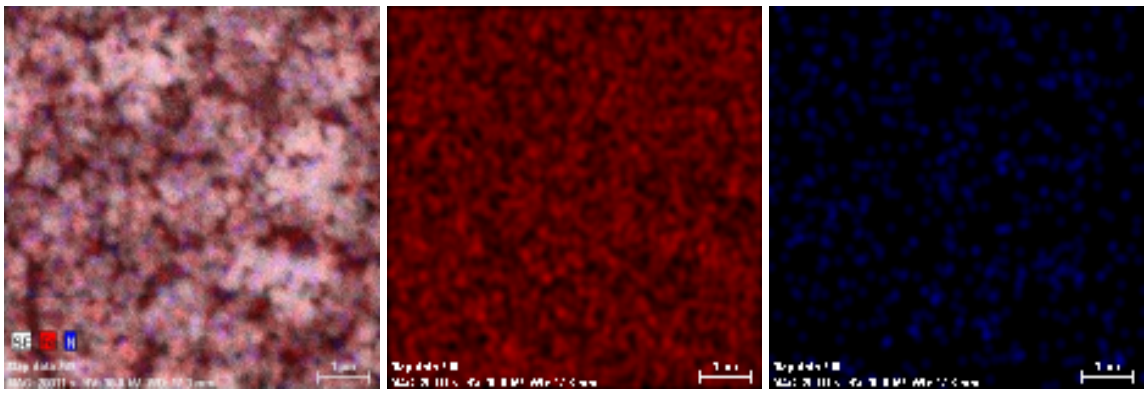

a) b) c)

Fig. 6. *Distributions of chemical elements in the deposited layer near the 5mm diameter hole: a) Fe, N distribution; b) Fe distribution; c) N distribution*

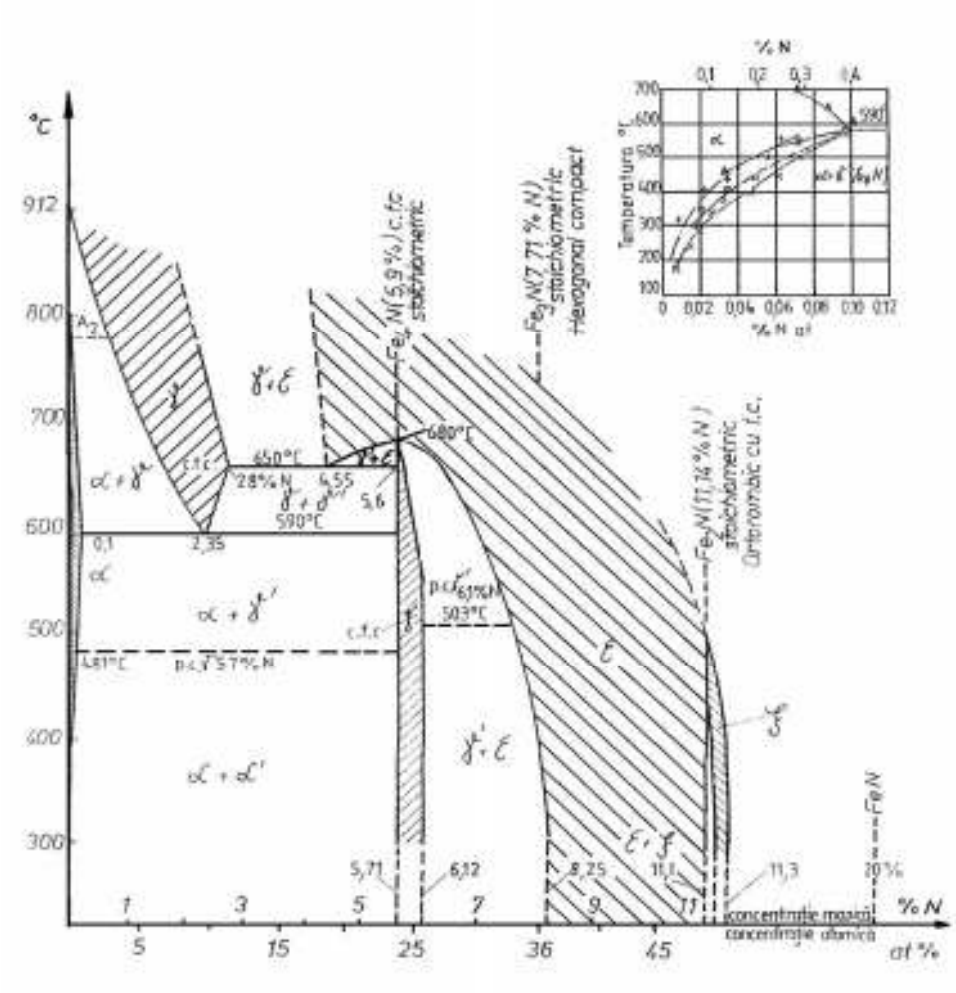

Fig. 7. *Equilibrium diagram for Fe-N alloy*

The study of the EDX analysis in areas 1, 2 and 3 (see tables 2, 3 and 4) shows that near the hole edge, the C and the N percent drops. This is explained by the fact that on the edge there has been a concentration of plasma (two negative glows). Also the hollow cathode effect and the edge effect are competing in that specific circular area. This effect, on classic plasma nitriding meets even stronger in edge areas, and fading color rings are present. This means a more obvious decrease in the amount of C and N, due to the temperature rising because the electrons are accelerated between the opposite surfaces of the walls [6].

If the temperature diffusion process is lower than the eutectoid transformation (591˚C), on the steel surface is formed the first phase α (solid solution of nitrogen in Feα), and when overcome the saturation limit will occur in order the following phases: γ' (nitride Fe_4N) and ε (solid solution based Fe_3N); consequently.

As temperatures drop, α and ε phases decompose and precipitate the γ 'excess phase (Figure 7). Therefore, at room temperature, the phase sequence present in the nitrided layer (from surface to core) is the following: ε→ε+γ'→γ'→α+γ'→α. If nitriding is performed at a temperature above the eutectoid, example 600˚C, α phase is formed first and after the saturation limit of successive phases occur γ, γ' and ε phases occurs. At the diffusion temperature, the nitrided layer will consist of the following phases: ε→ε→ γ' → γ → α [6].

The slow cooling causes decomposition of α and ε phases, precipitates excess γ' phase, while the γ phase undergoes eutectoid transformation, creating a mechanical mixture of α and γ'. Nitrided layer will contain the following phases at room temperature (from surface to core): ε→ε+γ', γ', α+ γ' (eutectoid), α+ γ' (secondary) → α.

Note that the N absorbed on the edge in the structure is less than on the surfaces, due to the fact that the edge temperature is higher than the middle zone and can exceed the amount of 590˚C, [3]. The nitrogen solubility degree in structures at T>600˚C is smaller than T<590˚C.

Usually diffusion is directly proportional to the thermochemical treatment temperature, but for nitrogen it is smaller at temperatures higher than 590˚C and higher at temperatures smaller than this. This results in a smaller thickness of nitrided layer and diffusion layer in edge areas.

4. Conclusions

1. The active screen grid main result is reducing sample surface damage by an intense sputtering, comparing to the classical plasma nitriding technology. This fact is highlighted by the lowest values of the studied surface.

2. The hollow cathode effect generally occurs on the surfaces of parts at a distance less than the cahodic falling distance is decreased by the presence of the grid but not canceled, because in the nearest area to the hole, a slight decarburising is observed and also a slight decreasing nitrogen concentration in the surface layer. For the classical plasma nitriding treatment these effects are much more powerful.

3. The edge effect which is present at classical plasma nitriding treatment showed by the fading color rings on the edge area is almost canceled with this active screen grid technology.

Acknowledgement

This paper was realised with the support of POSDRU CUANTUMDOC "DOCTORAL STUDIES FOR EUROPEAN PERFORMANCES IN RESEARCH AND INOVATION" ID79407 project funded by the European Social Found and Romanian Government.

References

[1]. Alves C. Jr. et al. - *Nitriding of titanium disks and industrial dental implants using hollow cathode discharge*, Surface & Coatings Technology 194, pp 196–202, (2005).
[2]. Axinte M. et. al. - *Facility for study heating and diffusion process, using a ionic triode in a plasma nitriding installation*, Tehnomus XV, Suceava, pp. 223-228, (2009).
[3]. Corujeira Gallo S., Dong H. - *Study of active screen plasma processing conditions for carburising and nitriding austenitic stainless steel*, Surface & Coatings Technology 203, pp. 3669–3675, (2009).
[4]. Janosi S. et al. - *Controlled hollow cathode effect: new possibilities for heating low-pressure furnaces*, Metal Science and Heat Treatment, Vol. 46, Nos.7–8, pp. 310-316, (2004).
[5]. Li C. X. et al. - *Active screen plasma nitriding of austenitic stainless steel*, Surface Engineering, Vol. 18, No. 6, pp. 453-457, (2002).
[6]. Vermesan G., Deac V. - *Procese fizico-chimice la nitrurarea ionica,* Bazele tehnologice ale nitrurarii ionice, Editura Universitatii din Sibiu, pp. 26-35, Sibiu, (1992).
[7]. S.D. de Souza, M. Kapp, M. Olzon-Dionysio, M. Campos - *Influence of gas nitriding pressure on the surface properties of ASTM F138 stainless steel.* Surface & Coatings Technology 204 pp. 2976–2980, (2010).
[8]. K.J.B. Ribeiro et al. - *Industrial application of AISI 4340 steels treateated in cathodic cage plasma nitriding technique,* Materials Science and Engineering A 479 pp 142–147, (2008).

THE ANNALS OF "DUNAREA DE JOS" UNIVERSITY OF GALATI.
FASCICLE IX. METALLURGY AND MATERIALS SCIENCE
N^0. 1 – 2013, ISSN 1453 – 083X

THE BEHAVIOUR OF ACID SLAG IN THE TUNDISH

Sinziana ITTU, Paul Petrus MOGOS
University Politehnica of Bucharest, Faculty of Materials Science and Engineering
email: suzu_joi2@yahoo.com

ABSTRACT

In the tundish, purification of steel is given by the use of an oxide powder on the steel surface. This powder perform several important functions, such as thermal insulation, protection against liquid steel surface oxidation and capturing inclusions from the bath. This paper presents an experiment carried out with an acid powder based on thermal power plant ash to the casting of steel with carbon content from 0.30 to 0.33% and 1.00 - 1.15% manganese. Powder behavior during casting can be summarized as follows: rapid spreading of liquid steel surface, good thermal insulation, revealed by the gradient temperature from the slag. The average specific consumption recorded was very low, 0.4 kg / t liquid steel. It has been analyzed the chemical composition of the slag from the tundish during casting, to prelevate 6 consecutive samples taken during casting. The compositions of these slags were compared to the oxide powder composition initially given on the liquid steel. There was a good absorption of inclusions, as evidenced by the last composition of the analyzed slag sample. There was a strong increase of MnO content and changes in values of the other oxide compounds, such as SiO2.

The paper highlights the experimental slag capacity, a hard acid slag based on thermal power plant ash, to capture the MnO type inclusions, up to 38%. This process can be interpreted as negative, meaning that the acid slag is absorbed from the steel alloying element, manganese.

KEYWORDS: fly ash, covering powder, acid slag, tundish, casting steel

1. Introduction

Many aspects of performing metallurgy require an upgraded role of the tundish, not only as a tundish of the liquid steel, but also this aggregate must be like an active reactor. In this sense, an ideal tundish should have a best mixing of the liquid steel [1], with a view to optimizing the flow conditions, the stability of refractory lining. In the first area, the steel jet flows, while in the following areas reactions to reach completion and for emergence of the inclusions take place. The tundish powder has an important role in the steel cleaning by the catch and the absorption of the inclusions in the liquid slag layer. The tundish powder was an acide powder based on fly ash. The experimentations took place at the Continuous Casting Sector, Steel Plant no. 2, Mechel, Targoviste.

The experimental conditions were the following:

- tundish with attached cover, on the four strand (ø13 mm) continuous casting machine, the cover with two orifices, gunited with magnesia mixes mass, 5 tones operative capacity;
- bloom size: (80x80) ÷(140x140)mm;
- casting speed: 1.4–1.6m/min; medium casting time: 80 minutes/batch;
- steel temperature in the tundish: 1555-1545^{0}C;
- the quality of continuous casting steel: carbon steel for constructions;
- casting series of minimum 2 batches, maximum 4 batches;
- casting without protection stream.

The results of the tundish powder industrial tests, and the conclusions, were presented in the following part of the work.

2. Experimental research

The powder characteristics are shown in table 1, it was used in fourteen casting sequences, each included minimum two batches. The tested powder was administrated through the orifices in the cover of the tundish, 2 bags of 5kg, through each hole.

Table 1. *The main characteristics of experimental tundish powder*

Physical characteristics			
Bulk density	**Humidity**	**Spreading surface**	**Melting temperature**
[g/cm^3]	[%]	[cm^2/220g]	[^{0}C]
0.48-0.56	0.53-max0.6	780-830	1300-1320

Chemical characteristics, %								
SiO_2	**Al_2O_3**	**CaO**	**MgO**	**Na_2O K_2O**	**Fe_2O_3**	**TiO_2**	**MnO**	**I.L***
50-53	15-18	3-4	3.5-4.5	0.7-0.9 2.0-2.5	5.5 -6.5	0.4-0.6	< 0.1	min.15

* ignition lost

Table 2. *Steel quality casting in experiment*

Steel quality	**Chemical composition,** % (main elements)			
	C	**Mn**	**Si**	**Cr**
"60 Grade"	0.30-0.33	1.00-1.15	0.27-0.30	0.19-0.33
	For any steel: max. 0,17 % S; max. 0,03 % P			

In table 2, the compositions of different steel qualities used in the experiments are shown.

When the continuous casting takes place in a covered tundish, the melted powder forms a slag layer that is maintained during the whole series and ensures an optimal thermal isolation of the steel surface. The powder addition at the second batch casting is not necessary, and does not improve the thermal isolation. Hence, at continuous casting series, tundish powder is added only at the beginning of the first batch then the tundish is covered.

The used experimental powder quantity was 20-30kg per batch. It was analyzed the evolution of the slag composition in the tundish during two batches casting in series.

The sampling slag from the tundish, during the continuous casting batches took place as follows:

- the first sample, (P1), was taken after about 15 minutes from the beginning of the casting;
- the second sample, (P2), was taken after casting half of the first batch, at 40 minutes from the beginning of the casting;
- the third sample, (P3), was taken with 3-5 minutes before finishing the casting of the first batch;
- the forth sample, (P4), was taken at the second batch at the beginning of the casting;
- the fifth sample, (P5), was taken after casting half of the second batch, at 120minutes from the beginning of the casting;
- the sixth sample was taken at the ending of the second batch casting.

5. Results regarding the tundish powder behaviour

The powder was easily spread, maintaining the dark grey colour on the steel bath, for about 15 minutes, then the melting process takes place, the dark red slag layer is formed, and this protected the steel, surface. In the tundish liquid steel three temperatures on each batch were measured: the first, at the beginning of the casting, the second at the middle and the last at the end.

The heat losses were very low, the difference between the second temperature registered in the tundish, 1555-1550^{0}C, and the third of about 1550-1545^{0}C, at the end of the continuous casting, was of maximum 5^{0}C. On the other hand, it is known that the covered tundish ensures its own thermal isolation.

The maximum consumption powder to the first casting batch was of 30kg/71 tone, with medium specific consumption 0.42kg/t liquid steel, and minimum quantity of powder used, was 20kg/71 tone, with medium specific consumption of 0.28kg/t steel.

If this powder quantity is reported to the entire series, because at the second batch, another powder quantity is not used, and the medium specific consumption is very low. The tundish slag entrapment capacity of steel inclusions was pointed out through the chemical analysis of the samples.

The classical X-ray diffraction on the melted powder showed amorphous structure mass. At the same time, a few samples from the slags were investigated by scanning analysis, EDS.

A few of these analyses are shown in Figures 3 and 4.

6. Discussions

It is known that the tundish powders based on fly ash form silicate acid slag with high viscosity comparatively to the basic powders and during the melting process thus give amorphous or semi-amorphous slags.

The molten powder composition, table 3, over 60% SiO_2, about 20% Al_2O_3 and very low level of MnO, provides a high absorption capacity of basic oxides.

Table 3. *The main oxide compounds of a molten powder sample*

Chemical analysis, %						
SiO_2	Al_2O_3	CaO	MgO	MnO	Fe_2O_3	I.L.
62.01	19.87	4.97	5.51	0.08	7.60	0.16

Table 4. *The level of chemical analysis of the tundish slag*

Batch-sample	SiO_2	Al_2O_3	MnO
	[%]		
I - P1	51.25	19.27	2.22
I - P2	48.22	17.60	11.22
I - P3	40.58	12.82	32.50
II- P4	38.33	9.70	31.06
II- P5	33.84	7.51	34.88
II- P6	24.30	7.20	38.83

At the same time, the slags that have below 20% Al2O3 content, can very well catch Al2O3 inclusions, when the tundish powder is used to casting aluminium deoxidized steel.

The results of chemical analyses values of the main oxydics compounds in the slag, during the continuous casting of two batches, are shown in table 4 and the graphs, Figures 1 and 2.

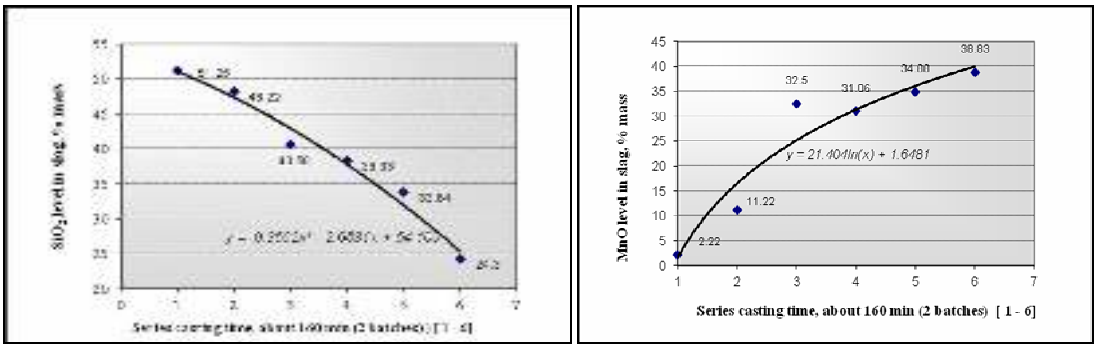

Fig. 1. *The level of SiO_2 and MnO from tundish slag samples during continuous casting*

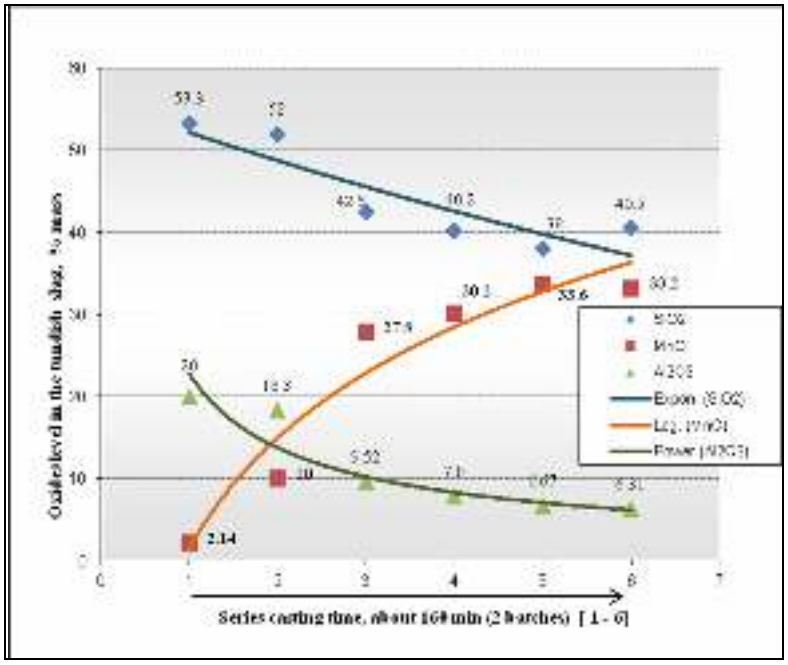

Fig. 2. *The values of main compounds from tundish slag during the experiment*

One of the spot compositions EDAX analysed, on a sample of slag, is shown in Figure 3.

The analysis of the experimental slag inclusions is presented in Figure 4.

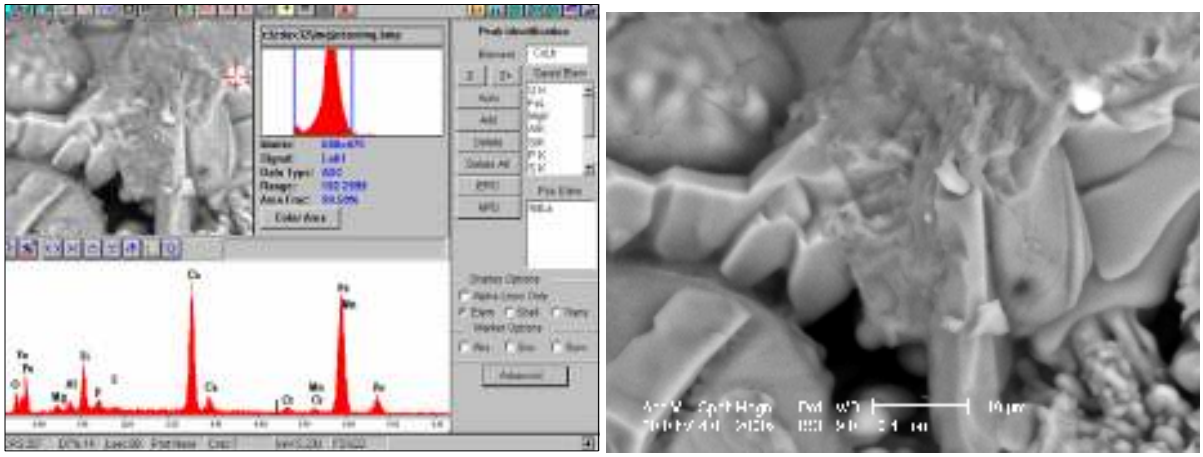

Fig. 3. *Microscopic image of a sample of slag and the elemental composition of a zone*

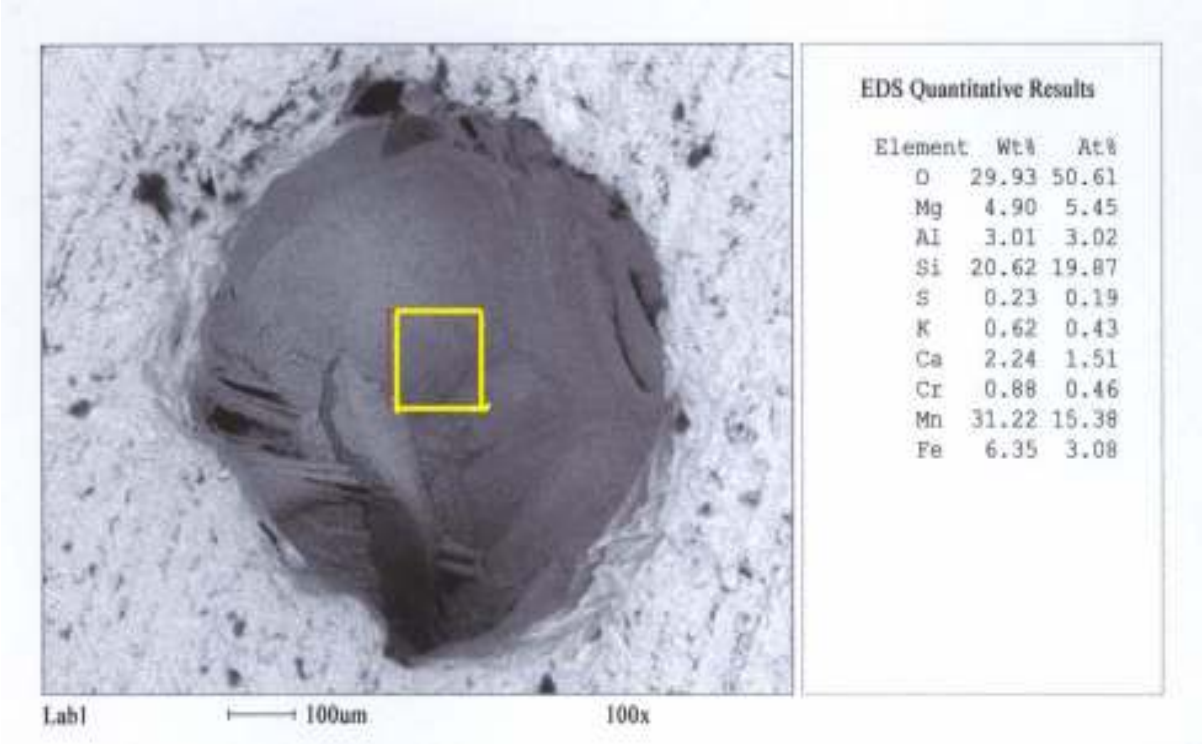

Fig. 4. *The EDS analysis on the last sample slag P6 (an inclusion)*

The data presented in last table show that during the continuous casting of the first batch, an important increase of the MnO content took place, as well as a decrease in the content of the other oxide compounds, SiO_2, Al_2O_3, caused by dilution. For the second batch casting, these tendencies have been maintained: high increasement of MnO content, and decrease of SiO_2 and Al_2O_3 content. The microstructures aspect by EDS, showed a heterogeneous slag.

The elementary composition from the various points of the slag is different, function of the analyzed point location. If the medium composition of these points is calculated, it is observed that there is a relative concordance of the EDS results with the chemical analysis.

In the EDS analyses, many inclusions inserted manganese-silicate, probable tephroite $2MnO \cdot SiO_2$, or, MnO - black globular inclusions it has shown. Light globular inclusions may be magnesia-spinel, $MgO \cdot Al_2O_3$, or wustite $FeO \cdot MnO$, or other silicates. A wide range of solid solubility exists between manganosite (MnO) and several metal oxides, Me(II)-

oxides [2], and it is very difficult to know exactly the identity of the oxide. The industrial tests of tundish powder, based on fly ash, have shown that the formed slag absorbs and partially it dissolves the metallic or nonmetallic, inclusions, especially MnO compounds witch can be dissolved in the silicate network.

The high content of MnO in slag was caused by the presumed reasons:

- the MnO inclusions passing from the casting ladle into the tundish;
- direct oxidizing of Mn in the slag, surface interactions between the slag and the liquid steel; the acid slag oxidizes manganese at the steel interface and retains it. This is a detrimental phenomenon and must be avoided by the usage of the acid powder tundish at the casting of alloyed and micro alloyed steel, with V, Al, Si. The cause of the moderate increase of MgO in the slag is the occuring of refractory inclusions, most often from the tundish lining. At the same time it was observed that the magnesia lining is quite stable, because MgO amount in the last slag is below 7% and the initial composition of powder is about 4%.

7. Conclusions

An acid tundish powder based on fly ash was tested at continuous casting carbon steel and the results of the tests were presented in this paper.

The principal aspects are presented as follows. When the continuous casting takes place in covered tundish, the melted powder forms a bath slag that overcasts the steel surface. This is maintained during the whole casting batches and ensure an optimal thermal isolation.

The evolution of tundish slag composition during casting steel of two batches in sequence has shown the process of cleaning steel. The main oxide compounds of the tundish slag composition were: MnO, SiO_2, MgO and Al_2O_3. The EDS results confirm the amount of inclusions and chemical analysis.

The powder behaviour can be resumed as follows:

1. fast spreading on the steel surface;
2. very good thermal isolation (the gradient in the tundish was about 5^0C);
3. low consumption, the specific consumption was maximum 0,42 kg/ t liquid steel;
4. very good absorption of inclusions, with prevailing MnO.

Formally, regarding the last point, it can be interpreted as it shows, the high capacity of tundish powder based on fly ash, to catch the steel inclusions, thus helping at cleaning continuous casting steel.

This process can be interpreted as negative, meaning that the acid slag is absorbed from the steel alloying element, manganese.

Although the steel quality was not affected by manganese absorption (up to 38%), the manganese colletion in the acid slag is an undesirable phenomenon.

References

[1]. P Tolve, A Praitoni, A Ramacciotti - *Perspectives on tundish metallurgy*, Steel Time, march, (1987).

[2]. R Kiessling, N Lange - *Non-metallic inclusions in steel, Part I: Inclusions belonging to the pseudo-ternary system MnO-SiO_2-Al_2O_3 and related systems*, Second Edition, 1978, book.nr.194, published by The Metals Society, London, UK.

THE ANNALS OF "DUNAREA DE JOS" UNIVERSITY OF GALATI.
FASCICLE IX. METALLURGY AND MATERIALS SCIENCE
N^0. 1 – 2013, ISSN 1453 – 083X

REGENERATION OF USED ENGINE LUBRICATION OIL BY SOLVENT EXTRACTION. THE SOLVENT INFLUENCE ON OIL RATIO

Ancaelena Eliza STERPU, Anca Iuliana DUMITRU, Anişoara Arleziana NEAGU
"Ovidius" University of Constanta
email: asterpu@univ-ovidius.ro

ABSTRACT

Huge amounts of used lubricating oils from automotive sources are disposed of as a harmful waste into the environment. For this reason, means to recover and reuse these wastes need to be found. Problems arising from acid treatment include environmental problems associated with the disposal of acid sludge and spent earth, low product yield (45–65%) and incomplete removal of metals.

The processes of re-refining of used lubricating oils depend greatly on the nature of the oil base stock and on the nature and amount of contaminants in the lubricant resulting from operations. The study was carried out on a sample of 15W40 type of used oil collected from one automobile. The re-refining process of used oil consists of dehydration, solvent extraction, solvent stripping and vacuum distillation. This study aims to investigate a process of solvent extraction of an alcohol–ketone mixture as a pre-treatment step followed by vacuum distillation at 5 mmHg. The primary step was conducted before the solvent extraction that involves dehydration to remove the water and fuel contaminants from the used oil by vacuum distillation. The solvent extraction and vacuum distillation steps were used to remove higher molecular weight contaminants. The investigated solvent to oil ratios was 2, 3, 4, 5 and 6. The solvent composition is 25% 2-propanol, 50% 1-butanol and 25% butanone or methyl ethyl ketone (MEK). The percentage of oil recovery for the solvent to oil ratio of 6:1 is further improved, but for the ratio values higher than 6:1, the operation was considered economically not feasible. Finally, the re-refined oil properties were compared to the commercial virgin lubricating oil properties.

KEYWORDS: regeneration used oil, solvent extraction, vacuum distillation, ash content

1. Introduction

Large and increasing amounts of lubricating oil are produced each year that, after use, are considered a hazardous waste because of their high content of pollutants (thermal degradation products from the base oil and additives and combustion products from the fuel and lubricant). Nevertheless, the used oil still contains a large proportion of valuable base oil that may be used to formulate new lubricants if undesirable pollutants are separated from the oil by an appropriate recycling procedure [1]. Thus, not only environmental but also economical reasons justify the waste oil regeneration process.

The principal obstacle of regeneration process is that cleaning used motor oil by filtering or centrifuging does not ensure that the products of aging, contained in fine particles (0.5–5.0 μm), are not totally removed.

Those contaminants can form sludge and promote the formation of varnish, carbon deposits, and other deposits on engine parts, thus shortening their service life.

Clarification of oil during cleaning to remove mechanical impurities and water is a necessary operation in the technology of reprocessing collected oil, although this requires special conditions and materials and improved equipment. [2].

Used Oil Recovery Processes

There are a large number of physical and chemical processes for reclamation, re-refining and reprocessing of used lubricating oil [3-5]. The earliest process known was the acid–clay treatment process. This treatment involves mixing the used oil with 93 to 98% sulfuric acid. The sulfuric acid acts as an extraction medium for the removal of asphaltenes, unsaturates, dirt, additives, color bodies and other impurities from the used oil. The acid treated oil will be then mixed with clay and filtered to remove mercaptans and other contaminants and to improve oil color. 30-42% of acid sludge can be combusted, whereas the remaining portion is called combustion residual. Problems arising from acid treatment include environmental problems associated with the disposal of acid sludge and spent earth, low product yield (45–65%) and incomplete removal of metals, especially lead. An alternate process using dehydration, distillation and hydro finishing consists in passing feed oil through a flash furnace and a tower to separate water and gasoline fractions. The oil is then heated up to 360–370^{o}C and passed to vacuum fractionators operating at 400^{o}C and 34 mBar. The column separates the oil into light and heavy oil products [6]. The main problems encountered in vacuum distillation processes are plugging of the lines, fractionators and furnace tubes due to formation of a resinous material that fouls the equipment. All modern technologies have included a physical or chemical pre-treatment step in order to avoid or eliminate these problems. Some authors [3, 7] describe a method of treating the dehydrated used oil with a mixture of one part 2-propanol, two parts 1-butanol and one part MEK. The solvent to oil ratio was 3 to 1 by volume. By this treatment the alcohol – ketone mixture will reduce coking and fouling problems during distillation.

2. Experimental results

The experimental procedure of solvent extraction process is presented schematically in Fig.1.

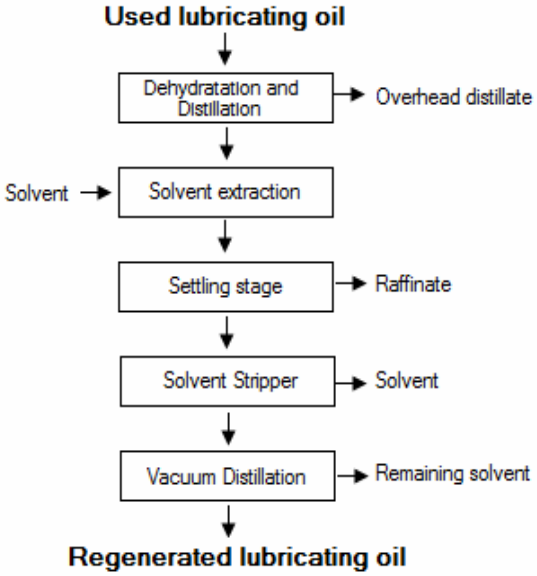

Fig. 1. *Detail of the solvent extraction process*

2.1. Dehydratation

The dehydration of used lubricating oil was performed in a simple batch vacuum distillation (Fig. 2) to eliminate water and light hydrocarbons (gasoline). In this process used lubricating oil is firstly filtrated to remove debris and other solid particles.

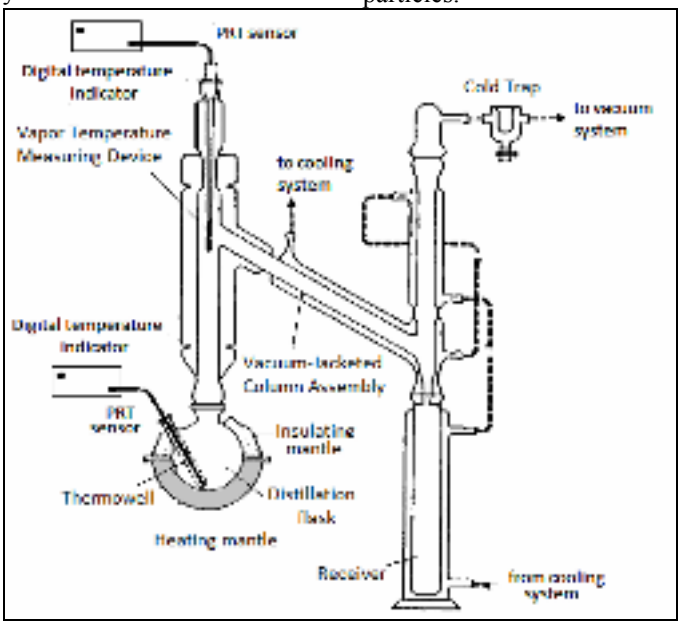

Fig. 2. *Vacuum distillation apparatus*

Water and gasoline fractions were separated under vacuum at 5 mmHg and 210^{o}C (atmospheric equivalent temperature).

Distillation was carried out until no further distillate was produced.

The dehydrated used oil was collected and then used for the next step of solvent extraction.

2.2. Solvent Extraction

The dehydrated used oil was prepared in amount of 100 ml for each experiment. The solvent composition was fixed to one part 2-propanol, two parts 1-butanol and one part MEK (25% 2-propanol, 50% 1-butanol and 25% MEK) as reported by some authors [7]. The main solvent properties are presented in Table.1.

Table 1. *The main solvent properties*

Test	**2-propanol**	**1-butanol**	**MEK**
Formula	C_3H_7OH	C_4H_9OH	C_4H_8O
Molecular weight, g/mol	60.1	74.12	72.11
Density, g/cm^3, at 20^{o}C	0.786	0.81	0.8050
Viscosity, cP at 20^{o}C	2.46	3	0.43
Refractive index, n_d^{20}	1.3776	1.399	1.3788
Boiling point, ^{o}C	82	118	80
Pour point, ^{o}C	-89	-90	-86
Solubility in water g/l	miscible	63.2	275

According to Table 1, there are three solvents in the oil with large differences in boiling point temperature of two of the solvents, i.e., 2-propanol (82^{o}C) and MEK (80^{o}C), compared to the third solvent 1-butanol (118^{o}C). Thus, all atmospheric distillation experiments failed to recover all the solvent amounts at temperature below 250^{o}C, which is the degradation temperature of the oil, while 2-propanol and MEK were successfully recovered at 200 ^{o}C.

The investigated solvents to oil ratios were 2, 3, 4, 5 and 6. Solvent to oil ratio less than 2 produced viscous mixture during separation. For a solvent to oil ratio higher than 6 to 1, the operation is considered economically not feasible. According to these considerations, the solvent amounts added were 200, 300, 400, 500 and 600ml. Adequate mixing of the solvent–oil mixture was obtained by stirring for 30 minutes at 2.5 rot/s. The mixture was allowed to settle for 24 hours in order to separate the extract phase (solvents and base oil components dissolved) from the raffinate phase (contaminants or sludge). Separation of the two phases was carried out in 1 liter separating funnels. The extract phase was red to brown in color and of low viscosity, while the raffinate phase was black and semisolid. This procedure was repeated in all experiments for every solvent to oil ratio.

The extract phase was subjected to simple batch atmospheric distillation to recover the solvent from the oil by heating up to 200^{o}C.

2.3. Vacuum distillation

The vacuum distillation operation is done to recover the remaining 1-butanol from the amount of used oil after the solvent extraction process.

The vacuum distillation experiments were carried out according to ASTM D 1160 - 03 by the vacuum distillation apparatus described in Fig.2. The operation conditions of the vacuum distillation process of the treated oil were at 5mm Hg and 190^{o}C to minimize cracking and to maximize yield.

After each experiment, the vacuum distillation apparatus was washed with *n*-hexane solvent in order to remove any contaminants that accumulated in the column, condenser and vacuum lines. The *n*-hexane washed the contaminants and accumulated them at the bottom of the still pot where they can be removed. After washing, all connections and joints were re-lubricated, and prepared for the next experiment.

Vacuum distillation apparatus

The vacuum distillation apparatus, shown schematically in Fig. 2, consists of the components described below:

- *distillation Flask*, of 500ml capacity, made of borosilicate glass and having a heating mantle with insulating top;
- *vacuum-Jacketed Column Assembly*, of borosilicate glass, consisting of a distilling head and an associated condenser section. The head shall be enclosed in a completely silvered glass vacuum jacket with a permanent vacuum of less than 10^{-7} mm Hg. A vertical glass slide window along the column is available to observe the liquid and vapor behavior in the column. The attached condenser section shall be enclosed in water jackets as illustrated in Fig. 2;
- *vapor Temperature Measuring Device* and associated signal conditioning and processing instruments for the measurement of the vapor temperature. The system must produce readings with an accuracy of ±0.5°C over the range 0 to 400°C. The

location of the vapor temperature sensor is extremely critical. The vapor temperature measuring device shall be centered in the upper portion of the distillation column with the top of the sensing tip 3±1mm below the spillover point.

The vapor temperature measuring device shall be mounted through a compression ring type seal mounted on the top of the glass temperature sensor/vacuum adapter or fused into a ground taper joint matched to the distillation column. The boiler temperature measuring device may be either a thermocouple or PRT.

- *receiver* of borosilicate glass;
- *vacuum Gage*, capable of measuring absolute pressures with an accuracy of 0.01kPa in the range below 1kPa absolute and with an accuracy of 1% above this pressure;
- *cold trap* mounted between the top of the condenser and the vacuum source to recover the light boiling components in the distillate that are not condensed in the condenser section.

3. Results and discussions

Used lubricating oil was analyzed to investigate density, cinematic viscosity, flash point and ash content.

The analysis and tests used for analyzing the oil samples to evaluate their properties were done according to the standard methods as shown in Table 2.

Table 2. *Used lubricating oil properties*

Test	Method	Apparatus	Value
Density, (g/cm^3) at 20^{o}C	ASTM D 7042	Anton Paar SVM 3000	0.896
Viscosity, (cSt) at 20^{o}C	ASTM D 7042	Anton Paar SVM 3000	89
Ash content, % wt.	ASTM D 482-03	-	2.39
Flash point, ^{o}C	ISO 2592	Marcusson open cup	184

Flash point of the used oil showed evidence of gasoline dilution, which has to be removed by distillation during the dehydratation process.

The best dehydration results are obtained at lower vacuum pressure and even though there is a wide range in boiling point between water, gasoline and the base oil cut. Also lower vacuum pressure is preferred to ensure that the temperature will not rise above 250^{o}C, which is the oil degradation temperature. The final dehydration temperature depends on the amount of water and gasoline fractions in the used oil. The concentration of light hydrocarbons after this treatment was expected to be negligible. Both types of compounds are undesirable for the formulation of new lubricants. Elimination of water was also necessary because it may modify the solubility parameter of base oil components in solvent.

The amounts of water and gasoline separated in all dehydratation experiments were small due to low fuel dilution.

The results for mass balance for the optimum solvent to oil ratio experiments are tabulated in Table 3 while the tests percentage of oil recovery and of ash content are presented in Table 4. The properties of produced solvent treated oil, i.e., oil recovery, solvent recovery and ash reduction in relation to solvent to oil ratio are shown in Fig. 3.

Table 3. *Measurements of mass balance for optimum solvent to oil ratio experiments*

Solvent to oil ratio	Oil feed	Solvent	Extract	Raffinate	Extract		
					Oil	Solvent	Loss
	[mL]						
2:1	100	200	265.4	34.6	78.3	185.2	2
3:1	100	300	373.9	26.1	86.4	285.7	1.8
4:1	100	400	478.8	21.2	92.3	384.9	1.6
5:1	100	500	587.8	12.2	95.5	490.8	1.5
6:1	100	600	690.7	9.3	96.1	593	1.6

Table 4. *Test analysis of the optimum solvents to oil ratio experiments*

Solvent to oil ratio	2:1	3:1	4:1	5:1	6:1
Oil recovery (vol %)	78.3	86.4	92.3	95.5	96.1
Ash content (wt%)	1.91	1.45	1.23	1.42	1.87

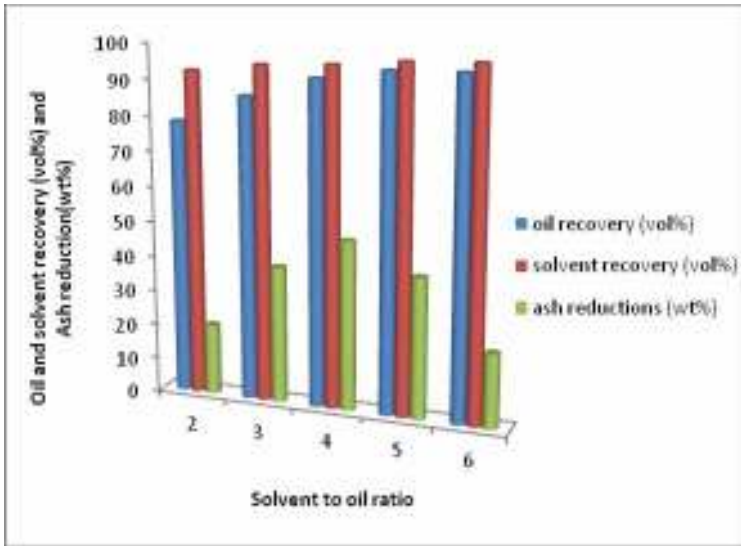

Fig. 3. *The percentage of oil recovery, solvent recovery and ash reduction vs. solvent to oil ratio*

The results of the investigation, Table 4 and Fig. 3 indicate that the maximum ash reduction is achieved for solvent to oil ratio of 4:1. The oil recovery and ash reduction for the same ratio are better than the ones obtained for solvent to oil ratio of 3:1 and 2:1.

This indicates that by increasing the solvent amount, the solvency power is improved. The percentage of oil recovery for the solvent to oil ratio of 6:1 is further improved, but this solvent to oil ratio produces an ash reduction lower than that obtained for the solvent to oil ratio of 4:1 and 5:1 as shown in Fig. 3. Ratios above 3:1 were not considered economically feasible by industry, but considering that the solvent can be recovered and reused, the ratio of 4:1 was considered to be the better solvent to oil ratio for the treatment of used lubricating oil.

A comparison between virgin oil and solvent treated oil (at solvent to oil ratio of 4:1) is presented in Table 5 which shows that the solvent treated oil is more pure than virgin oil as indicated by the lower ash content and the same density value.

Table 5*. Comparison between virgin oil and solvent treated oil properties*

Test	Method	Virgin oil	Solvent treated oil
Density, (g/cm^3) at 20^{o}C	ASTM D 7042	0.890	0.890
Viscosity, (cSt) at 20^{o}C	ASTM D 7042	117.5	98.4
Ash content % wt.	ASTM D 482-03	1.3	1.23
Flash point, ^{o}C	ISO 2592	225	212

The solvent extraction process can be followed by clay treatment or hydrotreatment to improve color and odor of regenerated oil.

4. Conclusion

Four process stages were studied, namely: dehydration, solvent extraction, solvent stripping, and vacuum distillation. The study was carried out on a sample of 15W40 of type used oil collected from one automobile.

All gasoline and water fractions were separated using vacuum distillation at 5 mm Hg and 210^{o}C for the dehydration process. Solvent to oil ratio of 4 to 1 with solvent composition of 25% 2-propanol, 50% 1-butanol and 25% MEK was found to be the optimum composition for solvent extraction. Solvent stripping was conducted by two stages: atmospheric distillation to recover 2-propanol and MEK solvents and vacuum distillation at 5mm Hg to remove the remaining 1-butanol.

Extraction reduces the contaminants (inorganic materials) to low level, i.e. 49% ash reduction, such that no further operational problems were encountered on vacuum distillation.

The best oil recovery and ash reduction by extraction were obtained using optimum evaluated solvent to oil ratio of 4 to 1 with solvent composition of 25% 2-propanol, 50% 1-butanol and 25% MEK were 49% ash reduction and 92% oil recovery. That means that solvent to oil ratio larger than 4:1 will lead to dissolution of some contaminants in the solvent

phase especially the ash forming material, which was considered to be undesirable.

As a result of the above mentioned facts, the solvent to oil ratio of 4:1 was considered to be the best solvent to oil ratio used for treatment of used lubricating oil.

Finally, it should be pointed out that these results can be very useful for the design of the continuous extraction process to recycle waste oil at industrial scale.

References

[1]. Rincon J., Canizares P., Garcia M.T. - *Regeneration of used lubricant oil by ethane extraction*, Journal of Supercritical Fluids, v. 39, p. 315-322, (2007).

[2]. Ostrikov V.V., Prokhorenkov V. D., Nagornov S. A. - *Industrial Ecology. Waste-Free Technology for Processing Used Lubricating Oil*, Chemical and Petroleum Engineering, v.39, n, 5–6, p. 292-297, (2003).

[3]. Whisman M.L., Reynolds J.W., Goetzinger J.E. and Cotton F.O. - *Re-refining makes quality oils*, Hydrocarbon Processing October, p141–145, (1978).

[4]. Ostrikov V.V., Prokhorenkov V.D. - *Waste-free technology for processing used lubricating oil*, Chemical and Petroleum Engineering v. 39, p. 5–6, (2003).

[5]. Bhaskar T., Azhar Uddin M., Muto A., Sakata Y., Omura Y., Kimura K., Kawakami Y. - *Recycling of waste lubricant oil into chemical feedstock or fuel oil over supported iron oxide catalysts,* Fuel v. 83, p. 9–15, (2004).

[6]. Snow R.J., Delaney S.F. - *Vacuum distillation of used lubricating oil,* Chemeca, 77, p. 14–16, (1977).

[7]. Awaja F., Pavel D. - *Design Aspects Of Used Lubricating Oil Re-Refining*, Elsevier Science Publisher B.V., Amsterdam, (2006).

THE ANNALS OF "DUNAREA DE JOS" UNIVERSITY OF GALATI.
FASCICLE IX. METALLURGY AND MATERIALS SCIENCE
N^0. 1 – 2013, ISSN 1453 – 083X

ELECTROCHEMICAL MODIFICATIONS OF TITANIUM AND TITANIUM ALLOYS SURFACE FOR BIOMEDICAL APPLICATIONS – A REVIEW

Eliza MARDARE, Lidia BENEA*, Iulian BOUNEGRU
"Dunarea de Jos" University of Galati, Metallurgy, Materials Science and Environment Faculty,
Competences Center: Interfaces-Tribocorrosion-Electrochemical Systems (CC-ITES),
47 Domneasca Street, RO-800008 Galati, Romania
*Corresponding author
email: Lidia.Benea@ugal.ro

ABSTRACT

The field of biomaterials requires the input of knowledge from very different areas such as biology, medicine and engineering so that the implanted material in a living body to not induce any adverse impacts. The paper focuses its attention mainly on titanium and titanium alloys, even though there are biomaterials manufactured from other metals, ceramics, polymers and composite materials. Both electrodeposition and anodic oxidation surface modification methods are discussed with several examples and a brief description of underlying theory, in order to improve the mechanical, chemical and biological properties of these materials.

KEYWORDS: titanium, titanium alloys, electrodeposition, anodic oxidation

1. Introduction

A biomaterial can be defined as any substance or combination of substances synthetic or biological in origin, used in the treatment of disease or lesion, to resolve pathology that cannot be straightened either by the natural healing process or conventional surgical intervention, using a multidisciplinary approach that requires involvement of science such as biology, medicine, and engineering. Biological biomaterials can be classified into soft (skin, tendon) and hard (bone, dentine,) tissue types. In the case of synthetic biomaterials, it is further classified into: metallic, polymeric, ceramic and composite [1-2]. The fundamental requirement of a biomaterial is that the material and the tissue environment of the body should coexist without having any undesirable or inappropriate effect on each other. The implanted material should not induce any adverse impacts like allergy, inflammation and toxicity either immediately after surgery or under post operative circumstances [3].

The necessity for biomaterials stems from an inability to treat many diseases, injuries and conditions with other therapies or procedures and biomaterials serve to replacement of body part that has lost function, correct abnormalities improve function and assist in healing.

The most important medical applications for biomaterials include orthopedic applications, dental implants, cardiovascular applications, skin repair devices, contact lenses, cochlear replacements, bone plates, bone cement, heart valves, artificial ligaments and tendons.

Metallic biomaterials represent the most highly used class of biomaterials and generally have attributes over other biomaterials in terms of strength, stiffness, toughness, impact resistance, and good processability [4]. The demand for metallic biomaterials is greatly increasing because of aging populations worldwide at a rapid rate and growing demand for a higher quality of life [5].

2. The most essential properties of a metallic biomaterial

In order to be used successfully, metallic biomaterials must have special properties that can be afforded to fulfill the requirements for their intended function, such as mechanical properties, biocompatibility, corrosion resistance, high fatigue and wear resistance.

However, depending on the application, differing requirements may appear. Sometimes these requirements can be completely reverse.

2.1. Mechanical properties

Mechanical properties of a biomaterial must be adjusted to its intended applications otherwise the implant is likely to fail. The mechanical properties such as hardness, tensile strength, modulus, elongation (strain), fracture resistance and fatigue strength or life play an important role in material selection for application in the human body [6].

The most common metals and metals alloys used for implants are fabricated from stainless steel, cobalt alloy and titanium and until nowadays have been used successfully [4-5]. These materials have the requisite strength characteristics but typically have not been resilient or flexible enough to form an optimum implant material. Also many alloys contain elements such as aluminum, vanadium, cobalt, nickel, molybdenum, and chromium which recent studies have suggested might have some long term adverse affects on human patients.

Strength of materials from which the implants are made has an influence on them, so that inadequate strength can cause fractures the implant. When the bone implant interface starts to fail, develops at the interface a soft fibrous tissue by releasing tiny particles of the implant and causes pain to the patient [5,7].

For major applications such as total joint replacement a low Young's modulus equivalent to that of human bone is basically essential in order to prevent bone absorption [8]. These metals typically used for traditional implants have elastic modules much higher than that of bone, for example, cortical bone has a modulus between 15 and 30GPa depending on the type of the bone and measurement direction – while 316 stainless steel has an elastic modulus of about 190GPa and that of cast heat-treated Co-Cr-Mo alloy is about 210GPa. Of these the alloy with the lowest elastic modulus is Ti-6Al-4V with an elastic modulus of about 110GPa [9-10].

Fatigue strength is defined as the highest periodic stress that does not initiate a failure of the material after a given number of cycles. Metal alloys are used for load bearing applications and must have sufficient fatigue strength to endure the rigors of daily activity (walking, chewing etc).

The comparison of mechanical properties of metallic biomaterials with bone is given in table 1 [11].

Table 1. *Comparison of mechanical properties of metallic biomaterials with bone*[*]

Material/ Parameter	Stainless steel	Co-Cr alloy	Pure Ti	Ti-6Al-4V	Cortical bone
Elastic modulus (GPa)	190	210-253	110	116	15-30
Yield Strength (Gpa)	221-1213	448-1606	485	896-1034	30-70
Tensile Strength (Mpa)	586-1351	655-1896	760	965-1103	70-150
Fatigue Limit (Mpa)	241-820	207-950	300	620	-
Density (g/cm^3)	7.9	8.4-9.2	4.5	4.5	-
Elongation (%)	12-40	5-30	15-24	10	1-2

**Adapted from J.B. Brunski. Metals, pp. 37–50 in B.D. Ratner, A.S. Hoffman, F.J. Shoen, and J.E. Lemons (eds.), Biomaterials Science: An Introduction to Materials in Medicine, Academic Press, San Diego (1996).*

2.2. Biocompatibility

There are several characteristics which influence implant biocompatibility. The first is that they should not be toxic to cells.

Toxicology deals with the substances that migrate out of biomaterials. It is convenient to say that a biomaterial should not give off anything from its mass unless specifically designed to do so. If a medical implant is fixed and it kills the surrounding cells, this would clearly cause difficulties for the patient. After a certain period the pain becomes insupportable and the implant must be substituted, a method that is called as a revision [7].

Another important factor is the compatibility of synthetic materials with blood and tissue. Interactions at the tissue-material interface may determine whether a material is tissue compatible and can coexist with the physiological environment.

A common problem with medical implants is rejection, because every biomaterial has the potential to induce biological dysfunctions such as inflammation and infection in the surrounding tissues after implantation [12]. The immune system identifies the substances from the implant as foreign and attempts to fight them and to remove them and so consequently the foreign materials to be extruded or walled off, in case they can not be removed from the body.

The degree of the tissue responses varies according to both physical and chemical nature of the implants. Pure metals tend to evoke a severe tissue reaction, due to the high-energy state or large free energy of them, which tends to lower the metal's free energy by oxidation or corrosion.

2.3. Corrosion

Corrosion, the graded degradation of materials by electrochemical attack, is of concern particularly when metallic biomaterials are placed in the hostile electrolytic environment provided by the human body. The body environment is very aggressive and contains water, complex organic compounds, dissolved oxygen, proteins, and ions such as hydroxide, sodium and chloride, small amounts of potassium, calcium, magnesium, phosphate, sulphate and amino acids [13-14]. These ions react electrochemically with the surface of metallic biomaterials to cause corrosion. The metallic components of the alloy are oxidized to their ionic forms and the dissolved oxygen is reduced to hydroxyl ions. During corrosion process, the total rates of oxidation and reduction reactions that are termed as electron production and electron consumption respectively, must be equal [13]. The corrosion of biomaterials depends on geometric, metallurgical, mechanical and solution chemistry parameters [15].

The nature of the passive oxide films formed, and the mechanical properties of the materials form some of the essential criteria for selection of alternative or development of new materials.

Resistance to corrosion is extremely important for a metallic material because corrosion can lead to rough surface, lower recovery, and release of elements from the metal or alloy. Release of elements can produce discoloration of adjacent soft tissues and allergic reactions in patients [16]. Corrosion products may be involved in causing local pain, tissue reactions and tumefactions in the region of the implant, in the lack of infection [17].

2.4. Wear properties

Wear properties of an implant material are important, especially for various joint replacements because wear of artificial joints releases particles into the body. Wear cannot be discussed without some understanding of friction between two materials. When metallic implant is subjected to wear, the passive layer can be removed allowing active corrosion to occur while the alloy is repassivates [18]. A fatigue wear process involving fretting causes the generation of wear debris which can produce acute host–tissue reactions and tend to aggravate the fatigue problems of the biomaterial by producing enzymes and chemicals (including fast multiplication of local fibroblast-like cells and activated macrophages) that are highly corrosive and finally implant loosening, a major cause of joint implant failure [19].

2.5. Tribocorrosion synergism

Tribocorrosion is a material degradation process which results from simultaneous mechanical (wear) and chemical or electrochemical (corrosion) effects [20]. It is well known in tribology that a corrosive environment can accelerate the wear rate [20-21]. The results obtained are not just a simply summation of the electrochemical and mechanical effects but represents a complex synergy between wear and corrosion [22]. Tribocorrosion behavior cannot be predicted from wear and corrosion taken separately [23]. If for the titanium and its alloys have been conducted and reported several results on their tribocorrosion behavior, the literature reveals the need for more robust testing techniques, in particular the need for analyze the tribocorrosion behavior of the coatings on their surfaces [24-27].

2.6. Osseointegration

Osseointegration is a recently introduced term that indicates a direct biochemical bond between a non-natural substance and a bony tissue [28]. Osseointegration has made possible the development of a number of clinical applications in the field of hand surgery and orthopedics: finger joint prostheses, thumb amputations, amputation of lower limb etc.

The initial observations of osseointegration were made in the 1952 by Professor Per-Ingva Brånemark of Sweden, in an experiment where embedded titanium device into rabbits' leg bones to study bone healing. At the conclusion of the experiment, after a few months he tried to remove these titanium devices and when he discovered that the bone had integrated so completely with the implant that could not be removed [29-30]. Since Branemark made first observations, osseointegration has been intensively studied and the research is ongoing. Osseointegration is a promising technique for providing function and quality of life.

3. Metallic implant materials

Metallic biomaterials are the most suitable for replacing failed hard tissue up to now. Metals and alloys have been widely used in various forms as implants materials in the medical and dental fields such as devices for bone fixation, partial and total joint replacement, external splints, and traction apparatus as well as dental amalgams, crowns, bridges, and dentures, which provide biocompatibility, the required mechanical strength, high corrosion and wear resistance. The commonly used metallic biomaterials are stainless steels, Co-based alloys, and titanium and its alloys.

3.1. The austenitic stainless steels

The austenitic stainless steels especially types 304, 316 and 316L – are used for implants fabrication because of a favorable combination of mechanical properties, good corrosion resistance, low cost,

availability and easy processing when compared to other metallic implant materials [4-5].

The austenitic class of stainless steels is nonmagnetic and offers the most resistance to corrosion in the stainless group, owing to its substantial nickel 8% content and higher levels of chromium 18%.

Types 316 and 316L stainless steels exhibit better corrosion resistance than type 304 or good elevated temperature strength. The "L" grades are used to provide extra corrosion resistance after welding. The only difference in composition between 316 and 316L stainless steel is the amount of carbon that is in the material, 316 has 0.08% maximum carbon content while 316L has a 0.03% maximum carbon content. The carbon is kept to 0.03% or under to avoid carbide precipitation. Carbon in steel when heated to temperatures in what is called the critical range (800 degrees F to 1600 degrees F) precipitates out, combines with the chromium and gathers on the grain boundaries. This deprives the steel of the chromium in solution and promotes corrosion adjacent to the grain boundaries. By controlling the amount of carbon, this is minimized.

Chromium is alloying element that is the essential stainless steel material for conferring corrosion resistance. Chromium has a great affinity for oxygen which allows the formation of a strongly adherent, self-healing and corrosion resistant film of chromium oxide on the surface of the steel Cr_2O_3, film that is too thin to be visible, and the metal remains lustrous [4, 7, 31]. A film that naturally forms on the surface of stainless steel self-repairs in the presence of oxygen if the steel is damaged mechanically or chemically, and thus prevents corrosion from occurring. Molybdenum in the presence of chromium enhances the corrosion resistance of stainless steel. The inclusion of molybdenum enhances resistance to pitting corrosion in salt water. Nickel is another alloying element used as a raw material for certain classes of stainless steel. Nickel provides high degrees of ductility (ability to change shape without fracture) as well as resistance to corrosion. The presence of nickel improves considerably the corrosion resistance when compared to the martensitic and ferritic grades.

Surgical implant application for stainless steel include: wire for surgical sutures, fractures plates, pins, screws hip nails and neurosurgical and microvascular clips [12]. Thus, stainless steels are suitable to use only in temporary implant devices because its fatigue strength that is less than other alloys. The wear resistance of austenitic stainless steel is relatively poor and therefore their use in orthopaedic joint prosthesis as metal-on-metal is limited because of high friction and large number of wear debris particles that occurring, resulting rapid loss of the implant [31]. In order to improve corrosion resistance, wear resistance and fatigue strength of these group of stainless steel, can be used surface modification methods such as anodization, passivation, hard coatings, bioceramics, ion-implantation, biomimetic coatings and glow-discharge.

3.2. Co-base alloys

Co-base alloys are generally used in applications which require wear resistance, corrosion resistance and/or thermal resistance. There are basically two types: one is the castable Co-Cr-Mo alloy, which usually has been used for many decades in dentistry and recently, in making joints, and the other is the wrought Co-Ni-Cr-Mo alloy which is a reletive newcomer now used for making the stems of prostheses for heavily loaded joints such as the knee and hip [4, 7].

Co-Cr alloys have an excellent corrosion resistance (better than that of stainless steel), which is provided by a thin adherent layer and passive of chromium-based oxides with additions of Mo on the surface even in chloride environments [7, 31-33]. Ly et al. [34] in their study they report the identification of different Cr and Co species in the passive films formed under different potentiostatic conditions, which play important roles in alloy passivation. Furthermore, they found that Mo is only present in the oxide layer if the film is air formed, but that it readily dissolves upon exposure to the solution [35]. The dissolution rate of Mo was too low to be measured, indicating that the passive film protected further oxidation of underlying Mo in the alloy [34, 36]. The modulus of elasticity for the Co-Cr alloys does not change with the changes in their ultimate tensile strength. These materials have a high elastic modulus (200–220 GPa) higher to that of stainless steel (approx. 200 GPa), and an order of magnitude higher than that of cortical bone (20–30 GPa) [4,7,32]. This may have some implications of different load transfer modes to the bone in artificial joint replacements, on contact with bone, the metallic devices will take most of the load due to their high modulus, producing stress shielding in the adjacent bone. The lack of mechanical stimuli on the bone may induce its resorption that will lead to the eventual failure and loosening of the implant [31,37].

Carbon additions between 0.1 and 0.3 wt% have been shown to favor the formation of carbides which increase wear resistance.

The Co-Ni-Cr-Mo alloy has a high degree of corrosion resistance to seawater under stres than Co-based alloys. The superior fatigue and ultimate tensile strength of the Co-Ni-Cr-Mo alloy make it very suitable for applications that require a long service life without fracture or stress fatigue.

3.3. Titanium and its alloys

Titanium and its alloys are used extensively for implant materials in the medical and dental fields, and offer many advantages such as superior biocompatibility, corrosion resistance, specific strength, relatively low modulus and strong osseointegration tendency compared with other metallic implant materials [38-39]. Among various titanium alloys, pure titanium and Ti-6Al-4V alloy have been and are still most widely used for biomedical applications. These groups of alloys, as those mentioned above are mainly used for substituting materials for hard tissues.

The greater *corrosion resistance* for titanium and its alloys derives from the spontaneous formation of a titanium oxide film on their surface as long as oxygen is present, its thickness has been evaluated to be approximately 5 nm and which possesses a low level of electronic conductivity [40-44]. This natural oxide layer for commercially pure titanium is composed of titanium oxide in different oxidation states (mainly consists of TiO_2, Ti_2O_3 and TiO), while for the alloys, aluminum, niobium, molybdenum or vanadium are additionally present in oxidized form (Al_2O_3, Nb_2O_5, MoO_2, MoO_3 or V-oxides) oxides which are thermodynamically stable at physiological pH values. The stable oxides are very insoluble in biological fluids and this lead to the excellent localized biocompatibility observed for these classes of alloys [42,45]. This film acts as an electrochemically passive film and inhibits negative ions from invading the matrix of the titanium or its alloys and in this way prevents the ion release or dissolution of titanium and alloyed elements into the body fluids. This high corrosion resistance of titanium alloys can be strongly decreased by damage of the passive film when the bending stress is loaded on the sample, even if the sample itself is not fractured [5,38,40].

The *modulus of elasticity* of these materials is about 100-110 GPa, which is half the value of Co-based alloy and is known that a lowest Young's modulus is favorable for homogeneous stress transfer between implant and bone and it was proved that an implanted Ti reduced biomechanical tissue problems, and the fatigue fracture rate following continuous physiological load-bearing is also far lower than it is with other known metals [12]. Niinomi [8] in his study reported that the level of Young's modulus is effective in inhibiting bone absorption after implantation and on the other hand a lowest Young's modulus, even similar to that of bone present some disadvantages because causes large amounts of shear motion between stem and bone, leading to the formation of fibrous tissue and finally failure.

Strong osseointegration tendency. After implantation, the oxygen atoms in the body fluid naturally react with Ti atoms and form the oxidized layer of titanium oxide (TiO_2), and the newly formed and fully mineralized bone is deposited directly upon the metal surface without any interposition [12].

4. Structure, properties and applications of titanium and Ti-6Al-4V titanium alloy

Depending on their microstructure after processing, titanium alloys may be classified into one of five classes: α, near-α, α+β, metastable β or stable β [46].

Alloying elements in Ti are classified into α, β and neutrals stabilizers on the basis of their effects on the α/β transformation temperature or on their differing solubility's in the α or β phases. Pure titanium exists in form of α-phase at temperatures above 882,5^{o}C and in form of β-phase at temperature below 882,5^{o}C [47]. The temperature of allotropic transformation of α-titanium to β-titanium is called Beta Transus Temperature. The α-stabilizing elements extend the α phase field to higher temperatures, while β-stabilizing elements shift the β phase field to lower temperatures. Neutral elements have only minor influence on the β-transus temperature. In crystallographic form of α-titanium atoms are arranged in hexagonal close packed structure (hcp), and in β-titanium atoms are arranged in body centered cubic structure (bcc) [9,46].

The substitutional element Al and the interstitial elements O, N, and C are all strong α stabilizers and increase the transus temperature with increasing solute content. Among the α stabilizers, aluminum is far the most important alloying element of titanium, because it is the only common metal raising the transition temperature and having large solubilities in both α and β phases. Other α stabilizers include B, Ga, Ge, and the rare earth elements but their solid solubilities are much lower as compared to Al or O and none of these elements is used commonly as an alloying element. The β stabilizing elements are divided into β isomorphous elements (V, Mo, Nb, Ta, Re) and β eutectoid forming elements (Cr, Fe, Si, Ni, Cu, Mn, W, Pd, Bi) depending on the details of the resulting binary phase diagrams. Sufficient concentrations of V, Mo, and Nb elements make it possible to stabilize the β phase at room temperature. The elements Zr and Sn that are found in some Ti alloys are considered to be 'neutral' alloying elements [46].

The α and near-α titanium alloys exhibit superior corrosion resistance but have limited low temperature strength. The β alloys also offer the unique characteristic of low elastic modulus and superior corrosion resistance. The alloys belonging to the α+β system contain one or more α stabilizing element with one or more β stabilizing element.

These alloys retain more β phase after solution treatment than do near-α alloys, the specific amont depending on the quantity of β stabilizers present and on heat treatment. The alpha-beta alloys, when properly treated have an excellent combination of higher strength, ductility and good hot formability. They are stronger than the alpha or the beta alloys due to the presence of both the α and β phases. Ti-6Al-4V is one of the most widely used titanium alloys for biomedical application and in generally is used in the (α+β)-annealed condition. Its total production is about half of all Ti alloys. It is an alpha-beta type containing 6 wt% Al and 4 wt% V. Aluminum is added to the alloys as α-phase stabilizer and hardener due its solution strengthening effect. Vanadium stabilizes ductile β-phase, providing hot workability of the alloy [47].

Applications of Ti-6Al-4V. Titanium is one material which receives equal attentions and interest from both the engineering and medical/dental fields. Because of their lightweight, high specific strength, low modulus of elasticity, and excellent corrosion resistance, titanium materials (both unalloyed and alloyed) have become important materials for the aerospace industry, automotive, surgery and medicine, chemical plant, power generation, oil and gas extraction, sports, and other major industries.

In aerospace industry since the early 1950s, was initially used for compressor blades in gas turbine engines. Today, wrought Ti-6Al-4V is used extensively for turbine engine and air frame applications. Engine components include blades, discs, and wheels. Ti-6Al-4V is used in a variety of airframe applications, including cargo – handling equipment, flow diverters, torque tubes for brakes, and helicopter rotor hubs. In missile and space applications, they are used for wings, missile bodies, optical sensor housings, and ordnance. Also, Ti-6Al-4V castings are used to attach the main external fuel tanks to the Space Shuttle and the boosters to the external tanks. In the automotive industry, wrought Ti-6Al-4V is used in special applications in high – performance and racing cars where is critical , usually in reciprocating and rotating parts, such as valves, valve springs, connecting rods, and rocker arms. It also has been used for drive shafts and suspension springs. Marine applications of wrought Ti-6Al-4V include armaments, sonar equipment, deep – submergence applications, hydrofoils, and capsules for telephone – cable repeater stations. Casting applications include water – jet inducers for hydrofoil propulsion and seawater ball valves for nuclear submarines. Major medical applications of this alloy are: dental applications, orthopedic applications, cardiovascular applications, cochlear implant, implantable cardiovascular devices, extracorporeal artificial organs, biomedical sensor and biosensors, bioelectodes – electrical stimulation and diagnostic devices. The popularity of titanium and its alloys in surgical implants fields can be recognized by counting the manuscripts published in literature reports. Thousands of experimental reports have addressed the excellent biocompatibility of titanium and titanium alloy.

5. Surface modification of Ti-6Al-4V for biomedical applications by electrochemical methods

Surface engineering can play a significant role in extending the performance of medical devices made of titanium and its alloys. Surface properties such composition, roughness and topography are the most important factors that depend on cellular interactions on surface engineering [48]. Surface modification is a process that changes a material's surface composition, structure, and morphology, leaving the mechanical properties intact [49].

Titanium and titanium alloys can not meet all of the clinical requirements because of its poor tribological properties such as poor wear resistance and a high co-efficient of friction which can cause problems [50]. In addition, it is dangerous for Ti-6Al-4V to stay in the human body for a long time because undergoes electrochemical exchange releasing metallic ions in the physiological environment and is known that aluminum element has strong neurotoxicity and vanadium is a strong cytotoxin, and over time, the alloy produced adverse reactions in the body tissues. The release of these elements, even in small amounts, may cause local irritation of the tissues surrounding the implant and sometimes can cause the implant failure [51-53]. Therefore, implants of titanium and titanium alloys are not used without some type of surface modification designed to provide a greater wear resistance and to add biofunction, because biofunction cannot be added during manufacturing processes [49]. Various surface modifications have been used for improving the wear, corrosion behaviour and bioactivity of Ti alloys.

The surface modification recently becomes active in the field of implants. In the biomedical domain, coatings have been used to modify the surface of implants, and sometimes to create an entirely new surface which gives the implant properties which are quite different from the uncoated device. There are a number of methods reported in the literature to modify titanium and titanium alloys for biomedical implants such thermal oxidation [54-56], plasma spraying [57-59], sol–gel method [60-62], biomimetic deposition [63-65], anodic oxidation [66-68], electrophoresis deposition [69-70] and electrochemical deposition [71-74].

5.1. Electrodeposition

Among these techniques which have been developed to deposit bioactive film on titanium and its alloys used for surface modification electrodeposition offers a number of combined advantages such as availability and inexpensive equipment, simple process, rigid control of coatings thickness, complex shapes and low process temperature [71-72, 74]. Electrodeposition parameters include bath composition, pH, temperature, overpotential, additives type, etc., while important microstructural features of the substrate are grain size, crystallographic texture, dislocation, density, and internal stress [75].

Table 2. *Various compositions of electrolytes used for electrodeposition of calcium phosphates*

Composition	**pH**	**Ref**
- 1.46 M $CaCl_2$ - 0.87 M NaH_2PO_4	3.89	[71]
- 0.1 M $Ca(NO_3)_2$ - 0.06 M $NH_4H_2PO_4$ - H_2O_2 10 mL/L	4.3	[79]
- 0.042 mol/L $Ca(NO_3)_2$ - 0.025 mol/L $(NH_4)_2HPO_4$	4.4 adjusted by dilute HNO_3 and NH_4OH	[80]
- 0.042 M $Ca_2(NO_3)_2$ x $4H_2O$ - 0.125 M $NH_4(H_2PO_4)$	4.4	[81]
- 0.04 mol/L $Ca(NO_3)_2$ - 0.027 mol/L $(NH_4)_2HPO_4$ - 0.1 mol/L $NaNO_3$	4.5	[82]
- 0.021 M $CaCl_2$ - 0.0225 M $NH_4H_2PO_4$	4.5	[83]
- 0.61 mM $Ca(NO_3)_2$ - 0.36 mM $NH_4H_2PO_4$	6	[84]
- 137.8 mmol/L NaCl - 1.7 mmol/L K_2HPO_4 x $3H_2O$ - 2.5 mmol/L $CaCl_2$	7.2 Adjusted with tris-hydroxymethylaminomethane $[(CH_2OH)_3CNH_2]$ and hydrochloric acid	[85]
- 1.67 mM phosphate containing salt, in the form of either $NH_4H_2PO_4$ or K_2HPO_4 - 2.5 mM calcium containing salt in the form of either $CaCl_2$ or $Ca(NO_3)_2$	7.2 by addition of tris(hydroxyl aminomethane), (hereafter referred as Tris) and hydrochloric acid	[72]

In order to prevent adverse tissue reactions resulting from hard tissue replacements, a bioinert material, which is stable in the human body and is immune at the interaction with body fluids and tissues, is preferred. Some bioactive materials, such as hydroxyapatite, bioactive glasses and glass ceramics are increasingly used as hard tissue replacements due to their ability to induce bone regeneration and bone in growth at the tissue–implant interface without the intermediate fibrous tissue layer by creating a bone-like apatite layer on their surface after implantation. Apatite formation is currently believed to be the main demand for the bone-bonding ability of materials [46, 76].

Hydroxyapatite $Ca_{10}(PO_4)_6(OH)_2$ (HA) is one of the first materials considered for coating metallic implants due to its close similarity of chemical composition and high biocompatibility with natural bone tissue [71-72]. Calcium phosphates are present in bone, teeth and tendons to give these organs

stability, hardness, and function [77]. Hydroxyapatite has been widely used for many years as a coating material on titanium and titanium alloys as implant devices in dental and orthopedic fields, and the most important reason for that was selected is its ability to accelerate bone in growth onto the surface of implant during the early stages after implantation. There are a number of additional benefits with this coating: faster adaptation of implant and surrounding tissue with reduced healing time, firmer implant bone attachment and the reduction of metallic ion release.

Several compositions of solutions indicated in Table 2, have been used as electrolytes in order to coat calcium phosphates using the electrodeposition method: acidic solution (pH≤4); basic solution (pH>9) and nearly neutral modified simulated body fluid (SBF) (pH=7.2–7.6) [78].

Today electrodeposition is much more than just a coatings technology. Recent literature on the electrodeposition of metallic and nonmetallic coatings containing nanosized particles is intensely investigated. The incorporation of nanosized particles can give an increased microhardness and corrosion resistance, modified growth to form a nanocrystalline deposit and a shift in the reduction potential of a metal ion [75].

Due to the rapid development of nanotechnology, the potential of nano-calcium phosphates has received considerable attention. Recent developments in biomineralization and biomaterials have demonstrated that nano-calcium phosphate particles play an important role in the formation of hard tissues [77]. Literature reports indicate that cumulative adsorption of proteins from body fluids is significantly higher on smaller nanometer grain size materials compared with conventional scale size [77].

In the past decades extensive research on hydroxyapatite coated implants have focused on the tissue–implant interface and also on the problems associated with the coating process and optimization of coating parameters to enhance tissue response [76]. Hydroxyapatite coating of Ti substrate by electrodeposition has been investigated by many research groups [69, 72, 86-87]. Electrochemical deposition of hydroxyapatite coating on titanium surface is an attractive process because irregular surfaces (porous, complex shape of substrate) can be coated relatively quickly at low temperatures and therefore unwanted phase changes could be avoided [72, 82]. Additionally, the thickness, chemical composition and microstructure of the deposit can be well controlled through adequate parameters of the electrodeposition process. Several recent studies have focused on the introduction of intermediate layers, as examples of controlled anodic TiO_2 film, between bioactive HA coating and metal substrate.

5.2. Anodic oxidation

Electrochemical anodizing is one of the simplest among the different techniques employed to form rough, porous and uniform films (generally oxide/hydroxide combination) across which oxygen ions can diffuse and oxidize the substrate, increasing the thickness of the film and in this way decreases ion release, modify and enhances the in vitro corrosion resistance and biocompatibility of Ti and its alloys [88]. Recently, anodic oxidation has become an attractive method for preparing oxide films on titanium, because the porous oxide films insure apatite formation in physiological environment in order to improve implant bioactivity for biomedical applications [66, 88-90]. It is generally accepted that rough and porous surfaces have a more pronounced and beneficial influence on cellular activity than smooth ones [68]. Porous implants layer have lower density than respective bulk and good mechanical strength is provided by bulk substrate [91].

Electrochemical anodic oxidation is an electrochemical process, which after application of direct-current voltages to electrodes immersed in electrolyte leads to oxidation of metal anode that forms a solid oxide layer on the surface [92]. The type, concentration and pH of electrolyte solution as well as the electrochemical parameters such as the applied current density, the voltage, the time of oxidation can affect the surface morphology, the chemical composition and the crystalline structure of the oxide films formed by anodic oxidation [93-95].

The electrolytes most commonly used to anodize Ti and its alloys are sulphuric and phosphoric acids at different degrees of dilution and Ca-P based solutions [93, 96]. An important condition which the electrolyte solution must meet is that should not chemically attack the growth of oxide, to prevent its dissolution during the anodization process, or at least it should be guarantee that the oxide growth percentage is higher than the dissolution one [93]. The rate of anodic film formation is much higher than its dissolution rate in acidic electrolytes like sulfuric acid, acetic acid, and phosphoric acid compared to alkaline electrolytes [97-98].

The electrical potential difference imposed between cathode and anode and the current density imposed to reach that value of potential difference can vary within a wide range of values. In fact, low potentials (1–130V) causes the formation of a smooth, amorphous oxide, about 3–300 nm thick, whose color changes as a function of thickness and, consequently, of applied voltage (interference color) [93, 99]. On the contrary high potentials (100–500 V), combined with high current densities, are the parameters used in anodic spark deposition (ASD) processes, which lead to a crystalline or semi-crystalline oxide that can range from few tens to

hundreds micrometers thick [93, 99]. The crystal structures of the titanium oxide have revealed different oxide structures at different thickness: TiO_2 with anatase structure was observed at 90 V [91, 100], mixture of anatase and rutile structure was formed at 155V and a single rutile phase was produced at 180V, respectively [91, 100].

The properties of anodic oxide films strongly depend on their composition, structure, and thickness. As the voltage increases, the thickness of the layer also increases and particular colors will arise at specific voltage rates. The transition from one color to another is not evident defined, but rather by nuances gradually through a limited spectrum. The apparent color transmitted to the metal is induced by interference between specific wavelengths of light reflecting off the metal and oxide coated surface [101]. Light which crosses through the oxide layer, then reflecting off of the metal, must pass farther than light reflecting directly off the surface of the oxide. If one wave type is not synchronized with the other, they will annul each other out, making that color "darker" or invisible. If through the thickness of the oxide layer is obtained a wave pattern whose path is similar to the path of a certain wavelength of light and it closely follows its path, then the wave amplitude will be increased, and this color would appear brighter. When the wave patterns cancel each other, the process it is called destructive interference, and when they match, it is constructive interference. Sometimes it is possible that the thickness of the oxide layer to create a combination of effects at the same time.

The main reactions leading to oxidation at the anode are as follows [46]:

At the Ti/Ti oxide interfaces:

$Ti \leftrightarrow Ti^{2+} + 2e^-$

At the Ti oxide/electrolyte interface:

$2H_2O \leftrightarrow 2O^{2-} + 4H^+$ (oxygen ions react with Ti to form oxide),

$2H_2O \leftrightarrow O_2$ (gas) $+ 4H^+ + 4e^-$ (O_2 gas evolves or stick at electrode surface).

At both interfaces:

$Ti^{2+} + 2O^{2-} \leftrightarrow TiO_2 + 2e^-$

The titanium and oxygen ions resulted from these redox reactions are actuated through the oxide by the externally applied electric field thus achieving the oxide film. Is know that titanium oxides obtained by anodic processes have a high resistivity relative to the electrolyte solution and the metallic components of the electrical circuit and therefore the applied voltage drop will mainly occurs across the oxide film of the anode.

As long as the electric field is high enough to lead the ions through the oxide, a current will flow and the oxide will continue to grow [46].

6. Conclusions

In this review, an overview of metallic implant application especially Ti and its alloy and the need of electrochemical surface modification methods used to improve the mechanical, chemical and biological properties of these have been given. The properties of titanium and its alloys can be upgraded to some extent after their surfaces are modified by electrochemical anodic oxidation and electrodeposition of HA.

Electrodeposition of HA to the titanium substrate is of utmost importance for the implant to function properly in physiological conditions. The application and prospective use of nano-calcium phosphate in the biological repair of bone and enamel are promising work. It is suggested that nano-HA may be the ideal biomaterial due to its good biocompatibility and bone/enamel integration.

One possible solution to improve the adhesion is to form an intermediate bonding layer between the titanium substrate and the HA coating, by anodic oxidation method. As a result of this anodic treatment, the surface of the Ti substrate is much rougher and porous. In summary, researches performed until now suggested that the anodic oxidation method followed by electrodeposition of HA is an effective way to prepare bioactive titanium surfaces.

With the development of the surface engineering, more new surface modification technologies will be introduced to improve the properties of titanium and its alloys for meeting the clinical needs.

Acknowledgements

The authors gratefully acknowledge both Bilateral Research Agreement between Competences Center: Interfaces-Tribocorrosion-Electrochemical Systems (CC-ITES) from Dunarea de Jos University of Galati and Department of Metallurgy and Materials Engineering (MTM) from Katholieke Universiteit Leuven and research project CEA-IFA C2-02 / 01-03-2012.

References

[1]. G. Binyamin, B.M. Shafi, C.M. Mery - Seminars in Pediatric Surgery **15**, 276 (2006).

[2]. B.D. Ratner, S.J. Bryant, - Annu. Rev. Biomed. Eng. **6**, 41 (2004).

[3]. G. Manivasagam, D. Dhinasekaran, A. Rajamanickam - Recent Patents on Corrosion Science **2**, 40 (2010).

[4]. M.B. Nasab, M.R. Hassan - Trends Biomater. Artif. Organs, **24**, 69 (2010).

[5]. K.H. Frosch, K.M. Stürmer - Eur J Trauma **32**, 149 (2006).

[6]. D.H. Kohn - Curr. Opin. Solid. State Mater. Sci. **3**, 309 (1998).

[7]. J. Alvarado, R. Maldonado, J. Marxuach, R. Otero - Mech.

Mater.–**I**, INGE 4011, 1 (2003).
[8]. M. Niinomi - Journal of the Mechanical Behavior Of Biomedical Materials **I**, 30 (2008).
[9]. M. Long, H.J. Rack - Biomaterials **19**, 1621 (1998).
[10]. K. Wang - Mater. Sci. Eng. A **213**, 134 (1996).
[11]. J.B. Brunski. **Metals, pp. 37–50 in B.D. Ratner, A.S. Hoffman, F.J. Shoen, and J.E. Lemons (eds.)** - Biomaterials Science: An Introduction to Materials in Medicine, Academic Press, San Diego (1996).
[12]. H. Suh, Yonsei - Med. J. **39**, 87 (1998).
[13]. U.K. Mudali, T.M. Sridhar, B. Raj - Sadhana **28**, 601 (2003).
[14]. D.C. Hansen - The Electrochemical Society Interface 31 (2008).
[15]. J.J. Jacobs, J.L. Gilbert, R.M. Urban, J Bone - Joint Surg Am. **80**, 268 (1998).
[16]. N. Adya, M. Alam, T. Ravindranath, A. Mubeen, B. Saluja - J. Indian Prosthodont. Soc. **5**, 126 (2005).
[17]. D. Sharan - Orthopaedic Update (India) **9**, 1 (1999).
[18]. M.A. Khan, R.L. Williams, D.F. Williams - Biomaterials **20**, 765 (1999).
[19]. S.H. Teoh - Int. J. Fatigue **22**, 825 (2000).
[20]. Y. Yan, A. Neville, D. Dowson, S. Williams - Tribol. Int. **39**, 1509 (2006).
[21]. J.R. Goldberga, J.L. Gilbert - Biomaterials **25**, 851 (2004).
[22]. M. Azzi, J.A. Szpunar - Biomol. Eng. **24**, 443 (2007).
[23] D Landolt - J. Phys. D: Appl. Phys. **39**, 3121 (2006).
[24] S. Barril, S. Mischler, D. Landolt - Wear **256**, 963 (2004).
[25]. J. Komotori, N. Hisamori, Y. Ohmori - Wear **263**, 412 (2007).
[26]. H. Ding, Z. Dai, F. Zhou, G. Zhou - Wear **263**, 117 (2007).
[27]. S. Kumar, B. Sivakumar, T.S.N.S. Narayanan, S.G.S. Raman, S.K. Seshadri - Wear **268**, 1537 (2010).
[28]. T. Albrektsson, C. Johansson - Eur. Spine. J. **10**, 96 (2001).
[29]. R. Brånemark, P.I. Brånemark, B. Rydevik, R.R. Myers - J. Rehabil. Res. Dev. **38**, 175 (2001).
[30]. R. Dimitriou, G.C. Babis - J Musculoskelet Neuronal Interact **7**, 253 (2007).
[31]. M. Navarro, A. Michiardi, O. Castaño, J.A Planell - J. R. Soc. Interface **5**, 1137 (2008).
[32]. J.J. Ramsden, D.M. Allen, D.J. Stephenson, J.R. Alcock, G.N. Peggs, G. Fuller, G. Goch - Annals of the CIRP **56**, 687 (2007).
[33]. R. Zupančič, A. Legat, N. Funduk - Mater. Tehnol. **41**, 295 (2007).
[34]. Y.S. Li, K. Wang, P. He, B.X. Huang, P. Kovacs - J. Raman. Spectrosc. **30**, 97 (1999).
[35]. A.W.E. Hodgson, S. Kurz, S. Virtanen, V. Fervel, C.-O.A. Olsson, S. Mischler - Electrochim. Acta **49**, 2167 (2004).
[36]. I. Milošev, H.-H. Strehblow - Electrochim. Acta **48**, 2767 (2003).
[37]. R. Huiskes, H. Weinans, B. Van Rietbergen - Clin. Orthop. Relat. Res. **274**, 124 (1992).
[38]. M. Niinomi - Mat. Sci. Eng. A **243**, 231 (1998).
[39]. M. Niinomi - Metall. Mater. Trans. A **33**, 477 (2002).
[40]. M. Masmoudi, M. Assoul, M. Wery, R. Abdelhedi, F. El Halouani, G. Monteil - Appl. Surf. Sci. **253**, 2237 (2006).
[41]. R. Chiesa, E. Sandrini, M. Santin, G. Rondelli, A. Cigada - J. Appl. Biomater. Biomech. **1**, 91 (2003).
[42]. C. Sittig, M. Textor, N.D. Spencer, M. Wieland, P.-H. Vallotton - J. Mater. Sci. – Mater. M. **10**, 35 (1999).
[43]. C. Fonseca, M.A. Barbosa - Corros. Sci. **43**, 547 (2001).
[44]. Y. Yang, N. Oh, Y. Liu, W. Chen, S. Oh, M. Appleford, S. Kim, K. Kim, S. Park, J. Bumgardner, W. Haggard, J. Ong - Journal of the Minerals, Metals and Materials Society **58**, 71 (2006).
[45]. J.A. Disegi - Injury, Int. J. Care Injured **31**, 14 (2000).
[46]. X. Liu, P.K. Chu, C. Ding - Mater. Sci. Eng. R **47**, 49 (2004).
[47]. C.E.B. Marino, S.R. Biaggio, R.C. Rocha-Filho, N. Bocchi - Electrochim. Acta. **51**, 6580 (2006).
[48]. M. Geetha, A.K. Singh, R. Asokamani, A.K. Gogia - Prog. Mater. Sci. **54**, 397 (2009).
[49]. T. Hanawa - Japanese Dental Science Review, **46**, 93 (2010).
[50]. K. Niespodziana, K. Jurczyk, M. Jurczyk - Rev. Adv. Mater. Sci. **18**, 236 (2008).
[51]. Boon Sing Ng, I. Annergren, A.M. Soutar, K.A. Khor, A.E.W. Jarfors - Biomaterials **26**, 1087 (2005).
[52]. Y. Okazakia, E. Gotoh - Biomaterials **26,** 11 (2005).
[53]. Y. Li, C. Wong, J. Xiong, P. Hodgson, C. Wen - J. Dent. Res. **89**, 493 (2010).
[54]. P.A. Dearnley, K.L. Dahm, H. Çimenoğlu - Wear **256**, 469 (2004).
[55]. S. Kumar, T.S.N.S. Narayanan, S.G.S. Raman, S.K. Seshadri - Mater. Chem. Phys. **119**, 337 (2010).
[56]. S. Kumar, T.S.N.S. Narayanan, S.G.S. Raman, S.K. Seshadri - Mater. Sci. Eng. C **30**, 921 (2010).
[57]. S. Yang, H.C. Man, W. Xing, X. Zheng - Surf. Coat. Tech. **203**, 3116 (2009).
[58]. H. Wang, N. Eliaz, Z. Xiang, H.-P. Hsuc, M. Spector, L.W. Hobbs - Biomaterials **27**, 4192 (2006).
[59]. C.H. Hager Jr., J.H. Sanders, S. Sharma - Wear **265**, 439 (2008).
[60]. L. Gan, J. Wang, R.M. Pilliar - Biomaterials **26**, 189 (2005).
[61]. D. Wang, C. Chen, T. He, T. Lei - J. Mater. Sci.-Mater. M. **19**, 2281 (2008).
[62]. Y.-M. Lim, K-S. Hwang, Y-J. Park - J. Sol-Gel Sci. Techn. **21**, 123 (2001).
[63]. Q. Zhang, Y. Leng, R. Xin - Biomaterials **26**, 2857 (2005).
[64]. J. Wang, P. Layrolle, M. Stigter, K. de Groot - Biomaterials **25**, 583 (2004).
[65]. F. Barrère, P. Layrolle, C.A. van Blitterswijk, K. de Groot - J. Mater. Sci.-Mater. M. **12**, 529 (2001).
[66] X. Cui, H.-M. Kim, M. Kawashita, L. Wang, T. Xio.ng, T. Kokubo, T. Nakamura - Dent. Mater. **25**, 80 (2009).
[67]. R. Narayanan, P. Mukherjee, S.K. Seshadri - J. Mater. Sci.-Mater. M. **18**, 779 (2007).
[68]. F. Variola, J.-H. Yi, L. Richert, J.D. Wuest, F. Rosei, A. Nanci - Biomaterials **29**, 1285 (2008).
[69]. I. Zhitomirsky, L. Gal-Or - J. Mater. Sci.-Mater. M. **8**, 213 (1997).
[70]. M. Wei, A.J. Ruys, B.K. Milthorpe, C.C. Sorrell, J.H. Evans - J. Sol-Gel Sci. Techn. **21**, 39 (2001).
[71]. A. Rakngarm, Y. Mutoh - Mater. Sci. Eng. C **29**, 275 (2009).
[72] A. Kar, K.S. Raja, M. Misra - Surf. Coat. Tech. **201**, 3723 (2006).
[73]. S. Miao, W. Weng, Z. Li, K. Cheng, P. Du, G. Shen, G. Han - J. Mater. Sci.-Mater. M. **20**, 131 (2009).
[74]. P. Kern, P. Schwaller, J. Michler - Thin Solid Films **494**, 279 (2006).
[75]. C.T.J. Low, R.G.A. Wills, F.C. Walsh - Surf. Coat. Tech. **201**, 371 (2006).
[76]. S.R. Paital, N.B. Dahotre - Mater. Sci. Eng. R **66**, 1 (2009).
[77]. Y. Cai, R. Tang - J. Mater. Chem. **18**, 3775 (2008).
[78]. Q. Yuan, T.D. Golden - Thin Solid Films **518**, 55 (2009).
[79]. Y.W. Song, D.Y. Shan, E.H. Han - Mater. Lett. **62**, 3276 (2008).
[80]. Y.-Y. Zhang, J. Tao, Y.-C. Pang, W. Wang, T. Wang - Trans. Nonferrous Met. Soc. China **16**, 633 (2006).
[81]. N. Dumelie, H. Benhayoune, D. Richard, D. Laurent-Maquin, G. Balossier - Mater. Charact. **59,** 129 (2008).
[82]. Y.-Q. Wang, J. Tao, L. Wang, P.-T. He, T. Wang - Trans. Nonferrous Met. Soc. China **18**, 631 (2008).
[83]. D.J. Blackwood, K.H.W. Seah - Mater. Sci. Eng. C **29**, 1233 (2009).
[84]. N. Eliaz, T. M. Sridhar - Crystal Growth & Design **8,** 3965 (2008).
[85]. X. Zhao, L. Yang, Y. Zuo, J. Xiong - Chinese J. Chem. Eng. **17**, 667 (2009).
[86]. N. Eliaz, M. Eliyahu - J. Biomed. Mater. **80A**, 621 (2007).
[87]. X. Cheng, M. Filiaggi, S.G. Roscoe - Biomaterials **25**, 5395 (2004).

[88]. R. Narayanan, S.K. Seshadri - J. Appl. Electrochem. **36**, 475 (2006).
[89]. D. Velten, V. Biehl, F. Aubertin, B. Valeske, W. Possart, J. Breme - J. Biomed. Mater. Res. **59**, 18 (2002).
[90]. E. Krasicka-Cydzik, K. Kowalski, I. Glazowska - Journal of Achievements in Materials and Manufacturing Engineering, **18**, 147 (2006).
[91]. J. Jakubowicz - Electrochem. Commun. **10,** 735 (2008).
[92]. H. Lukáčová, B. Plešingerová, M. Vojtko, G. Bán - Acta Metallurgica Slovaca, **16**, 186 (2010).
[93]. M.V. Diamanti, M.P. Pedeferri - Corros. Sci. **49**, 939 (2007).
[94]. H.H. Park, I.S. Park, K.S. Kim, W.Y. Jeon, B.K. Park, H.S. Kim, T.S. Bae, M.H. Lee - Electrochim. Acta. **55**, 6109 (2010).
[95]. J. Kunze, L. Müller, J.M. Macak, P. Greil, P. Schmuki, F.A. Müller - Electrochim. Acta. **53,** 6995 (2008).
[96]. H.Z. Abdullah, C.C. Sorrell - J. Aust. Ceram. Soc. **43**, 125 (2007).
[97]. A. Karambakhsh, A. Afshar, P. Malekinejad - J. Mater. Eng. Perform. **19**, 1 (2010).
[98]. Y.-T. Sul, C.B. Johansson, Y. Jeong, T. Albrektsson - Med. Eng. Phys. **23**, 329 (2001).
[99]. M.V. Diamanti, M. Ormellese, M.P. Pedeferri - Corros. Sci. **52**, 1824 (2010).
[100]. B. Yang, M. Uchida, H.-M. Kim, X. Zhang, T. Kokubo - Biomaterials **25**, 1003 (2004).
[101]. S. Van Gilsa, P. Mast, E. Stijns, H. Terryn - Surf. Coat. Tech. **185**, 303 (2004).

THE ANNALS OF "DUNAREA DE JOS" UNIVERSITY OF GALATI.
FASCICLE IX. METALLURGY AND MATERIALS SCIENCE
N^0. 1 – 2013, ISSN 1453 – 083X

THE ANALYSIS OF A WORKPLACE FROM AN ERGONOMICALLY CRITERION. CASE STUDY: PRELIMINARY CHARGE

Adrian VASILIU, Marian BORDEI
"Dunărea de Jos" University of Galaţi, 111, Domnească Street, 800201, Galaţi, Romania
email: avasiliu@email.ro

ABSTRACT

This paper presents a practical method of analyzing a wokplace from an ergonomically criterion based on an "ergonomic analysis questionnaire", and, also, the conclusions and proposed measures in order to improve the activity of the analyzed workplace.

KEYWORD: ergonomics, job, worker, ergonomic index

1. Introduction

The ergonomics is a branch of multi-disciplinary nature that emerged after The Second World War, having common knowledge with science, biology, medicine, psychology and sociology. Shortly, we can say that ergonomics is the science that studies human behavior in employment, and more often at the workplace. Ergonomics is an approach that allows people to work optimally and efficiently. The basic principle of ergonomics is to adapt the workplace to the worker.

The implementation and application of ergonomics in the workplace starts from the simple worker (individual) to the team (group level).

A solution for the ergonomic research is the research team which consists of specialists from different fields of science.

For a good team cooperation each member must acquire a minimum knowledge from the others domains. This will allow a better flow of information and a good cooperation during the investigation. The ergonomic research is the higher form of scientific research.

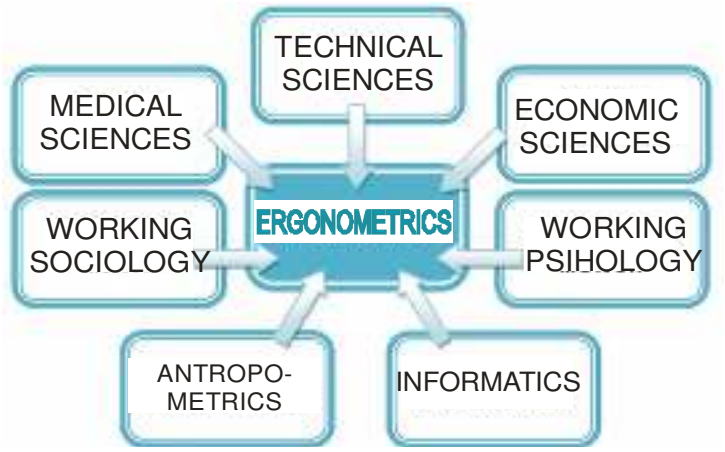

Fig. 1. *Ergonomics, interdisciplinary scientific field*

The purpose of applying ergonomic principles in the industry are the following:

- to improve the physical and mental well-being, eliminating the extra work (physical and mental) illness prevention and job satisfaction.
- to improve the social well-being by building relationships and contact with work colleagues, creating a adequate safe, comfortable and healthy system and working environment.
- to improving the human-machine system and establish a rational balance between technical, economic, and anthropological aspects, in order to increase its effectiveness.

2. Objectives

To ensure the effectiveness of the man-work-environment resources and minimize error opportunities under the conditions of reducing stress, at the samr time with the increase of job satisfaction, it is necessary, both for the designer and the organizers and work leaders to use appropriate methods that are based on possibilities knowledge and on human requirements during labor process. In these circumstances the analysis, design and ergonomic redesign of the workplace is very useful and a permanent necessity.

The ergonomic analysis of the workplace aimes at the constructive design optimization of workplace by improving the work safety and the physical environment factors, the reducing of the negative effects because of work monotony and decrease of physical and mental demands.

3. Work method

The process has as starting point the analysis of working conditions or proposed to be achieve in various ways for each workplace, based on evaluation factors and influence criteria. [1]. The research team applies the "ergonomic analysis questionnaire" individually at the workplace where the worker (contractor) develops his professional activity. For the analysis, we will use interview method during the stage of data collection (the questionnaire may be filled with other specific questions or others can be removed from the questionnaire).

The results will be analytically processed by calculating the ergonomic index (1) which reflects the aspects of the ergonomic organization for the job. The bigger the number of workers is the more important the results will be.

After analyzing the questionnaire, critical appreciations will be made regarding the ergonomic aspects of the job, conclusions and suggestions will be presented in order to improve the ergonomic situation at the analyzed workplace and the measures to improve the ergonomic factor will be proposed.

The ergonomic index calculation of a workplace (station) is made by the relation:

$$\mathbf{Ie = (\Sigma P + \Sigma N) / N\hat{i}} \quad (1)$$

where:

P = YES answers favorable (positive) - marked with 1;

N = NO answers unfavorable (negative) - marked with 1;

*** DO NOT KNOW Answers - marked with 0;

Nî = number of questions

Processing results

The ergonomic index will be calculated: the ergonomic index can take values between -1 and 1 resulting:

1. - the principles and ergonomic requirements, maximum satisfaction at work and therefore efficient activity;

0. - non-compliance of all ergonomics requirements, work is carried out in satisfactory conditions.

-1. - non-compliance of ergonomic requirements, minimalal satisfaction, inefficient activity.

Data collection and processing

The questionnaire was applied to a sample of 12 employees from the Agglomeration Department and to six employees from the Furnaces Stockade Sector Department of AMG. The samples included people working in shifts serving various specific installation, of different ages and sexes.

Table 1. *Ergonomic analysis questionnaire for batch preparatory work [2]*

No.	QUESTIONS	YES	DO NOT KNOW	NO
	A. Questions related to specific activity			
1.	Do you know the main function in the workplace?	1		
2.	But secondary function?		0	
3.	Do you know the basic requirements of the job?	1		
4.	Know the risk factors in your work?	1		
5.	When distributing the functions to take account of personal skills?			-1
6.	There are conditions permit exercise properly?			-1
7.	There are elements that disturb the activity (lack of space, lighting, noise, temperature, risk)?			-1
8.	There is a functional link between employees?	1		
9.	The links are appropriate?	1		

10.	Been taken into account in the preparation and distribution functions prior specialization?		0	
	Ie=(5-3)/10=0.2			
	B. Questions about the physical demands and posture during work			
11.	Physical efforts can be supported without danger of overload or impairment of work capacity?			-1
12.	Is the space enough?	1		
13.	But free space?	1		
14.	Where are prompted for an orthostatic position have taken measures to support and balance?			-1
15.	Doorways in height are provided with guard rails?	1		
16.	Area reserved knee and leg clearance satisfactory?			-1
17.	Motor vehicles are utilized?	1		
18.	Additional steps can be taken to ease the physical exertion of various materials handling?	1		
19.	The pace of work is appropriate?		0	
	Ie=(5-3)/9=0.2			
	C. Questions about applications perception, attention, skills			
20.	Is distracted attention by noise or other acoustic stimuli?	1		
21.	Routine activities and skill is running under visual control?	1		
22.	Education and training are dynamic and appealing?			-1
	Ie=(2-1)/3=0.33			
	D. Questions on adapting to ambient conditions, light, color, noise, dust			
23.	Sufficient illumination to be fulfilled her duties?	1		
24.	Light sources are installed?			-1
25.	There area each compartment lighting adequate?		0	
26.	There are contrasts of light on the most common directions?	1		
27.	There are contrasts of light on the most common directions?	1		
28.	Intensity artificial lighting is sufficient and steady?			-1
29.	Chromatic interior helps to improve lighting?		0	
30.	Wall color is pleasant and soothing?			-1
31.	The temperature at which the work is best?			-1
32.	We have taken steps to limit the effect of thermal radiation?			-1
33.	Warming winter appropriate?			-1
34.	The temperature of the surrounding surfaces is the same as that of air?	1		
35.	Working at high temperature in summer is accompanied by measures to prevent heat stroke?			-1
36.	Air exchange with the outside is appropriate?		0	
37.	We have taken measures to limit dust in your workspace?		0	
38.	Relative humidity corresponding physiological requirements?		0	
39.	Attention staff is disturbed by noise?	1		
40.	Perception and decision-making capacity are negatively influenced by noise?	1		
41.	They made arrangements for isolating noise producing?			-1
42.	We have taken steps to soundproof workspaces?			-1
	Ie=(7-8)/20= - 0.5			
	E. Questions about clothing and protective equipment			
43.	The equipment used in the movements of the performers creates difficulties?	1		
44.	There are protective equipment against microorganisms and dust?	1		

45.	Protective equipment bothers accomplishing tasks?	1		
46.	When purchasing or making clothing and protective equipment to take into account the proposals of the employees?			-1
	Ie=(3-1)/4=0.5			
	F. Questions regarding working hours and psychological environment			
47.	Perception, attention and dexterity is required in the normal range?	1		
48.	Working time is appropriate?	1		
49.	Function is sufficient motivation for the work efficiency and good humor?			-1
50.	Service members were able to form collective team spirit?	1		
51.	In making teams take account of options and affinity component members?			-1
52.	There is an atmosphere of collaboration, consultation and participation in enforcement activities?	1		
53.	Head customary to close with each subaltern speak?	1		
54.	The reward system is stimulating?			-1
55.	Known or particular staff tries knowledge unrest?			-1
	Ie=(5-4)/9=0.11			
	TOTAL	26	0	-21
	Ie=(26-21)/55=0.12 **Ie= 0. 12**			

Based on the results and the ergonomic index calculation the value 0.12 resulted, value which falls to the limit, to fully respect the ergonomic requirements; the activity of the worker at the analyzed workplace runs in satisfactory conditions.

4. Conclusions

Unsurprisingly, ergonomic index was positive but close to zero for all persons interviewed, which demonstrates clearly the need for more intense concerns from managers in this unit to ergonomics. Certainly there are negative aspects in this regard, aspects that can be improved by applying a set of appropriate measures.

Based on the questionnaire were determined following conclusions, and have proposed the following measures:

Specific activity (Ie = 0.2): It finds a good knowledge of the requirements of function (job) of the basic requirements of the job, the risks specific to the job by the employee. Some shortcomings are found in functional connections between employees, but the work is in satisfactory condition.

As recommended measures improving functional link between employees and better sharing of staff working on functions taking into account personal skills.

Physical demands and body position (Ie = 0.22): From the point of view of application and physical posture during work finds that space is sufficient and space and have taken the necessary steps to support and balance as and providing sufficient transport.

As recommended improving working conditions so as to minimize the danger of overloading.

Requests perception, attention, skills (Ie = 0.33): With regards to perception, attention, skills finds that the work is under major influence of acoustic stimuli (noise) and that the trainings are dynamic and appealing. Ergonomics index shows that the activity is conducted in a more than satisfactory.

As recommended measures are personal protective equipment against noise (ear) where the noise level is exceeded or limited and staff training in addition to training SMART.

Environmental conditions (Ie = -0.05): Regarding the ambient conditions is found that insufficient lighting at work, often appear large temperature contrasts and the work is near sources of noise insulated. Ie = -0.05 - shows that the overall activity is conducted in poor conditions.

As recommended improvement measures both natural and artificial lighting, equipping staff with appropriate equipment (summer - winter) and isolating noise and where it is not possible equipping staff with PPE against noise (earplugs).

Clothing and protective equipment (Ie = 0.5): Regarding the protective clothing and equipment are

clearly noted concern management to ensure the necessary equipment for the smooth running of the production process. As observed for management: when making supply protective equipment should be consulted and the staff uses to avoid difficulties in the use of and increase the range of appropriate protective equipment against temperature.

The work program and psychological environment (Ie = 0.11) on the program of work and psychological atmosphere is found (in terms of the employee) that: salary is insufficient in relation to the work performed; not take into account the composition of the collective choices of team members; reward system is not stimulating.

Final conclusions:

- job description was a constant concern, so the organizational structure is reasonable and appropriate in the circumstances, but not stimulating.

- report preparation and content of the posts did not work as a lever of efficiency and job satisfaction.

- management of documentation structures was powerless to counteract the wage provided humiliating and incompatible with the volume of work and the terms of existing work, which effectively reduced the authority of managers and staff motivation.

References

[1]. Burloiu, P. - *Managementul resurselor umane*. Bucureşti: Lumina Lex, (1997), p. 1272.
[2]. *** - *Les profils de postes*. Paris. Ed. Masson, (1976), p. 20-40
[3]. Grandjean, E. - *Principiile ergonomiei*. Bucureşti: Editura Ştiinţifică, (1972).
[4]. Mathis, R. Nica, P. - *Managementul resurselor umane.* Ed. Economică, (1997).
[5]. Nicolescu, O.; Verboncu, I. - Management. Bucureşti, Editura Economică, (1997).

THE ANNALS OF "DUNAREA DE JOS" UNIVERSITY OF GALATI.
FASCICLE IX. METALLURGY AND MATERIALS SCIENCE
N^0. 1 – 2013, ISSN 1453 – 083X

R.N.U.R. METHOD OF RISK ASSESSMENT BASED ON ERGONOMIC CRITERIA. CASE STUDY: CRANE MAINTENANCE ELECTRICIAN

Adrian VASILIU, Marian BORDEI
"Dunărea de Jos" University of Galaţi, 111, Domnească Street, 800201, Galaţi, Romania
email: avasiliu@email.ro

ABSTRACT

This paper presents a case study on the evaluation of a job (electrical maintenance) in AMG plant through a less used method in Romania, respectively Renault method, used especially in France. Means of work are analyzed on the basis of the technological equipment, the work task based on the job description and the work medium based on analyzes of made by occupational medicine. The test results are tabulated and graphically processed and they are taking into account to establish the conclusions and the measures to be imposed at the analyzed work place.

KEYWORD: ergonomics, risk assessment, Renault method, system work, physical environment, reduction efforts, job profile

1. Introduction

Ergonomics refers to the compatibility of people with their job: employee abilities and limits, ensurance of tasks, equipment, information and working environment that fit everyone. In assessing this compatibility it is taken into consideration: the degree of fulfilling the employee obligations, the equipment qualities (size, shape, and how appropriate are for service obligations), the information used during work activities (mode of presentation, access and change). The ergonomic analysis of the workplace has as objectives the optimization of constructive design of jobs by improving occupational safety and improving the physical environment factors, reducing the negative effects because of the work monotony and decrease of physical and mental demands.

To ensure the efficiency man - work means - environment and to minimize error possibilities, while reducing stress, the same time with increasing job satisfaction, it is necessary for organizers and leaders of work processes to use appropriate methods based on possibilities and human requirements during labor process. In these circumstances, the analysis, design and ergonomic redesign of the workplace is of great utility.

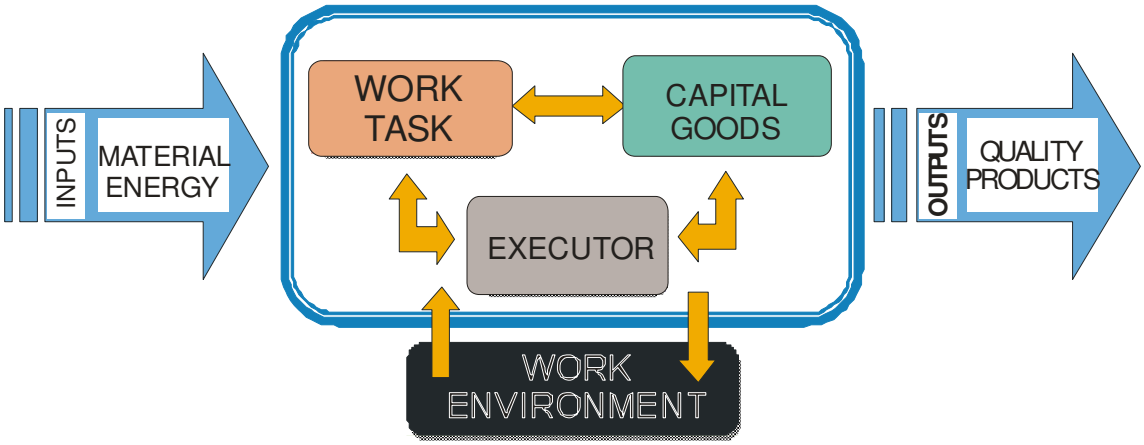

Fig. 1. *The components of the work system*

The work system can be defined as the assembly of inter-relationship components, developing during various activities, in order to transform the system inputs (materials, subassemblies, energy, etc. purchased / supplied) in system outputs (products, services, etc. delivered / sold) to meet the needs in the market.

The components of the work system are: work tasks, worker (executive), inputs, work environment (Figure 1).

2. Theoretical considerations

R.N.U.R. method assessment based on ergonomic criteria aims the analysis and redesign of the existing work systems and has been developed at the National Administration of Renault Plants, France. It is based on the interaction man - machine, which takes place in an environment of mutual dependencies between the components that are being investigated thoroughly, emphasizing possible problems highlighted in these interactions.

The process has as its starting point the analysis of existing working conditions (based on direct observation) or designed to perform in different ways and for each job, depending on the evaluation factors and criteria of influence. In order not to omit important ergonomic issues, the R.N.U.R. method analysis 27 influence criteria (Table 1), divided into 8 evaluation factors (A - H), with 5 fields of research, where the more favorable is level 1 and the worst is level 5, (Table 2).

Table 1. *Influence factors and evaluation criteria analytical work system*

Areas of investigation	**Factors of influence**		**Criteria of evaluation**	No.
Concept of the work place		A_0	Height - distance	1
			Feed and discharge	2
			Agglomeration – accessibility	3
			Commands - signals	4
Safety Factor		A	Work Security	5
Ergonomic factors	Physic ambience	B	Thermal Ambience	6
			Sound Ambience	7
			Artificial lighting	8
			Vibrations	9
			Hygiene atmospheric	10
			Workplace aspect	11
	Physic load	C	Physical main body	12
			Worst position	13
			Work effort	14
			Work position	15
			Handling effort	16
			Position during handling	17
Psychological and social factors	Mental task	D	Mental operations	18
			The level of attention	19
	Autonomy	E	Individual autonomy	20
			Autonomy in group	21
	Work relationships	F	Independences work relationships	22
			Dependences work relationships	23
	Repetitivity	G	Repetitivity of the work cycle	24
	Work content	H	Work potential	25
			Responsibility	26
			Work interest	27

The determination of ergonomic levels is done taking into account the significance of each criterion, adapted to the concrete situation of work (Table 2).

Assessing the degree of difficulty of each criterion previously met is carried out in order to:

- optimize of workplace;
- ensure security work;
- improve physical environment;
- reduce physical and mental demands;
- establish appropriate psychosocial working conditions
- interpret job profile.

Table 2. *Evaluation grill of method criteria*

Level	Evaluation factor						
	A	B	C - D	E	F	G	H
1	very good		very easy	< 30 min	group+ from outside	< 10 min	high
2	good		easy	15 - 30 min	group	5-10 min	
3	acceptable		normal	5-15 min	easy relationships	3-5 min	medium
4	danger	difficult	solicited	1 - 5 min	direct relationships	1-3 min	
5	very danger	very difficult	very solicited	< 1 min	isolated	< 1 min	low

Workplace concept ($\underline{A_0}$). The specialist attention will turn to the interaction between the work space and the human component of the system. It is checked if the height and distance between the arms and legs zones drive operator both work orthostatic position and sitting, are correlated with anthropometric measurements of the operator (A_{01}).

The possibility of feed and discharge of the pieces (A_{02}) is, also, related to anthropometric dimensions of the worker. At the same time, these activities are investigated based on the moving economy principles; so that the worker can feed and discharge the pieces based on the movements of the lower classes, the less energy consumers. It is preferred to use the solutions which use the law of gravity, reducing both worker effort and time required for these activities.

The agglomeration and accessibility at the workplace (A_{03}) involves a study of the organization of work and the possibility of movement at the workplace. It is useful to have an outline of the section or workshop on which mark the jobs, equipment, material storage items, boxes, tables, etc. In these sketches there will be shown the access roads and routes crossed by the worker to fulfill the task, emphasizing the agglomeration points and unnecessarily long routes.

The commands and signals (A_{04}) may generate problems for the interaction between workspace element and human components: the senses, etc.; consequently, the conception of the machine control actuators (buttons, cranks, levers, wheels, etc.) of the signals (sound, images, etc.), of the measuring apparatus will be verified in terms of the visualisation, the location, the clarity of message.

Work safety (A) is one of the main objectives of ergonomics (safety factor A_5). The conditions of producing accidents and incidents, and their severity are investigated, taking into account the equipment used and the nature of the activities implied.

Physical environment of work (B) is characterized by a set of influence criteria, bringing together both the physical state of air, air hygiene, appearance, and problems related to noise, vibration, lighting etc.

Thermal environment (B_6) assesses whether the workplace air temperature both in warm and cold seasons, coupled with dynamic work load, provides the operator the physiological status, appropriate to carry out work in a normal rhythm.

Sound environment (B_7) is characterized by measuring the sound pressure levels for continuously noises present in the workplace and for intermittent ones. The measurements are made by using precision sonometers with type A filter; the evaluation levels of this criterion are in accordance with ISO standards.

Visual comfort (B_8) involves measuring the levels of lighting with a help of a luxmeter and comparing these values with those recommended for the different activities, depending on the precision of the works. It also taken into account the luminance, both in terms of contrast and brightness of the distribution.

The frequency, amplitude and duration of exposure to vibration (B_9) are determined through their adverse effects on the health of the operator.

Atmospheric hygiene of the physical environment (B_{10}) refers to environmental pollution with: dust, fumes, gas, and vapor. The extent to which those pollutants and how they affect the health of the operator and his ability to work are considered.

Aspect of workplace (B_{11}), both in terms of cleanliness, space, chroma, and in terms of natural lighting - appreciated by fitting windows, floor surface, the distance between work and frontage windows.

Physical exertion (C) who is subject the operator is a fatigue generator, frequent cause of decreased of the work capacity. Based on the analysis of the work task and the work method, worker position during their activities are determined.

Postural solicitation gived by the main position once of the operator body (C_{12}), correlated with time-keeping in that position, should be determined not only the most important activity such as processing itself on a machine tool, but for all activities which are carried by the operator to achieve the task, eg training activities and closing operation for the operator make an effort (lift, push, pull, push, grip, etc..) request generated is estimated by the strain time and effort to maintain the position and frequency of efforts.

This evaluation is done for the step of converting the product (C_{14}) and for the step of handling thereof (C_{16}). The position of the worker requests, generated during the effort in both the step

of the product converting (C_{15}) and the step of handling (C_{17}) are examined and evaluated.

Nervous solicitation (D*)* of the operator during the work aimed at overloading the nervous system, resulting in time to exhaustion. In assessing the application date nervous mental operations (DL8), depending on the number of information received and processed in a minute and duration for implementation of these operations without affecting the smooth running of the process. Request nervous due care level (D_{19}) is determined taking into account the care and precision required by the tasks.

Autonomy in the work activity (E) is a factor with which to appreciate enables the operator to leave the workplace in order to consume the time for rest and physiological needs, without disrupting production. Check both individual autonomy (E_{20}), depending on the maximum duration of leaving the job of a performer and group autonomy (E_{21}) by the maximum in which many performers may leave the workplace without affecting the production process, for example to take a break superimposed during machine operation.

Labor relations (F) man-machine system environment in which the work is the use and the organization of work, including social problems. The nature of the task and work organization influences independent labor relations (F_{22}) between operators, seen through the extra-communication during the work, without negatively impacting its deployment.

Investigation dependent relations to work (F_{22}) covers the possibility of communication with the next higher hierarchical organs, control staff, refinish, repair, transport, etc.., In the interest of the service.

Repetitive work cycle (G) tires the operator by monotony. Depends on the number of operations is repeated identical cycle work, the number of different jobs that can rotate performer, and rotation period.

Labor content (H) is a factor that investigates the relationship between the human and tasks. The necessary skills to perform the task, correlated with activity during adaptation are taken into account by potential employment criterion (H_{25}).

Responsibility criteria (H_{26}) focuses the ergonomist attention to the potential for error because of the nature of the task, for the consequences of producing errors and operator's ability to solve the errors and labor problems incurred.

Working interest (H_{27}) is a criterion which addresses the extent to which task work gives satisfaction operator. Check that the operator runs several phases necessary to manufacture a product or has met only one task, if his work is recognized in the product, making the whole product or only parts of the whole, if it can decide and choose the order of technological operations, machinery, tools, appliances, checkers needed.

3. Case study: maintenance electrician risk assessment

This step is done at work which operates under review. It will collect information on the existing technical conditions, for example, equipment, tools, devices, checkers, wear and so on, and on specific issues of work organization.

The work task is studying by the analysis method applied to measure the activities and time for the exercise of these work activities. For the data collected to be realistic and complete, will discuss these issues with the operators involved in working with specialists from the slot.

The work process is aimed at maintaining, repairing, supervision, adjustments and interventions to remedy defects in components of lifting equipment and transport (the cranes, hoist, etc.) of the Furnaces Department.

4. The components of the system of work reviewed

Means of production: lifting equipment (cranes, hoist, jib cranes etc.) with related equipment (electrical, mechanical, etc.); panels and / or internal service switchboards DC and AC.

Gears on the side panels of automation and protection: AMC: meter, ammeters, voltmeters; relays; switchgear; electrical protection; strings of terminals for conductors; medium voltage cables.

Motors, synchronous, asynchronous and current; DC voltage converters; DC generators; Process computer and peripherals; Electricity transmission systems cables MV, LV, control and signaling.

Specific tools, accessories and devices: locksmith T.S.L. kit; electrician kit; voltage detector; measuring devices (multimeters, oscilloscopes, signal generators, testers, etc.); field equipment (limiters, proximity detectors, pressure transducers, flow, displacement, position); flashlight; portable scale; shorted; voltage detectors (test);

Workshop engines: universal drilling machine; fixed electric grinder; vice; various kits for verification; solders; wire brushes; pick; shovel; pickaxe; shovel; fire extinguishers; electrical heating unit; workbenches; transformer oil; painted gun; paint thinner, alcohol technical brushes; installation of fluorescent and mercury vapor.

Inputs to the electrician performing work or in contact during work: DC motors; AC motors; ventilation systems; controls; control cable, power and low voltage; bridge, well, basement, electrical cable tunnel; drilling machine; car stopped; tipping

trough; oxygen distribution facilities; installation of methane gas distribution and gas protection; compressed air systems; electrical installations; automation systems; other specific work activities occurring within the department furnaces.

Working tasks

According to the documentation provided by the department, the burden of work is shown mainly by the following documents:

- work and safety instructions for the maintenance and repair of cranes;
- ISCIR technical requirements;
- safe work practices for working at heights;
- workplace description for the position maintenance electrician platform.

Besides the work tasks of the documents listed above, maintenance electrician has the following job responsibilities:

- have to come to work in full capacity to perform work tasks smoothly incumbent;
- is obliged to strictly observe the rules laid down by the laws and regulations of the interior order;
- must be committed to work, presenting before starting the program without delays or interruptions;
- has an obligation to perform quality work and meet the technical standards of maintenance and repair;
- performs the binding of pregnancy (pregnancy related authorized);
- does not leave work without the driver or without good reason;
- works only with specific equipment sector approved, verified and approved by the responsible factors;
- is required to make and maintain cleanliness in the workplace;
- responsible for compliance with OHS and general and sector-specific SU activity;
- responsible for compliance with RI, CCM and occupational standards.

In this assessment were checked electricians job descriptions of CM (no brand 86xxx), MG (no brand 69xxx).

Work environment

Electrician work is conducted on the premises which houses the production areas and outside the Department furnaces (stoves raw sewage / fine dosing skip drive, chargers, etc.). From the analysis report no. 88 - 100 of 12/08/2013, are found to be exceeding the allowable values for the following pollutants in the work environment: noise and dust. In addition we can remark during unloading iron, air temperature, and (within legal allowable) the presence of particulates, carbon monoxide, silicon oxide, air currents and IR radiation emission.

Work system analysis method based on specific criteria

Work system analysis method was used RNUR This method is typical of industrial usability. Analyzing employment situation - taking into account the factors of influence - has the advantage of allowing an overview of all aspects that define the work system interacting not only assign a single decisive factor, which would be easily visible and easier Mitigation.

As each factor is defined by values and characteristics, compliance levels ergonomic factors under evaluation grid is done with precision, without interpretation.

This means analyzing and evaluating ergonomic ensure, through systemic vision that has on labor activity, the fact that improvements in one area does not entail negative effects in other areas of influence.

Evaluation Criteria

The evaluation criteria are the number of 27 organized so as not to omit any issue that would be important in terms of ergonomics the system work and hence the health and safety of workers operating in job analysis.

The evaluation criteria are divided into eight evaluation factors and are valued using valuation scale from 1-5, where level 1 is the most favorable, and level 5 the worst.

As a result of analysis of the working of the system, each component of the working part, and the evaluation levels are obtained for evaluation criteria summarized in Table 3.

Table 3. *Evaluation criteria*

Factors of influences	**Evaluation criteria**	**Level evaluatedt**
A_0 1	Fall on same level as the imbalance by sliding the drive, by tripping, etc. and falls from height: by stepping into the void, the balance is lost, the drive, sliding etc., falls from height due to inadequate spontaneous reactions in case of danger.	2
A_0 2	Slipping, rolling of parts, materials, assemblies, subassemblies, etc. stored without stability.	3

A_0 3	Visits and stationary in hazardous areas - ex. on the access roads and rail cars under suspended load lifting hook, right next to the furnace platform work equipment that is in working order (ie in the vicinity of the discharge chute, cast iron machine gauge stopped or drilling, etc.) adjacent mounting holes, bearing the guard rails provided in areas where there is the possibility of falling from height, crossing gutters clay through undeveloped places, travel out work tasks in the vicinity of installations etc. energized.	3
A_0 4	Making electrical drives by identifying erroneous cells and / or items of electrical equipment. Means not checking electrical protection (electrical poles, voltage indicator, etc.) and individual protection means. Run memory electrical connections. Using makeshift control lamps. Running the wrong power cable connections from the connection terminals of electric motors. Putting accidental electrical voltage of a cell that has not been removed or CLP scurtcircuitorul coupled. The power supply of an electric cell located in pregnancy (running) by operating (opening) separator line or bar etc. The drive switching devices without protective cover. Use fuse handle M.P.R. defective without ferrules etc. Remove fuses M.P.R. high voltage without de-energize the associated circuit before performing this activity.	2
A 5	Unexpected activities performing work activities (outside work tasks) do work for which no qualifications and / or authorization required. Making operations, activities, work, etc. in a different manner than those of working instructions, instructions for safety, work procedures and manufacturing requirements for safety and health at work, etc. ISCIR prescriptions.	3
B 6	High air temperature in some work areas, especially near the iron and slag troughs, etc. Low air temperature in cool season in some areas of work.	3
B 7	High noise level - as attached determinations ballot - more than the maximum allowable.	2
B 8	Low light in some areas of it.	3
B 9	No vibration.	1
B 10	Accumulation of toxic gases - carbon monoxide presence in some areas of work (as ballot measures linked to below the maximum allowable), the occurrence of toxic gases from certain insulation piercing (epoxy resins, PVC, etc..) Current transformers and / or electric motors, complex gases from burning insulation of electrical conductors, etc..	2
B 11	High contrast between the iron and clay, and general background incandescent lighting of the hall, a visual overload. Ionizing radiation (IR) from the flow of liquid iron gutters, etc.	3
C 12	Postures mixed forced vicious	3
C 13	Forced postures, vicious - ex. interventions to be carried out at height, in confined spaces, etc..	3
C 14	Dynamic effort than intervention route.	3
C 15	Complete of major routes for interventions	3
C 16	Dynamic effort handling tasks.	3
C 17	Lumbar spine disorders handling large electric motors	3
D 18	Difficult decisions to be taken in short time to remedy situations of "incident" or "failure".	2
D 19	Mental stress related to risk of injury	2
E 20	There are individual autonomy depending on the time of leaving the workplace	2
E 21	There is autonomy grouped by time of leaving job	2
F 22	There are interdependent relationships in the band working without affecting the work.	2
F 23	Communication with hierarchical structures and other operators in the work stations, radio stations directly or through	2
G 24	Operations repetitive short cycle time repair shop engine	2
H 25	High work pace on some days of service (scheduled repairs or damage).	2
H 26	Performing operations with high degree of responsibility	2
H 27	Solving multiple and diverse work tasks	2

Evaluation grid (method criteria)

The evaluation grid is evaluated for the 8 levels of evaluation factors, labeled A to H. The level of each factor is calculated as average of criteria related influence. After analyzing the work system under evaluation in terms of ergonomics, we obtained values of levels of assessment factors entered in Table 4.

Table 4. *Levels of assessment factors*

Evaluation factors	A	B	C	D	E	F	G	H
Evaluated level	2.6	2.3	3	2	2	2	2	2

The workplace profile interpretation

Levels ergonomic listed in Table 3 translates to a graphic in the assessment levels are noted at equal distances on the abscissa and the ordinate are ranked the 27 influential factors, in order of their current numbers.

After analyzing the work system using the R.N.U.R. method each criterion investigated revealed interactions between different blocks of the system and was rated with the evaluation grid. These results can be plotted to highlight areas of poor system design.

Analytical profile of the work system consists of a graphical representation of all levels of evaluation criteria influence. The analysis shows the normal operation of the system work, but may be searched for ways to improve the performance of the whole system work and not just one of its components. Influence criteria considered are those listed in Table 1.

Overall picture of the system work gives an overview of the system, the level of each factor yielding the arithmetic mean of the respective criteria of highlighting the weight factor and the difficulty accordingly. As shown in Figure 3, the physical load limit reaches normal levels remaining evaluation factors ranging between good and very good.

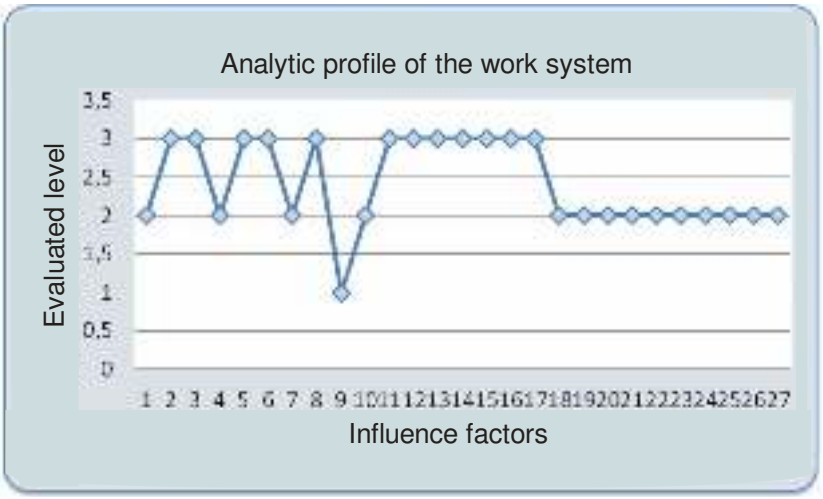

Fig. 2. *Graphic representation of the analytical profile of the work system*

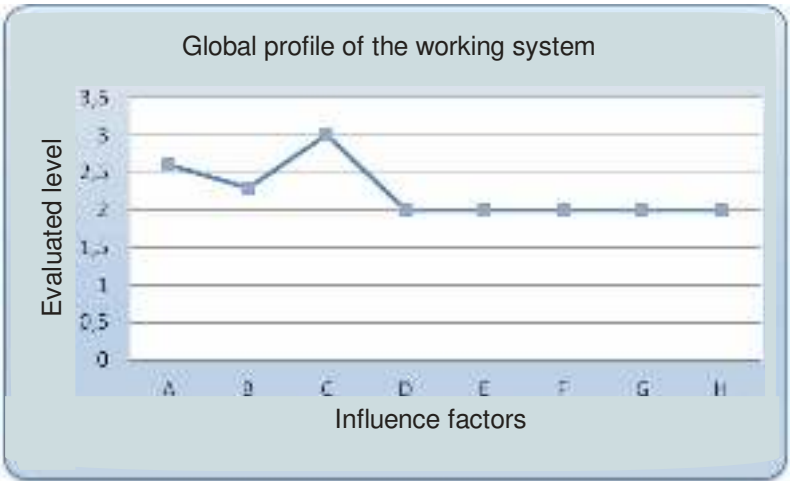

Fig. 3. *Graphical representation of the overall profile of the work system*

Assessment factors analyzed are: (legend): A concept of employment and security B-physical environment, physical exertion C-, D-load nervous, E-autonomy F-relations work; G-repetitive H-labor content.

5. Conclusions

R.N.U.R. method assured the opportunity to analyze the interactions between the worker and the other system components, linking possibilities morphological, functional, psychological, etc. with its technical, economic, organizational, social system works, for which all determinants of the method can be considered ergonomic.

The analysis work performed on *electrical maintenance and repair bridges* in the section of the Mechanical repairs furnaces Department, we can draw the following conclusions:

- overall picture of the work system has values between 1 and 3 These values are within normal limits, demonstrating the existence of a safe workplace, no major influence, in terms of worker health and safety ergonomics.

-higher values are observed in the workplace, physical environment and physical exertion;

-analyzing the graph profile analytical work system see detailed criteria influence the values close to the danger zone. If the global situation is normal, the criteria of influence should be studied and treated individually, according to the assessment made for corrective action to improve the performance of the whole system and not just one of its components.

Measures

We recommend certain technical and organizational measures which can translate into practice the following:

- proper storage of parts and devices to ensure stability;
- marking of access roads and security with guard rail mounting holes;
- training and verification of compliance with work instructions and ISCIR technical requirements;
- work load will be distributed during periods of high thermal discomfort on a larger number of employees by a system of rotation and breaks;
- the arrangement of locations in which workers to regulate body temperature;
- providing the facilities department to ensure microclimate;
- leveling platform furnace to eliminate bumps;
- providing intervention to prevent vehicles traveling on long routes;
- after performing operations requiring the worker to work in orthostatic position for long periods will necessarily perform some gentle exercise warming-up of the body;
- use of mechanical devices for lifting handling and transport operations by response personnel.

References

[1]. Burloiu, P. - *Managementul resurselor umane.* Bucureşti: Lumina Lex, (1997), p. 1272.
[2]. *** - *Les profils de postes*. Paris:Ed. Masson, (1976), p. 20-40
[3]. Grandjean, E. - *Principiile ergonomiei*. Bucureşti: Editura Ştiinţifică, (1972).
[4]. Vasiliu A - *Asigurarea mediului de muncă* – uz intern Galaţi (2013).
[5]. *** - SR EN ISO 6385:2004 – Principii ergonomice de proiectare a sistemelor de muncă.

MANUSCRISELE, CARŢILE ŞI REVISTELE PENTRU SCHIMB, PRECUM SI ORICE CORESPONDENTE SE VOR TRIMITE PE ADRESA:

MANUSCRIPTS, REVIEWS AND BOOKS FOR EXCHANGE COOPERATION, AS WELL AS ANY CORRESPONDANCE WILL BE MAILED TO:

LES MANUSCRIPTS, LES REVUES ET LES LIVRES POUR L'ECHANGE, TOUT AUSSI QUE LA CORRESPONDANCE SERONT ENVOYES A L'ADRESSE:

MANUSCKRIPTEN, ZIETSCHRITFTEN UND BUCHER FUR AUSTAUCH SOWIE DIE KORRESPONDENZ SID AN FOLGENDE ANSCHRIFT ZU SEDEN:

After the latest evaluation of the journals achieved by National Center for the Science and Scientometry Politics (**CENAPOSS**), as recognition of its quality and impact at national level, the journal is included in B^+ category, 215 code (http://www.cncsis.ro/2006_evaluare_rev.php).

The journal is indexed in:
CSA: http://www.csa.com/ids70/serials_source_list.php?db=mechtrans-set-c
EBSCO: http://www.ebscohost.com/titleLists/a9h-journals.pdf
Copernicus: http://journals.indexcopernicus.com/karta.php

The papers published in this journal can be visualized on the "Dunarea de Jos" University of Galati site, the Faculty of Materials and Environmental Engineering, page: www.fimm.ugal.ro.

Publisher's Name and Address:
Contact person: Antoaneta CĂPRARU
Galati University Press - GUP
47 Domneasca St., 800008 - Galati, Romania
Phone:+40 336 130139, Fax: +40 236 461353
Email: gup@ugal.ro

Editor's Name and Address:
Prof. Dr. Eng. Marian BORDEI
Dunarea de Jos University of Galati, Faculty of Materials and Environmental Engineering
111 Domneasca St., 800201 - Galati, Romania
Phone: +40 336 130223, Phone/Fax: +40 236 460750
Email: mbordei@ugal.ro

AFFILIATED WITH:

- *ROMANIAN SOCIETY FOR METALLURGY*
- *ROMANIAN SOCIETY FOR CHEMISTRY*
- *ROMANIAN SOCIETY FOR BIOMATERIALS*
- *ROMANIAN TECHNICAL FOUNDRY SOCIETY*
- *THE MATERIALS INFORMATION SOCIETY (ASM INTERNATIONAL)*

Annual subscription (4 issues per year)

Edited under the care of
Faculty of
MATERIALS AND ENVIRONMENTAL ENGINEERING

Edited date: 30.03.2013
Issues number: 200
Printed by
Galati University Press
accredited CNCSIS
47 Domnească Street, 800036
Galati, Romania